EUROPEAN JOURNAL OF PURE AND APPLIED MATHEMATICS
2025, Vol. 18, Issue 4, Article Number 7228
ISSN 1307-5543 – ejpam.com
Published by New York Business Global

Artificial Intelligence-Enhanced Framework for Complex Double-Valued Neutrosophic Soft Sets and Emotional Affinity Evaluation via Cotangent Similarity

Maha Noorwali[1], Raed Hatamleh[2], Ahmed Salem Heilat[3], Haitham Qawaqneh[4], Arif Mehmood[5,*], Aqeedat Hussain[5], Jamil J. Hamja[6], Cris L. Armada[7,8]

[1] *Department of Mathematics, King Abdulaziz University, P.O. Box 80203, Jeddah 21589, Saudi Arabia*
[2] *Department of Mathematics, Faculty of Science, Jadara University, P.O. Box 733, Irbid 21110, Jordan*
[3] *Department of Mathematics, Jadara University, P. O. Box (733), 21111, Irbid, Jordan*
[4] *Al-Zaytoonah University of Jordan, Amman 11733, Jordan*
[5] *Department of Mathematics, Institute of Numerical Sciences, Gomal University, Dera Ismail Khan 29050, KPK, Pakistan*
[6] *Mathematics and Sciences Department, College of Arts and Sciences, Mindanao State University-Tawi-Tawi College of Technology and Oceanography, 7500 Philippines*
[7] *National University Ho Chi Minh City, Linh Trung Ward, Thu Duc City, Ho Chi Minh City, Vietnam*
[8] *Department of Applied Mathematics, Faculty of Applied Science, Ho Chi Minh City University of Technology (HCMUT), 268 Ly Thuong Kiet, Ward 14, District 10, Ho Chi Minh City, Vietnam*

Abstract. This work introduces a novel hybrid emotion signal/template mapping system that combines the artificial intelligence (AI) validation layer with complex two-valued neutrosophic soft sets (DNSS). Next, by describing a comprehensive DNSS topology, fundamental operations, and properties, we create a rigorous mathematical foundation. Its analytical center measures emotional alignment using a Cotangent Similarity Measure (Cot SM), which shows a discernible hierarchy of connectedness between signal channels ($S_1 - S_4$) and emotional foci ($T_1 - T_4$). The multi-method visualization displays a hierarchy between cases of absolute dissonance (T_2S_4: 0.1431) and strong and stable pairs (e.g., T_2S_3: 0.3776). To guarantee the consistency of the paradigms, a nonlinear verification technique was implemented using an Artificial Neural Network (ANN). Strong performance metrics (Precision = 0.86, Recall = 0.83, F_1-Score = 0.84, ROC-AUC = 0.91) verified that ANN was able to replicate the analytical hierarchy. The integration of the symbolic cotangent model with numerical ANN validation demonstrates statistical consistency and structural harmony across computation domains. In order to establish a repeatable paradigm of affective computing and quantification of uncertainty in emotional connections, this research presents a theoretically and AI-checkable model of emotional analytic.

2020 Mathematics Subject Classifications: 54A05

Key Words and Phrases: Complex double-valued neutrosophic soft sets (CDVNS-sets), union, intersection, difference, AND, OR operations, interior and closure, bi-dimensional uncertainty modeling

*Corresponding author.
DOI: https://doi.org/10.29020/nybg.ejpam.v18i4.7228

Email addresses: mnorwali@kau.edu.sa (M. Noorwali), raed@jadara.edu.jo (R. Hatamleh), ahmed_heilat@yahoo.com (A. S. Heilat), h.alqawaqneh@zuj.edu.jo (H. Qawaqneh), mehdaniyal@gmail.com (A. Mehmood), aqeedathussain04@gmail.com (A. Hussain), jamilhamja@msutawi-tawi.edu.ph (J. J. Hamja), cris.armada@hcmut.edu.vn (C. L. Armada)

1. Introduction

The study of intuitionistic fuzzy sets (IFSs), which expanded on conventional fuzzy logic by introducing the independent membership and non-membership degrees, was essentially the first to establish this field [1]. In order to better represent the degree of data imprecision, [2] extended this paradigm to interval-valued intuitionistic fuzzy sets (IVIFSs), using these degrees as intervals. These models' practical utility in data clustering was quickly recognized, leading to the development of an algorithm that employed intuitionistic fuzzy equivalent relations and a maximal tree clustering technique that made use of fuzzy graphs [3]-[4]. Since the earliest methods, including the smallest spanning subtree of [5] and the shortest connection networks [6], served as the basis for more recent work, the application of graph theory to clustering is not new. The early gestalt cluster detection methods of [7] continue to use this technique, which was first introduced in graph theory by hierarchical clustering, a form of fuzzy connectedness, in [8]. By [9], the development of the uncertainty theory had advanced significantly with the introduction of neutrosophic logic and sets. This framework creates a three-part framework of truth, indeterminacy, and falsity, generalizing IFSs by including an independent indeterminacy membership. In their paper on fuzzy and neutrosophic cognitive maps, [10] was able to theoretically delve deeper into this area of research. Single valued neutrosophic sets (SVNSs) were later defined by [11] to increase computing utility, which resulted in widespread use. While [13] and [14] also employed neutrosophic sets to image thresholding and color texture segmentation, respectively, [12] examined a soft semantic web services agent as an example. This was added to the work of [15], who segmented images based on watersheds using a neutrosophic approach. Social sciences were also included, as demonstrated by [16]'s investigation of e-learning systems and [17]'s extensive socio-medical research on migrant workers who use neutrosophic cognitive maps. Multiple Attribute Decision-Making (MADM) has been one of the most important areas in which these sophisticated sets have been implemented. In this context, a lot of work has gone into developing sophisticated aggregation operators. These are the single-valued neutrosophic normalized weighted Bonferonni mean by [19], the normal neutrosophic generalized weighted power averaging operator by [20], and the Hamacher aggregation operators of numbers of the generalized neutrosophic number by [18]. The generalized hybrid weighted average operator by using interval neutrosophic hesitant sets of [22], the power generalized aggregation operators of [23], and the standard neutrosophic Bonferonni mean operators of [21] comprise additional input. Next, we followed the interval neutrosophic prioritized OWA operator of [24]. However, other authors have made important contributions using a number of MADM techniques, including single-valued neutrosophic cross-entropy, correlation coefficient-based, aggregate operators of simplified neutrosophic sets, and a single-valued neutrosophic minimum spanning tree clustering technique [25] [26] [27] [28].
The convergence of graph theory and uncertainty modeling in clustering is one of the most advanced study fields. It was heavily influenced by the gene expression clustering based on MSTs of [30] and the classical clustering methods of [29]. The intuitionistic fuzzy MST cluster algorithms of [32] and the hesitant fuzzy MST cluster analysis of [31] both combine modern uncertainty theories.

1.1. Literature Review

Based on the neutrosophic sets solid foundation, researchers sought to increase their applicability by fusing them with other useful uncertainty theories.The foundation of uncertainty theory today was established by Zadeh [33], and the introduction of fuzzy set theory revolutionized traditional set theory by giving the elements a membership grade, enabling the mathematical representation of partial truth. The merging of neutrosophic sets with soft set theory, which resulted in the initial concept of the neutrosophic soft set by [34], was one significant advancement in that area. With a neutrosophic set tied to each parameter, this hybrid model provides

a parameterized approach to handling uncertainty and provides a two-dimensional framework that is incredibly adaptable for simulating complex real-world scenarios. This structure's parameterization makes it possible to describe data in a more thorough and organized manner, and it would be particularly suitable in a decision-making setting where characteristics are defined by a number of criteria. The development of some topological structure soon solidified the conceptual underpinnings of this new form. Neutrosophic soft set, neutrosophic soft open set, neutrosophic soft closed set, neutrosophic soft interior set, neutrosophic soft closure set, and neutrosophic soft continuity were all fundamentally described by the Neutrosophic Soft Topology in [35]. This formalization was crucial because it provided the means to analyze the convergence, compactness, and separation axioms in the neutrosophic soft domain. This advanced the latter's application to complex computational models and brought it up to par with the important implications. Due to the need for even greater precision in scenarios requiring fine-grained distinctions, the theory evolved further, with new value domains becoming complex. Refined Neutrosophic Soft Sets were introduced by [36] at this time.

Numerous fields of study have demonstrated the superior structures' practical utility. For instance, in a neutrosophic soft set context, [37] suggested a decision-making system that uses similarity metrics to provide effective object ranking and selection techniques. Simultaneously, [38] has explored the application of such sets in data analysis and prediction, demonstrating their superiority in handling incomplete and irregular data streams. Following the development of the algebraic framework, the features of neutrosophic soft topology were thoroughly examined in [39], which further enhanced the theoretical complex by introducing concepts like connectedness and compactness. In order to address the intricate and contradictory nature of such strategic decisions, [40] has more recently proposed an expanded model of the selection of sustainable energy sources using an integrated method that makes use of the capabilities of sophisticated neutrosophic soft sets. From the early hybridization of neutrosophic with soft sets [34], to their topological formalization [35], refinement into multi-valued structures [36], and usage in various contexts [37]-[40], this trajectory reflects a continuous drive for more expressive, structured, and potent mathematical tools to deal with the whims of contemporary information systems.

1.2. Motivation and Significance

Because of the nature of the current neutrosophic and fuzzy models, it is necessary to redefine the operations on Complex Double-Valued Neutrosophic Soft Sets (CDVNS-sets) in order to handle information that has a dual phase of uncertainty and is multidimensional in its ambiguity. While classic complex-valued neutrosophic sets do not reflect the interplay between truth and falsity grades between connected domains, real-value systems sometimes overlook the rhythmic or cyclic nature of truth. By modeling each membership element-truth, indeterminacy, and falsity-with a real and imaginary component to represent the amplitude and phase components of uncertainty, the suggested CDVNS procedures overcome these shortcomings. The CDVNS structures can more accurately and adaptably model inconsistent, time-varying, and phase-shifted information because to this dual encoding. In theory, the redefined operations follow logical features such as complementarity and De Morgan duality and are mathematically consistent and closed. When it comes to the construction of improved topological, algebraic, and decision-making models that require sensitivity to the degree and directional orientation of the uncertainty, they offer a shared algebraic base. As a result, the CDVNS framework offers a powerful analytical tool for multi-criteria evaluation, pattern recognition, and complex systems analysis in the context of high-dimensional indeterminacy, enabling the bridge to be closed between abstract neutrosophic logic and practical computational intelligence.

The limitations of the conventional similarity and correlation measures, which do not take into account nonlinear, asymmetric, and cross-modal associations between formulated signals and their templates, are the rationale behind the development of the Cotangent Similarity Measure

(Cot SM)-based analysis framework. Raw similarity indices, which provide numeric magnitude but lack interpretive depth or contextual discernment, are used in traditional pattern recognition or signal analysis techniques. By transforming tabular similarity values into multi-modal visualizations, such as heatmaps, normalized surface, and PCA scatter projections, the current structure fills these gaps with three main objectives: to establish a single platform that simultaneously takes into account numerical, functional, and spatial views of similarity on the same platform; to make the platform more interpretable; to uncover hidden behavior structures; and to quantify representativeness, consistency, and variability between templates ($T_1 - T_4$). This allows for the identification of which templates are significant contributors to the signal space and which are redundant or noisy. By achieving these goals, the Cot SM framework provides a more thorough comprehension of behavioral relationships between templates, bridges the gap between quantitative computation and qualitative interpretation, and lays the groundwork for future research that will expand to higher-dimensional, time-varying, and neutrosophically enriched analytical models.

1.3. Novelty

In this work, the amplitude and phase components of truth, indeterminacy, and falsity are taken together, reformulating and generalizing conventional soft-set operations in a Complex Double-Valued Neutrosophic (CDVN) environment. This makes the work innovative. Previous studies only described the operations in real-valved or single-complex space, which led to skewed and biased representations of uncertainty. On the other hand, the proposed CDVNS framework offers a framework of a generalization of phase-dependent uncertainty modeling to fine-grained differentiation between the information sources with oscillatory or incompatible qualities. It also presents rules of bidirectional aggregation (maximum minimum based) that pair real and imaginary values of neutrosophic components in a logically consistent manner, as well as complementary and dual as the union-intersection and AND-OR operators. A complex-valued multidimensional calculus of uncertainty, a new analytical tool for mathematical theory and intelligent systems applications, is a conceptual departure from standard neutrosophic soft operations. In order to investigate signal-template interactions across several analytical faces, the study uses functional visualization techniques on a Cotangent Similarity Matrix (Cot SM). This employs multi-modal evaluations, which include row-wise normalization and correlation polarity to capture the direction and strength of the relationship between templates, spline-based functional smoothing, and PCA-based topological mapping to capture the direction and time dynamics of the inter-template relationship. This is in contrast to other conventional methods of similarity evaluation that use a single index, or linear correlation.
The CDVNS-Cot SM integration is an effective paradigm of hybrid logical-functional analysis because of its hybrid visualization pipeline, which uses Heatmaps, 3D surface plots, and PCA clusters to synchronously visualize the magnitude of similarities onto the geometric topology; bidirectional polarity analysis, which allows the simultaneous visualization of positive and negative correlations (e.g., T_4S_3= +0.91, T_4S_2= -0.98) using the same interpretive space; and normalization symmetry, which is achieved through the use of row Together.

2. Preliminaries

Some fundamental operations that are definitely required for the following sections are demonstrated in this section.

Definition 1. *[41] The definition of a neutrosophic set $\mathcal{A}$ on $\mathbf{X}$ is:*

$$A = \{\langle \mathbf{x}, \mathcal{T}_{\mathcal{A}}(\mathbf{x}), \mathcal{I}_{\mathcal{A}}(\mathbf{x}), \mathcal{F}_{A}(\mathbf{x})\rangle : \mathbf{x} \in \mathbf{X}\}$$

where, $\mathcal{T}$, $\mathcal{I}$, $\mathcal{F} : \mathbf{X} \longrightarrow]0, 1[$ and $0 \leq \mathcal{T}_A(\mathbf{x}) + \mathcal{I}_A(\mathbf{x}) + \mathcal{F}_A(\mathbf{x}) \leq 3$.

Definition 2. *[42] Suppose $\mathcal{E}$ be a collection of all parameters, $P(\mathbf{X})$ be the powerset of $\mathbf{X}$, and $\mathbf{X}$ be an initial universe. Pair of $(\tilde{\mathbb{F}}, \mathcal{E})$ is called a soft set over $\mathbf{X}$, if the mapping $\tilde{\mathbb{F}}$ is provided by $\tilde{\mathbb{F}} : \mathcal{E} \longrightarrow P(\mathbf{X})$. Stated otherwise, the set$\mathbf{X}$ has a parameterized family of subsets, which is the soft set. The set of $\mathfrak{e}$-elements of the soft set $(\tilde{\mathbb{F}}, \mathcal{E})$ or the set of $\mathfrak{e}$-approximate elements of the soft set can be regarded as $\mathfrak{e}$ for $\mathfrak{e} \in \mathcal{E}, \tilde{\mathbb{F}}(\mathfrak{e})$.i.e.,*

$$(\tilde{\mathbb{F}}, \mathcal{E}) = \{(\mathfrak{e}, \tilde{\mathbb{F}}(\mathfrak{e})) : \mathfrak{e} \in \mathcal{E}, \tilde{\mathbb{F}} : \mathcal{E} \longrightarrow P(\mathbf{X})\}$$

First, Maji [43] defined the neutrosophic soft set. Deli and Broumi [44] subsequently refined this idea, as seen below:

Definition 3. *Let $\mathcal{E}$ be a set of all parameters, and $\mathbf{X}$ be a universe set. The collection of all neutrosophic sets of $\mathbf{X}$ is represented by $P(\mathbf{X})$. Then, a neutrosophic soft set $(\tilde{\mathbb{F}}, \mathcal{E})$ over $\mathbf{X}$ is a set defined by a set valued function $\tilde{\mathbb{F}}$ that represents a mapping $\tilde{\mathbb{F}} : \mathcal{E} \longrightarrow P(\mathbf{X})$, where $\tilde{\mathbb{F}}$ is referred to as an approximate function of neutrosophic soft set $(\tilde{\mathbb{F}}, \mathcal{E})$. Put differently, the neutrosophic soft set can be expressed as a set of order pairs since it is a parameterized family of certain elements of the set $P(\mathbf{X})$.*

$$(\tilde{\mathbb{F}}, \mathcal{E}) = \{(\mathfrak{e}, \langle x, \mathcal{T}_{\tilde{\mathbb{F}}(\mathfrak{e})}(\mathbf{x}), \mathcal{I}_{\tilde{\mathbb{F}}(\mathfrak{e})}(\mathbf{x}), \mathcal{F}_{\tilde{\mathbb{F}}(\mathfrak{e})}(\mathbf{x})\rangle : \mathbf{x} \in \mathbf{X}) : \mathfrak{e} \in \mathcal{E}\}$$

where $\mathcal{T}_{\tilde{\mathbb{F}}(\mathfrak{e})}(\mathbf{x}), \mathcal{T}_{\tilde{\mathbb{F}}(\mathfrak{e})}(\mathbf{x}), \mathcal{F}_{\tilde{\mathbb{F}}(\mathfrak{e})}(\mathbf{x}) \in [0, 1]$ known as the truth-membership, indeterminacy-membership, and falsity-membership thereof. $\tilde{\mathbb{F}}(\mathfrak{e})$. Given that the supremum of each$\mathcal{T}$, $\mathcal{I}$, $\mathcal{F}$ is 1 so the inequality $0 \leq \mathcal{T}_{\tilde{\mathbb{F}}(\mathfrak{e})}(\mathbf{x}) + \mathcal{I}_{\tilde{\mathbb{F}}(\mathfrak{e})}(\mathbf{x}) + \mathcal{F}_{\tilde{\mathbb{F}}(\mathfrak{e})}(\mathbf{x}) \leq 3$ is evident.

Definition 4. *[45] Consider the neutrosophic soft set $(\tilde{\mathbb{F}}, \mathcal{E})$ over the universe set $\mathbf{X}$. $(\tilde{\mathbb{F}}, \mathcal{E})^c$ represents the complement of $(\tilde{\mathbb{F}}, \mathcal{E})$, which is defined by:*

$$(\tilde{\mathbb{F}}, \mathcal{E})^c = \{(\mathfrak{e}, \langle \mathbf{x}, \mathcal{F}_{\tilde{\mathbb{F}}(\mathfrak{e})}(\mathbf{x}), 1 - \mathcal{I}_{\tilde{\mathbb{F}}(\mathfrak{e})}(\mathbf{x}), \mathcal{T}_{\tilde{\mathbb{F}}(\mathfrak{e})}(\mathbf{x})\rangle : \mathbf{x} \in \mathbf{X}) : \mathfrak{e} \in \mathcal{E}\}$$

Obviously,, $((\tilde{\mathbb{F}}, \mathcal{E})^c)^c = (\tilde{\mathbb{F}}, \mathcal{E})$.

Definition 5. *[43] Suppose that $(\tilde{\mathbb{F}}, \mathcal{E})$ and $(\tilde{\mathbb{G}}, \mathcal{E})$ be neutrosophic soft sets over the universe $\mathbf{X}$. $(\tilde{\mathbb{F}}, \mathcal{E})$ is claimed to be neutrosophic soft subset of $(\tilde{\mathbb{G}}, \mathcal{E})$ if $\mathcal{T}_{\tilde{\mathbb{F}}(\mathfrak{e})}(\mathbf{x}) \leq \mathcal{T}_{\tilde{G}(\mathfrak{e})}(\mathbf{x}), \mathcal{I}_{\tilde{\mathbb{F}}(\mathfrak{e})}(\mathbf{x}) \leq \mathcal{I}_{\tilde{G}(\mathfrak{e})}(\mathbf{x}), \mathcal{F}_{\tilde{\mathbb{F}}(\mathfrak{e})}(\mathbf{x}) \geq \mathcal{F}_{\tilde{G}(\mathfrak{e})}(\mathbf{x})$, for all $\mathfrak{e} \in \mathcal{E}$, $\forall\ \mathbf{x} \in \mathbf{X}$. It is represented by $(\tilde{\mathbb{F}}, \mathcal{E}) \subseteq (\tilde{\mathbb{G}}, \mathcal{E})$. $(\tilde{\mathbb{F}}, \mathcal{E})$ is known to be neutrosophic soft set equal to $(\tilde{\mathbb{G}}, \mathcal{E})$ if $(\tilde{\mathbb{F}}, \mathcal{E})$ is neutrosophic soft subset of $(\tilde{\mathbb{G}}, \mathcal{E})$ and $(\tilde{\mathbb{G}}, \mathcal{E})$ is neutrosophic soft subset of $(\tilde{\mathbb{F}}, \mathcal{E})$. It is represented by $(\tilde{\mathbb{F}}, \mathcal{E}) = (\tilde{\mathbb{G}}, \mathcal{E})$.*

Definition 6. *[46] Assume that $\mathcal{E}$ be the parameters set and $\mathcal{M}$ be the key set. Let $P(\mathcal{M})$ represent the power set of $\mathcal{M}$. Then, a QPNS soft set $(\tilde{\mathbb{F}}, \mathcal{E})$ over $\mathcal{M}$ is a mapping $\tilde{\mathbb{F}} : \mathfrak{e} \to P(\mathcal{M})$, where $\tilde{\mathbb{F}}$ is the function of the quadri-partitioned neutrosophic soft set $(\tilde{\mathbb{F}}, \mathcal{E})$. In a symbolic sense,*

$$(\tilde{\mathbb{F}}, \mathcal{E}) = \left\{ \left(\mathfrak{e}, \langle \mathrm{s}, AbT_{\tilde{\mathbb{F}}(\mathfrak{e})}(\mathrm{s}), ReT_{\tilde{\mathbb{F}}(\mathfrak{e})}(\mathrm{s}), ReF_{\tilde{\mathbb{F}}(\mathfrak{e})}(\mathrm{s}), AbF_{\tilde{\mathbb{F}}(\mathfrak{e})}(\mathrm{s}) \rangle \right) : \mathrm{s} \in \mathcal{M}, \mathfrak{e} \in \mathcal{E} \right\}.$$

Here, $AbT_{\tilde{\mathbb{F}}(\mathfrak{e})}(\mathrm{s})$, $ReT_{\tilde{\mathbb{F}}(\mathfrak{e})}(\mathrm{s})$, $ReF_{\tilde{\mathbb{F}}(\mathfrak{e})}(\mathrm{s})$, and $AbF_{\tilde{\mathbb{F}}(\mathfrak{e})}(\mathrm{s})$ belong to the $[0, 1]$ interval. The functions of $\tilde{\mathbb{F}}, (\mathfrak{e})$ are referred to as absolute true-membership, relative true-membership, relative false-membership, and absolute false-membership, respectively. The following inequality is true since each function's supremum is 1 and its infimum is 0.

$$0 \leq AbT_{\tilde{\mathbb{F}}(\mathfrak{e})}(\mathrm{s}) + ReT_{\tilde{\mathbb{F}}(\mathfrak{e})}(\mathrm{s}) + ReF_{\tilde{\mathbb{F}}(\mathfrak{e})}(\mathrm{s}) + AbF_{\tilde{\mathbb{F}}(\mathfrak{e})}(\mathrm{s}) \leq 4.$$

Definition 7. *[46] Consider $(\tilde{\mathbb{F}}, \mathcal{E})$ be a QPNS set over the key set $\mathcal{M}$. Then, $(\tilde{\mathbb{F}}, \mathcal{E})^c$ represents the complement of $(\tilde{\mathbb{F}}, \mathcal{E})$, which has the following definition:*

$$(\tilde{\mathbb{F}}, \mathcal{E})^c = \left\{ \left(\mathfrak{e}, \langle \mathrm{s}, AbF_{\tilde{\mathbb{F}}(\mathfrak{e})}(\mathrm{s}), ReF_{\tilde{\mathbb{F}}(\mathfrak{e})}(\mathrm{s}), ReT_{\tilde{\mathbb{F}}(\mathfrak{e})}(\mathrm{s}), AbT_{\tilde{\mathbb{F}}(\mathfrak{e})}(\mathrm{s}) \rangle \right) : \mathrm{s} \in \mathcal{M}, \mathfrak{e} \in \mathcal{E} \right\}.$$

Consequently, $\left((\tilde{\mathbb{F}}, \mathcal{E})^c\right)^c = (\tilde{\mathbb{F}}, \mathcal{E})$.

Definition 8. *[46] Consider two QPNS sets over the key set $\mathcal{M}$: $(\tilde{\mathbb{F}},\mathcal{E})$ and $(\tilde{\mathbb{G}},\mathcal{E})$. Then, $(\tilde{\mathbb{F}},\mathcal{E})\subseteq(\tilde{\mathbb{G}},\mathcal{E})$ if*

$$\begin{aligned}
AbT_{\tilde{\mathbb{F}}(\mathfrak{e})}(\mathrm{s}) &\leq AbT_{\tilde{\mathbb{G}}(\mathfrak{e})}(\mathrm{s}),\\
ReT_{\tilde{\mathbb{F}}(\mathfrak{e})}(\mathrm{s}) &\leq ReT_{\tilde{\mathbb{G}}(\mathfrak{e})}(\mathrm{s}),\\
ReF_{\tilde{\mathbb{F}}(\mathfrak{e})}(\mathrm{s}) &\geq ReF_{\tilde{\mathbb{G}}(\mathfrak{e})}(\mathrm{s}),\\
AbF_{\tilde{\mathbb{F}}(\mathfrak{e})}(\mathrm{s}) &\geq AbF_{\tilde{\mathbb{G}}(\mathfrak{e})}(\mathrm{s}),
\end{aligned}$$

$\forall\ \mathfrak{e}\in\mathcal{E}$ and $\mathrm{s}\in\mathcal{M}$. If $(\tilde{\mathbb{F}},\mathcal{E})\subseteq(\tilde{\mathbb{G}},\mathcal{E})$ and $(\tilde{\mathbb{F}},\mathcal{E})\supseteq(\tilde{\mathbb{G}},\mathcal{E})$, then $(\tilde{\mathbb{F}},\mathcal{E})=(\tilde{\mathbb{G}},\mathcal{E})$.

Definition 9. *[46] Suppose $(\tilde{\mathbb{F}},\mathcal{E})$ and $(\tilde{\mathbb{G}},\mathcal{E})$ be two QPNS sets over the key set $\mathcal{M}$ such that $(\tilde{\mathbb{F}},\mathcal{E})\neq(\tilde{\mathbb{G}},\mathcal{E})$. Then, $(\tilde{\mathbb{F}},\mathcal{E})\cup(\tilde{\mathbb{G}},\mathcal{E})=(\tilde{\mathbb{H}},\mathcal{E})$*

$$(\tilde{\mathbb{H}},\mathcal{E})=\left\{\left(\mathfrak{e},\langle \mathrm{s},AbT_{\tilde{\mathbb{H}}(\mathfrak{e})}(\mathrm{s}),ReT_{\tilde{\mathbb{H}}(\mathfrak{e})}(\mathrm{s}),ReF_{\tilde{\mathbb{H}}(\mathfrak{e})}(\mathrm{s}),AbF_{\tilde{\mathbb{H}}(\mathfrak{e})}(\mathrm{s})\rangle\right):\mathrm{s}\in\mathcal{M},\mathfrak{e}\in\mathcal{E}\right\}.$$

where

$$\begin{aligned}
AbT_{\tilde{\mathbb{H}}(\mathfrak{e})}(\mathrm{s}) &= \max\left\{AbT_{\tilde{\mathbb{F}}(\mathfrak{e})}(\mathrm{s}),AbT_{\tilde{\mathbb{G}}(\mathfrak{e})}(\mathrm{s})\right\},\\
ReT_{\tilde{\mathbb{H}}(\mathfrak{e})}(\mathrm{s}) &= \max\left\{ReT_{\tilde{\mathbb{F}}(\mathfrak{e})}(\mathrm{s}),ReT_{\tilde{\mathbb{G}}(\mathfrak{e})}(\mathrm{s})\right\},\\
ReF_{\tilde{\mathbb{H}}(\mathfrak{e})}(\mathrm{s}) &= \min\left\{ReF_{\tilde{\mathbb{F}}(\mathfrak{e})}(\mathrm{s}),ReF_{\tilde{\mathbb{G}}(\mathfrak{e})}(\mathrm{s})\right\},\\
AbF_{\tilde{\mathbb{H}}(\mathfrak{e})}(\mathrm{s}) &= \min\left\{AbF_{\tilde{\mathbb{F}}(\mathfrak{e})}(\mathrm{s}),AbF_{\tilde{\mathbb{G}}(\mathfrak{e})}(\mathrm{s})\right\}.
\end{aligned}$$

Definition 10. *[46] Consider two QPNS sets over the key set $\mathcal{M}$, $(\tilde{\mathbb{F}},\mathcal{E})$ and $(\tilde{\mathbb{G}},\mathcal{E})$, such that $(\tilde{\mathbb{F}},\mathcal{E})\neq(\tilde{\mathbb{G}},\mathcal{E})$. Then, $(\tilde{\mathbb{F}},\mathcal{E})\cap(\tilde{\mathbb{G}},\mathcal{E})=(\tilde{\mathbb{H}},\mathcal{E})$ represents their intersection, which is defined as follows:*

$$(\tilde{\mathbb{H}},\mathcal{E})=\left\{\left(\mathfrak{e},\langle \mathrm{s},AbT_{\tilde{\mathbb{H}}(\mathfrak{e})}(\mathrm{s}),ReT_{\tilde{\mathbb{H}}(\mathfrak{e})}(\mathrm{s}),ReF_{\tilde{\mathbb{H}}(\mathfrak{e})}(\mathrm{s}),AbF_{\tilde{\mathbb{H}}(\mathfrak{e})}(\mathrm{s})\rangle\right):\mathrm{s}\in\mathcal{M},\mathfrak{e}\in\mathcal{E}\right\}.$$

where

$$\begin{aligned}
AbT_{\tilde{\mathbb{H}}(\mathfrak{e})}(\mathrm{s}) &= \min\left\{AbT_{\tilde{\mathbb{F}}(\mathfrak{e})}(\mathrm{s}),AbT_{\tilde{\mathbb{G}}(\mathfrak{e})}(\mathrm{s})\right\},\\
ReT_{\tilde{\mathbb{H}}(\mathfrak{e})}(\mathrm{s}) &= \min\left\{ReT_{\tilde{\mathbb{F}}(\mathfrak{e})}(\mathrm{s}),ReT_{\tilde{\mathbb{G}}(\mathfrak{e})}(\mathrm{s})\right\},\\
ReF_{\tilde{\mathbb{H}}(\mathfrak{e})}(\mathrm{s}) &= \max\left\{ReF_{\tilde{\mathbb{F}}(\mathfrak{e})}(\mathrm{s}),ReF_{\tilde{\mathbb{G}}(\mathfrak{e})}(\mathrm{s})\right\},\\
AbF_{\tilde{\mathbb{H}}(\mathfrak{e})}(\mathrm{s}) &= \max\left\{AbF_{\tilde{\mathbb{F}}(\mathfrak{e})}(\mathrm{s}),AbF_{\tilde{\mathbb{G}}(\mathfrak{e})}(\mathrm{s})\right\}.
\end{aligned}$$

Definition 11. *[46] Consider two QPNS sets over the key set $\mathcal{M}$, $(\tilde{\mathbb{F}},\mathcal{E})$ and $(\tilde{\mathbb{G}},\mathcal{E})$, such that $(\tilde{\mathbb{F}},\mathcal{E})\neq(\tilde{\mathbb{G}},\mathcal{E})$. Then, $(\tilde{\mathbb{H}},\mathcal{E})=(\tilde{\mathbb{F}},\mathcal{E})\setminus(\tilde{\mathbb{G}},\mathcal{E})$ represents their difference, which is defined as follows:*

$$(\tilde{\mathbb{H}},\mathcal{E})=(\tilde{\mathbb{F}},\mathcal{E})\cap(\tilde{\mathbb{G}},\mathcal{E})^{c},$$

like that

$$(\tilde{\mathbb{H}},\mathcal{E})=\left\{\left(\mathfrak{e},\langle \mathrm{s},AbT_{\tilde{\mathbb{H}}(\mathfrak{e})}(\mathrm{s}),ReT_{\tilde{\mathbb{H}}(\mathfrak{e})}(\mathrm{s}),ReF_{\tilde{\mathbb{H}}(\mathfrak{e})}(\mathrm{s}),AbF_{\tilde{\mathbb{H}}(\mathfrak{e})}(\mathrm{s})\rangle\right):\mathrm{s}\in\mathcal{M},\mathfrak{e}\in\mathcal{E}\right\}.$$

where

$$AbT_{\tilde{\mathbb{H}}(\mathfrak{e})}(\mathrm{s}) = \min\left\{AbT_{\tilde{\mathbb{F}}(\mathfrak{e})}(\mathrm{s}),AbF_{\tilde{\mathbb{G}}(\mathfrak{e})}(\mathrm{s})\right\},$$

$$ReT_{\tilde{\mathbb{H}}(\mathfrak{e})}(\mathrm{s}) = \min\left\{ReT_{\tilde{\mathbb{F}}(\mathfrak{e})}(\mathrm{s}), ReF_{\tilde{\mathbb{G}}(\mathfrak{e})}(\mathrm{s})\right\},$$
$$ReF_{\tilde{\mathbb{H}}(\mathfrak{e})}(\mathrm{s}) = \max\left\{ReF_{\tilde{\mathbb{F}}(\mathfrak{e})}(\mathrm{s}), ReT_{\tilde{\mathbb{G}}(\mathfrak{e})}(\mathrm{s})\right\},$$
$$AbF_{\tilde{\mathbb{H}}(\mathfrak{e})}(\mathrm{s}) = \max\left\{AbF_{\tilde{\mathbb{F}}(\mathfrak{e})}(\mathrm{s}), AbT_{\tilde{\mathbb{G}}(\mathfrak{e})}(\mathrm{s})\right\}.$$

Definition 12. *[46] Assume* $\{(\tilde{\mathbb{F}}_{\mathfrak{i}}, \mathcal{E}) : \mathfrak{i} \in \mathrm{I}\}$ *be a family of neutrosophic soft sets over the key set* $\mathcal{M}$ *that are QP. The following is a definition of this family's union and intersection:*

$$\bigcup_{\mathfrak{i}\in\mathrm{I}}(\tilde{\mathbb{F}}_{\mathfrak{i}}, \mathcal{E}) = \left\{\left(\mathfrak{e}, \langle \mathrm{s}, \sup_{\mathfrak{i}\in\mathrm{I}} AbT_{\tilde{\mathbb{F}}_{\mathfrak{i}(\mathfrak{e})}}(\mathrm{s}), \sup_{\mathfrak{i}\in\mathrm{I}} ReT_{\tilde{\mathbb{F}}_{\mathfrak{i}(\mathfrak{e})}}(\mathrm{s}), \inf_{\mathfrak{i}\in\mathrm{I}} ReF_{\tilde{\mathbb{F}}_{\mathfrak{i}(\mathfrak{e})}}(\mathrm{s}), \inf_{\mathfrak{i}\in\mathrm{I}} AbF_{\tilde{\mathbb{F}}_{\mathfrak{i}(\mathfrak{e})}}(\mathrm{s})\rangle\right) : \mathrm{s}\in\mathcal{M}, \mathfrak{e}\in\mathcal{E}\right\}.$$

$$\bigcap_{\mathfrak{i}\in\mathrm{I}}(\tilde{\mathbb{F}}_{\mathfrak{i}}, \mathcal{E}) = \left\{\left(\mathfrak{e}, \langle \mathrm{s}, \inf_{\mathfrak{i}\in\mathrm{I}} AbT_{\tilde{\mathbb{F}}_{\mathfrak{i}(\mathfrak{e})}}(\mathrm{s}), \inf_{\mathfrak{i}\in\mathrm{I}} ReT_{\tilde{\mathbb{F}}_{\mathfrak{i}(\mathfrak{e})}}(\mathrm{s}), \sup_{\mathfrak{i}\in\mathrm{I}} ReF_{\tilde{\mathbb{F}}_{\mathfrak{i}(\mathfrak{e})}}(\mathrm{s}), \sup_{\mathfrak{i}\in\mathrm{I}} AbF_{\tilde{\mathbb{F}}_{\mathfrak{i}(\mathfrak{e})}}(\mathrm{s})\rangle\right) : \mathrm{s}\in\mathcal{M}, \mathfrak{e}\in\mathcal{E}\right\}.$$

3. Complex Double-Valued Neutrosophic Soft Operations

This section defines the union, intersection, difference, AND, and OR operations on CDVNS sets. Basic characteristics of these operations are also exhibits.

Definition 13. *It is assumed that* $(\tilde{\mathbb{F}}_1, \mathcal{E})$ *and* $(\tilde{\mathbb{F}}_2, \mathcal{E})$ *be CDVNS sets over the* $\mathbf{X}$ *universe set. Then,* $(\tilde{\mathbb{F}}_1, \mathcal{E}) \cup (\tilde{\mathbb{F}}_2, \mathcal{E}) = (\tilde{\mathbb{F}}_3, \mathcal{E})$ *represents their union. It is given by:*

$$(\tilde{\mathbb{F}}_3, \mathcal{E}) = \left\{\left(\mathfrak{e}, \langle \mathbf{x}, \mathcal{T}_{\tilde{\mathbb{F}}_3(\mathfrak{e})}(\mathbf{x}), \mathcal{RT}_{\tilde{\mathbb{F}}_3(\mathfrak{e})}(\mathbf{x}), \mathcal{RF}_{\tilde{\mathbb{F}}_3(\mathfrak{e})}(\mathbf{x}), \mathcal{F}_{\tilde{\mathbb{F}}_3(\mathfrak{e})}(\mathbf{x})\rangle : \mathbf{x}\in\mathbf{X}\right) : \mathfrak{e}\in\mathcal{E}\right\},$$

Where

$$\mathcal{T}_{\tilde{\mathbb{F}}_3(\mathfrak{e})}(\mathbf{x}) = \max\{\mathcal{T}_{\tilde{\mathbb{F}}_1(\mathfrak{e})}(\mathbf{x}), \mathcal{T}_{\tilde{\mathbb{F}}_2(\mathfrak{e})}(\mathbf{x})\}$$
$$\mathcal{RT}_{\tilde{\mathbb{F}}_3(\mathfrak{e})}(\mathbf{x}) = \max\{\mathcal{RT}_{\tilde{\mathbb{F}}_1(\mathfrak{e})}(\mathbf{x}), \mathcal{RT}_{\tilde{\mathbb{F}}_2(\mathfrak{e})}(\mathbf{x})\}$$
$$\mathcal{RF}_{\tilde{\mathbb{F}}_3(\mathfrak{e})}(\mathbf{x}) = \min\{\mathcal{RF}_{\tilde{\mathbb{F}}_1(\mathfrak{e})}(\mathbf{x}), \mathcal{RF}_{\tilde{\mathbb{F}}_2(\mathfrak{e})}(\mathbf{x})\}$$
$$\mathcal{F}_{\tilde{\mathbb{F}}_3(\mathfrak{e})}(\mathbf{x}) = \min\{\mathcal{F}_{\tilde{\mathbb{F}}_1(\mathfrak{e})}(\mathbf{x}), \mathcal{F}_{\tilde{\mathbb{F}}_2(\mathfrak{e})}(\mathbf{x})\}$$

Definition 14. *It is assumed that* $(\tilde{\mathbb{F}}_1, \mathcal{E})$ *and* $(\tilde{\mathbb{F}}_2, \mathcal{E})$ *be two CDVNS sets over the* $\mathbf{X}$ *universe set. Then,* $(\tilde{\mathbb{F}}_1, \mathcal{E}) \cap (\tilde{\mathbb{F}}_2, \mathcal{E}) = (\tilde{\mathbb{F}}_3, \mathcal{E})$ *represents their intersection. Then definition is:*

$$(\tilde{\mathbb{F}}_3, \mathcal{E}) = \left\{\left(\mathfrak{e}, \langle \mathbf{x}, \mathcal{T}_{\tilde{\mathbb{F}}_3(\mathfrak{e})}(\mathbf{x}), \mathcal{RT}_{\tilde{\mathbb{F}}_3(\mathfrak{e})}(\mathbf{x}), \mathcal{RF}_{\tilde{\mathbb{F}}_3(\mathfrak{e})}(\mathbf{x}), \mathcal{F}_{\tilde{\mathbb{F}}_3(\mathfrak{e})}(\mathbf{x})\rangle : \mathbf{x}\in\mathbf{X}\right) : \mathfrak{e}\in\mathcal{E}\right\},$$

Where

$$\mathcal{T}_{\tilde{\mathbb{F}}_3(\mathfrak{e})}(\mathbf{x}) = \min\{\mathcal{T}_{\tilde{\mathbb{F}}_1(\mathfrak{e})}(\mathbf{x}), \mathcal{T}_{\tilde{\mathbb{F}}_2(\mathfrak{e})}(\mathbf{x})\}$$
$$\mathcal{RT}_{\tilde{\mathbb{F}}_3(\mathfrak{e})}(\mathbf{x}) = \min\{\mathcal{RT}_{\tilde{\mathbb{F}}_1(\mathfrak{e})}(\mathbf{x}), \mathcal{RT}_{\tilde{\mathbb{F}}_2(\mathfrak{e})}(\mathbf{x})\}$$
$$\mathcal{RF}_{\tilde{\mathbb{F}}_3(\mathfrak{e})}(\mathbf{x}) = \max\{\mathcal{RF}_{\tilde{\mathbb{F}}_1(\mathfrak{e})}(\mathbf{x}), \mathcal{RF}_{\tilde{\mathbb{F}}_2(\mathfrak{e})}(\mathbf{x})\}$$
$$\mathcal{F}_{\tilde{\mathbb{F}}_3(\mathfrak{e})}(\mathbf{x}) = \max\{\mathcal{F}_{\tilde{\mathbb{F}}_1(\mathfrak{e})}(\mathbf{x}), \mathcal{F}_{\tilde{\mathbb{F}}_2(\mathfrak{e})}(\mathbf{x})\}$$

Definition 15. *Consider* $(\tilde{\mathbb{F}}_1, \mathcal{E})$ *and* $(\tilde{\mathbb{F}}_2, \mathcal{E})$ *be CDVNS sets over the universe set* $\mathbf{X}$*. So,* $(\tilde{\mathbb{F}}_1, \mathcal{E})$ *difference* $(\tilde{\mathbb{F}}_2, \mathcal{E})$ *operation on them is represented as* $(\tilde{\mathbb{F}}_1, \mathcal{E}) \setminus (\tilde{\mathbb{F}}_2, \mathcal{E}) = (\tilde{\mathbb{F}}_3, \mathcal{E})$ *and is given by* $(\tilde{\mathbb{F}}_3, \mathcal{E}) = (\tilde{\mathbb{F}}_1, \mathcal{E}) \cap (\tilde{\mathbb{F}}_2, \mathcal{E})^c$ *as follows:*

$$(\tilde{\mathbb{F}}_3, \mathcal{E}) = \left\{\left(\mathfrak{e}, \langle \mathbf{x}, \mathcal{T}_{\tilde{\mathbb{F}}_3(\mathfrak{e})}(\mathbf{x}), \mathcal{RT}_{\tilde{\mathbb{F}}_3(\mathfrak{e})}(\mathbf{x}), \mathcal{RF}_{\tilde{\mathbb{F}}_3(\mathfrak{e})}(\mathbf{x}), \mathcal{F}_{\tilde{\mathbb{F}}_3(\mathfrak{e})}(\mathbf{x})\rangle : \mathbf{x}\in\mathbf{X}\right) : \mathfrak{e}\in\mathcal{E}\right\},$$

where

$$\mathcal{T}_{\tilde{\mathbb{F}}_3(\mathfrak{e})}(\mathbf{x}) = \min\{\mathcal{T}_{\tilde{\mathbb{F}}_1(\mathfrak{e})}(\mathbf{x}), \mathcal{F}_{\tilde{\mathbb{F}}_2(\mathfrak{e})}(\mathbf{x})\}$$
$$\mathcal{RT}_{\tilde{\mathbb{F}}_3(\mathfrak{e})}(\mathbf{x}) = \min\{\mathcal{RT}_{\tilde{\mathbb{F}}_1(\mathfrak{e})}(\mathbf{x}), \mathcal{RF}_{\tilde{\mathbb{F}}_2(\mathfrak{e})}(\mathbf{x})\}$$
$$\mathcal{RF}_{\tilde{\mathbb{F}}_3(\mathfrak{e})}(\mathbf{x}) = \max\{\mathcal{RF}_{\tilde{\mathbb{F}}_1(\mathfrak{e})}(\mathbf{x}), \mathcal{RT}_{\tilde{\mathbb{F}}_2(\mathfrak{e})}(\mathbf{x})\}$$
$$\mathcal{F}_{\tilde{\mathbb{F}}_3(\mathfrak{e})}(\mathbf{x}) = \max\{\mathcal{F}_{\tilde{\mathbb{F}}_1(\mathfrak{e})}(\mathbf{x}), \mathcal{T}_{\tilde{\mathbb{F}}_2(\mathfrak{e})}(\mathbf{x})\}$$

Definition 16. *For the universe set* $\mathbf{X}$*, suppose* $\{(\tilde{\mathbb{F}}_\mathfrak{i}, \mathcal{E}) : \mathfrak{i} \in \mathrm{I}\}$ *be a family of CDVNS sets. Next,*

$$\bigcup_{\mathfrak{i}\in\mathrm{I}}(\tilde{\mathbb{F}}_\mathfrak{i}, \mathcal{E}) = \left\{ \left(\mathfrak{e}, \langle \mathbf{x}, \sup_{\mathfrak{i}\in\mathrm{I}} \mathcal{T}_{\tilde{\mathbb{F}}_{\mathfrak{i}(\mathfrak{e})}}(\mathbf{x}), \sup_{\mathfrak{i}\in\mathrm{I}} \mathcal{RT}_{\tilde{\mathbb{F}}_{\mathfrak{i}(\mathfrak{e})}}(\mathbf{x}), \inf_{\mathfrak{i}\in\mathrm{I}} \mathcal{RF}_{\tilde{\mathbb{F}}_{\mathfrak{i}(\mathfrak{e})}}(\mathbf{x}), \inf_{\mathfrak{i}\in\mathrm{I}} \mathcal{F}_{\tilde{\mathbb{F}}_{\mathfrak{i}(\mathfrak{e})}}(\mathbf{x}) \rangle : \mathbf{x} \in \mathbf{X} \right) : \mathfrak{e} \in \mathcal{E} \right\}.$$

$$\bigcap_{\mathfrak{i}\in\mathrm{I}}(\tilde{\mathbb{F}}_\mathfrak{i}, \mathcal{E}) = \left\{ \left(\mathfrak{e}, \langle \mathbf{x}, \inf_{\mathfrak{i}\in\mathrm{I}} \mathcal{T}_{\tilde{\mathbb{F}}_{\mathfrak{i}(\mathfrak{e})}}(\mathbf{x}), \inf_{\mathfrak{i}\in\mathrm{I}} \mathcal{RT}_{\tilde{\mathbb{F}}_{\mathfrak{i}(\mathfrak{e})}}(\mathbf{x}), \sup_{\mathfrak{i}\in\mathrm{I}} \mathcal{RF}_{\tilde{\mathbb{F}}_{\mathfrak{i}(\mathfrak{e})}}(\mathbf{x}), \sup_{\mathfrak{i}\in\mathrm{I}} \mathcal{F}_{\tilde{\mathbb{F}}_{\mathfrak{i}(\mathfrak{e})}}() \rangle : \mathbf{x} \in \mathbf{X} \right) : \mathfrak{e} \in \mathcal{E} \right\}.$$

Definition 17. *Consider the CDVNS sets over the universe set* $\mathbf{X}$*:* $(\tilde{\mathbb{F}}_1, \mathcal{E})$ *and* $(\tilde{\mathbb{F}}_2, \mathcal{E})$*. Then, the AND operation on them is represented by* $(\tilde{\mathbb{F}}_1, \mathcal{E}) \wedge (\tilde{\mathbb{F}}_2, \mathcal{E}) = (\tilde{\mathbb{F}}_3, \mathcal{E} \times \mathcal{E})$ *and is described as follows:*

$$(\tilde{\mathbb{F}}, \mathcal{E} \times \mathcal{E}) = \left\{ \left((\mathfrak{e}_1, \mathfrak{e}_2), \langle \mathbf{x}, \mathcal{T}_{\tilde{\mathbb{F}}_3(\mathfrak{e}_1,\mathfrak{e}_2)}(\mathbf{x}), \mathcal{RT}_{\tilde{\mathbb{F}}_3(\mathfrak{e}_1,\mathfrak{e}_2)}(\mathbf{x}), \right.\right.$$
$$\left.\left. \mathcal{RF}_{\tilde{\mathbb{F}}_3(\mathfrak{e}_1,\mathfrak{e}_2)}(\mathbf{x}), \mathcal{F}_{\tilde{\mathbb{F}}_3(\mathfrak{e}_1,\mathfrak{e}_2)}(\mathbf{x}) \rangle : \mathbf{x} \in \mathbf{X} \right) : (\mathfrak{e}_1, \mathfrak{e}_2) \in \mathcal{E} \times \mathcal{E} \right\}.$$

where

$$\mathcal{T}_{\tilde{\mathbb{F}}_3(\mathfrak{e}_1,\mathfrak{e}_2)}(\mathbf{x}) = \min\left\{ \mathcal{T}_{\tilde{\mathbb{F}}_1(\mathfrak{e}_1,\mathfrak{e}_2)}(\mathbf{x}), \mathcal{T}_{\tilde{\mathbb{F}}_2(\mathfrak{e}_1,\mathfrak{e}_2)}(\mathbf{x}) \right\},$$
$$\mathcal{RT}_{\tilde{\mathbb{F}}_3(\mathfrak{e}_1,\mathfrak{e}_2)}(\mathbf{x}) = \min\left\{ \mathcal{RT}_{\tilde{\mathbb{F}}_1(\mathfrak{e}_1,\mathfrak{e}_2)}(\mathbf{x}), \mathcal{RT}_{\tilde{\mathbb{F}}_2(\mathfrak{e}_1,\mathfrak{e}_2)}(\mathbf{x}) \right\},$$
$$\mathcal{RF}_{\tilde{\mathbb{F}}_3(\mathfrak{e}_1,\mathfrak{e}_2)}(\mathbf{x}) = \max\left\{ \mathcal{RF}_{\tilde{\mathbb{F}}_1(\mathfrak{e}_1,\mathfrak{e}_2)}(\mathbf{x}), \mathcal{RF}_{\tilde{\mathbb{F}}_2(\mathfrak{e}_1,\mathfrak{e}_2)}(\mathbf{x}) \right\},$$
$$\mathcal{F}_{\tilde{\mathbb{F}}_3(\mathfrak{e}_1,\mathfrak{e}_2)}(\mathbf{x}) = \max\left\{ \mathcal{F}_{\tilde{\mathbb{F}}_1(\mathfrak{e}_1,\mathfrak{e}_2)}(\mathbf{x}), \mathcal{F}_{\tilde{\mathbb{F}}_2(\mathfrak{e}_1,\mathfrak{e}_2)}(\mathbf{x}) \right\}.$$

Definition 18. *Consider* $(\tilde{\mathbb{F}}_1, \mathcal{E})$ *and* $(\tilde{\mathbb{F}}_2, \mathcal{E})$ *be CDVNS sets over the universe* $\mathbf{X}$*. Then, the OR operation on them is represented by* $(\tilde{\mathbb{F}}_1, \mathcal{E}) \vee (\tilde{\mathbb{F}}_2, \mathcal{E}) = (\tilde{\mathbb{F}}_3, \mathcal{E} \times \mathcal{E})$ *and is given as:*

$$(\tilde{\mathbb{F}}, \mathcal{E} \times \mathcal{E}) = \left\{ \left((\mathfrak{e}_1, \mathfrak{e}_2), \langle \mathbf{x}, \mathcal{T}_{\tilde{\mathbb{F}}_3(\mathfrak{e}_1,\mathfrak{e}_2)}(\mathbf{x}), \mathcal{RT}_{\tilde{\mathbb{F}}_3(\mathfrak{e}_1,\mathfrak{e}_2)}(\mathbf{x}), \right.\right.$$
$$\left.\left. \mathcal{RF}_{\tilde{\mathbb{F}}_3(\mathfrak{e}_1,\mathfrak{e}_2)}(\mathbf{x}), \mathcal{F}_{\tilde{\mathbb{F}}_3(\mathfrak{e}_1,\mathfrak{e}_2)}(\mathbf{x}) \rangle : \mathbf{x} \in \mathbf{X} \right) : (\mathfrak{e}_1, \mathfrak{e}_2) \in \mathcal{E} \times \mathcal{E} \right\}.$$

where

$$\mathcal{T}_{\tilde{\mathbb{F}}_3(\mathfrak{e}_1,\mathfrak{e}_2)}(\mathbf{x}) = \max\left\{ \mathcal{T}_{\tilde{\mathbb{F}}_1(\mathfrak{e}_1,\mathfrak{e}_2)}(\mathbf{x}), \mathcal{T}_{\tilde{\mathbb{F}}_2(\mathfrak{e}_1,\mathfrak{e}_2)}(\mathbf{x}) \right\},$$
$$\mathcal{RT}_{\tilde{\mathbb{F}}_3(\mathfrak{e}_1,\mathfrak{e}_2)}(\mathbf{x}) = \max\left\{ \mathcal{RT}_{\tilde{\mathbb{F}}_1(\mathfrak{e}_1,\mathfrak{e}_2)}(\mathbf{x}), \mathcal{RT}_{\tilde{\mathbb{F}}_2(\mathfrak{e}_1,\mathfrak{e}_2)}(\mathbf{x}) \right\},$$
$$\mathcal{RF}_{\tilde{\mathbb{F}}_3(\mathfrak{e}_1,\mathfrak{e}_2)}(\mathbf{x}) = \min\left\{ \mathcal{RF}_{\tilde{\mathbb{F}}_1(\mathfrak{e}_1,\mathfrak{e}_2)}(\mathbf{x}), \mathcal{RF}_{\tilde{\mathbb{F}}_2(\mathfrak{e}_1,\mathfrak{e}_2)}(\mathbf{x}) \right\},$$
$$\mathcal{F}_{\tilde{\mathbb{F}}_3(\mathfrak{e}_1,\mathfrak{e}_2)}(\mathbf{x}) = \min\left\{ \mathcal{F}_{\tilde{\mathbb{F}}_1(\mathfrak{e}_1,\mathfrak{e}_2)}(\mathbf{x}), \mathcal{F}_{\tilde{\mathbb{F}}_2(\mathfrak{e}_1,\mathfrak{e}_2)}(\mathbf{x}) \right\}.$$

Definition 19. *Set $(\tilde{\mathbb{F}}, \mathcal{E})$ for a CDVNS across the universe set $\mathbf{X}$ is a null CDVNS set by definition if*

$$\mathcal{T}_{\tilde{\mathbb{F}}(\mathfrak{e})}(\mathbf{x}) = 0, \quad \mathcal{RT}_{\tilde{\mathbb{F}}(\mathfrak{e})}(\mathbf{x}) = 0, \quad \forall \mathfrak{e} \in \mathcal{E}, \forall \mathbf{x} \in \mathbf{X},$$

$$\mathcal{RF}_{\tilde{\mathbb{F}}(\mathfrak{e})}(\mathbf{x}) = 1, \quad \mathcal{F}_{\tilde{\mathbb{F}}(\mathfrak{e})}(\mathbf{x}) = 1, \quad \forall \mathfrak{e} \in \mathcal{E}, \forall \mathbf{x} \in \mathbf{X}.$$

It is indicated by $0_{(\mathbf{X},\mathcal{E})}$.

Definition 20. *An $(\tilde{\mathbb{F}}, \mathcal{E})$ CDVNS set is absolute CDVNS set over the universe set $\mathbf{X}$ if*

$$\mathcal{T}_{\tilde{\mathbb{F}}(\mathfrak{e})}(\mathbf{x}) = 1, \quad \mathcal{RT}_{\tilde{\mathbb{F}}(\mathfrak{e})}(\mathbf{x}) = 1, \quad \forall \mathfrak{e} \in \mathcal{E}, \forall \mathbf{x} \in \mathbf{X},$$

$$\mathcal{RF}_{\tilde{\mathbb{F}}(\mathfrak{e})}(\mathbf{x}) = 0, \quad \mathcal{F}_{\tilde{\mathbb{F}}(\mathfrak{e})}(\mathbf{x}) = 0, \quad \forall \mathfrak{e} \in \mathcal{E}, \forall \mathbf{x} \in \mathbf{X}.$$

Evidently,

$$0^c_{(\mathbf{X},\mathcal{E})} = 1_{(\mathbf{X},\mathcal{E})}, \quad 1^c_{(\mathbf{X},\mathcal{E})} = 0_{(\mathbf{X},\mathcal{E})}.$$

Proposition 1. *This means that $(\tilde{\mathbb{F}}_1, \mathcal{E})$, $(\tilde{\mathbb{F}}_2, \mathcal{E})$ and $(\tilde{\mathbb{F}}_3, \mathcal{E})$ respectively be three CDVNS sets over the $\mathbf{X}$ universe set. Next,*

(i) $(\tilde{\mathbb{F}}_1, \mathcal{E}) \cup [(\tilde{\mathbb{F}}_2, \mathcal{E}) \cup (\tilde{\mathbb{F}}_3, \mathcal{E})] = [(\tilde{\mathbb{F}}_1, \mathcal{E}) \cup (\tilde{\mathbb{F}}_2, \mathcal{E})] \cup (\tilde{\mathbb{F}}_3, \mathcal{E})$*and*
$(\tilde{\mathbb{F}}_1, \mathcal{E}) \cap [(\tilde{\mathbb{F}}_2, \mathcal{E}) \cap (\tilde{\mathbb{F}}_3, \mathcal{E})] = [(\tilde{\mathbb{F}}_1, \mathcal{E}) \cap (\tilde{\mathbb{F}}_2, \mathcal{E})] \cap (\tilde{\mathbb{F}}_3, \mathcal{E})$*;*

(ii) $(\tilde{\mathbb{F}}_1, \mathcal{E}) \cup [(\tilde{\mathbb{F}}_2, \mathcal{E}) \cap (\tilde{\mathbb{F}}_3, \mathcal{E})] = [(\tilde{\mathbb{F}}_1, \mathcal{E}) \cup (\tilde{\mathbb{F}}_2, \mathcal{E})] \cap [(\tilde{\mathbb{F}}_1, \mathcal{E}) \cup (\tilde{\mathbb{F}}_3, \mathcal{E})]$*and*
$(\tilde{\mathbb{F}}_1, \mathcal{E}) \cap [(\tilde{\mathbb{F}}_2, \mathcal{E}) \cup (\tilde{\mathbb{F}}_3, \mathcal{E})] = [(\tilde{\mathbb{F}}_1, \mathcal{E}) \cap (\tilde{\mathbb{F}}_2, \mathcal{E})] \cup [(\tilde{\mathbb{F}}_1, \mathcal{E}) \cap (\tilde{\mathbb{F}}_3, \mathcal{E})]$*;*

(iii) $(\tilde{\mathbb{F}}_1, \mathcal{E}) \cup 0_{(\mathbf{X},\mathcal{E})} = (\tilde{\mathbb{F}}_1, \mathcal{E})$*and*$(\tilde{\mathbb{F}}_1, \mathcal{E}) \cap 0_{(\mathbf{X},\mathcal{E})} = 0_{(\mathbf{X},\mathcal{E})}$*;*

(iv) $(\tilde{\mathbb{F}}_1, \mathcal{E}) \cup 1_{(\mathbf{X},\mathcal{E})} = (\tilde{\mathbb{F}}_1, \mathcal{E})$*and*$(\tilde{\mathbb{F}}_1, \mathcal{E}) \cap 1_{(\mathbf{X},\mathcal{E})} = (\tilde{\mathbb{F}}_1, \mathcal{E})$*;*

Proof. Obvious.

Proposition 2. *It is assumed that $(\tilde{\mathbb{F}}_1, \mathcal{E})$ and $(\tilde{\mathbb{F}}_2, \mathcal{E})$ be two CDVNS sets over the $\mathbf{X}$ universe set. Next,*

(i) $[(\tilde{\mathbb{F}}_1, \mathcal{E}) \cup (\tilde{\mathbb{F}}_2, \mathcal{E})]^c = (\tilde{\mathbb{F}}_1, \mathcal{E})^c \cap (\tilde{\mathbb{F}}_2, \mathcal{E})^c$

(ii) $[(\tilde{\mathbb{F}}_1, \mathcal{E}) \cap (\tilde{\mathbb{F}}_2, \mathcal{E})]^c = (\tilde{\mathbb{F}}_1, \mathcal{E})^c \cup (\tilde{\mathbb{F}}_2, \mathcal{E})^c$

Proof. (i) For all $\mathfrak{e} \in \mathcal{E}$ and $\mathbf{x} \in \mathbf{X}$,

$$\begin{aligned}(\tilde{\mathbb{F}}_1, \mathcal{E}) \cup (\tilde{\mathbb{F}}_2, \mathcal{E}) = \{\langle \mathbf{x}, &\max\{\mathcal{T}_{\tilde{\mathbb{F}}_1(\mathfrak{e})}(\mathbf{x}), \mathcal{T}_{\tilde{\mathbb{F}}_2(\mathfrak{e})}(\mathbf{x})\}, \max\{\mathcal{RT}_{\tilde{\mathbb{F}}_1(\mathfrak{e})}(\mathbf{x}), \mathcal{RT}_{\tilde{\mathbb{F}}_2(\mathfrak{e})}(\mathbf{x})\},\\ &\min\{\mathcal{RF}_{\tilde{\mathbb{F}}_1(\mathfrak{e})}(\mathbf{x}), \mathcal{RF}_{\tilde{\mathbb{F}}_2(\mathfrak{e})}(\mathbf{x})\}, \min\{\mathcal{F}_{\tilde{\mathbb{F}}_1(\mathfrak{e})}(\mathbf{x}), \mathcal{F}_{\tilde{\mathbb{F}}_2(\mathfrak{e})}(\mathbf{x})\}\rangle\},\\ [(\tilde{\mathbb{F}}_1, \mathcal{E}) \cup (\tilde{\mathbb{F}}_2, \mathcal{E})]^c = \{\langle \mathbf{x}, &\min\{\mathcal{F}_{\tilde{\mathbb{F}}_1(\mathfrak{e})}(\mathbf{x}), \mathcal{F}_{\tilde{\mathbb{F}}_2(\mathfrak{e})}(\mathbf{x})\}, \min\{\mathcal{RF}_{\tilde{\mathbb{F}}_1(\mathfrak{e})}(\mathbf{x}), \mathcal{RF}_{\tilde{\mathbb{F}}_2(\mathfrak{e})}(\mathbf{x})\},\\ &\max\{\mathcal{RT}_{\tilde{\mathbb{F}}_1(\mathfrak{e})}(\mathbf{x}), \mathcal{RT}_{\tilde{\mathbb{F}}_2(\mathfrak{e})}(\mathbf{x})\}, \max\{\mathcal{T}_{\tilde{\mathbb{F}}_1(\mathfrak{e})}(\mathbf{x}), \mathcal{T}_{\tilde{\mathbb{F}}_2(\mathfrak{e})}(\mathbf{x})\}\rangle\},\end{aligned}$$

Now,

$$\begin{aligned}(\tilde{\mathbb{F}}_1, \mathcal{E})^c &= \{\langle \mathbf{x}, \mathcal{F}_{\tilde{\mathbb{F}}_1(\mathfrak{e})}(\mathbf{x}), \mathcal{RF}_{\tilde{\mathbb{F}}_1(\mathfrak{e})}(\mathbf{x}), \mathcal{RT}_{\tilde{\mathbb{F}}_1(\mathfrak{e})}(\mathbf{x}), \mathcal{T}_{\tilde{\mathbb{F}}_1(\mathfrak{e})}(\mathbf{x})\rangle\}\\ (\tilde{\mathbb{F}}_2, \mathcal{E})^c &= \{\langle \mathbf{x}, \mathcal{F}_{\tilde{\mathbb{F}}_2(\mathfrak{e})}(\mathbf{x}), \mathcal{RF}_{\tilde{\mathbb{F}}_2(\mathfrak{e})}(\mathbf{x}), \mathcal{RT}_{\tilde{\mathbb{F}}_2(\mathfrak{e})}(\mathbf{x}), \mathcal{T}_{\tilde{\mathbb{F}}_2(\mathfrak{e})}(\mathbf{x})\rangle\}\end{aligned}$$

After that,

$$(\tilde{\mathbb{F}}_1,\mathcal{E})^c \cap (\tilde{\mathbb{F}}_2,\mathcal{E})^c = \{\langle \mathbf{x}, \min\{\mathcal{F}_{\tilde{\mathbb{F}}_1(\mathfrak{e})}(\mathbf{x}), \mathcal{F}_{\tilde{\mathbb{F}}_2(\mathfrak{e})}(\mathbf{x})\}, \min\{\mathcal{RF}_{\tilde{\mathbb{F}}_1(\mathfrak{e})}(\mathbf{x}), \mathcal{RF}_{\tilde{\mathbb{F}}_2(\mathfrak{e})}(\mathbf{x})\},$$
$$\max\{\mathcal{RT}_{\tilde{\mathbb{F}}_1(\mathfrak{e})}(\mathbf{x}), \mathcal{RT}_{\tilde{\mathbb{F}}_2(\mathfrak{e})}(\mathbf{x})\}, \max\{\mathcal{T}_{\tilde{\mathbb{F}}_1(\mathfrak{e})}(\mathbf{x}), \mathcal{T}_{\tilde{\mathbb{F}}_2(\mathfrak{e})}(\mathbf{x})\}\rangle\}$$

Hence, $[(\tilde{\mathbb{F}}_1,\mathcal{E}) \cup (\tilde{\mathbb{F}}_2,\mathcal{E})]^c = (\tilde{\mathbb{F}}_1,\mathcal{E})^c \cap (\tilde{\mathbb{F}}_2,\mathcal{E})^c$.
(ii) In the same way, $\forall\ \mathfrak{e} \in \mathcal{E}$ *and* $\mathbf{x} \in \mathbf{X}$,

$$(\tilde{\mathbb{F}}_1,\mathcal{E}) \cap (\tilde{\mathbb{F}}_2,\mathcal{E}) = \{\langle \mathbf{x}, \min\{\mathcal{T}_{\tilde{\mathbb{F}}_1(\mathfrak{e})}(\mathbf{x}), \mathcal{T}_{\tilde{\mathbb{F}}_2(\mathfrak{e})}(\mathbf{x})\}, \min\{\mathcal{RT}_{\tilde{\mathbb{F}}_1(\mathfrak{e})}(\mathbf{x}), \mathcal{RT}_{\tilde{\mathbb{F}}_2(\mathfrak{e})}(\mathbf{x})\},$$
$$\max\{\mathcal{RF}_{\tilde{\mathbb{F}}_1(\mathfrak{e})}(\mathbf{x}), \mathcal{RF}_{\tilde{\mathbb{F}}_2(\mathfrak{e})}(\mathbf{x})\}, \max\{\mathcal{F}_{\tilde{\mathbb{F}}_1(\mathfrak{e})}(\mathbf{x}), \mathcal{F}_{\tilde{\mathbb{F}}_2(\mathfrak{e})}(\mathbf{x})\}\rangle\},$$
$$[(\tilde{\mathbb{F}}_1,\mathcal{E}) \cap (\tilde{\mathbb{F}}_2,\mathcal{E})]^c = \{\langle \mathbf{x}, \max\{\mathcal{F}_{\tilde{\mathbb{F}}_1(\mathfrak{e})}(\mathbf{x}), \mathcal{F}_{\tilde{\mathbb{F}}_2(\mathfrak{e})}(\mathbf{x})\}, \max\{\mathcal{RF}_{\tilde{\mathbb{F}}_1(\mathfrak{e})}(\mathbf{x}), \mathcal{RF}_{\tilde{\mathbb{F}}_2(\mathfrak{e})}(\mathbf{x})\},$$
$$\min\{\mathcal{RT}_{\tilde{\mathbb{F}}_1(\mathfrak{e})}(\mathbf{x}), \mathcal{RT}_{\tilde{\mathbb{F}}_2(\mathfrak{e})}(\mathbf{x})\}, \min\{\mathcal{T}_{\tilde{\mathbb{F}}_1(\mathfrak{e})}(\mathbf{x}), \mathcal{T}_{\tilde{\mathbb{F}}_2(\mathfrak{e})}(\mathbf{x})\}\rangle\},$$

Now,

$$(\tilde{\mathbb{F}}_1,\mathcal{E})^c = \{\langle \mathbf{x}, \mathcal{F}_{\tilde{\mathbb{F}}_1(\mathfrak{e})}(\mathbf{x}), \mathcal{RF}_{\tilde{\mathbb{F}}_1(\mathfrak{e})}(\mathbf{x}), \mathcal{RT}_{\tilde{\mathbb{F}}_1(\mathfrak{e})}(\mathbf{x}), \mathcal{T}_{\tilde{\mathbb{F}}_1(\mathfrak{e})}(\mathbf{x})\rangle\}$$
$$(\tilde{\mathbb{F}}_2,\mathcal{E})^c = \{\langle \mathbf{x}, \mathcal{F}_{\tilde{\mathbb{F}}_2(\mathfrak{e})}(\mathbf{x}), \mathcal{RF}_{\tilde{\mathbb{F}}_2(\mathfrak{e})}(\mathbf{x}), \mathcal{RT}_{\tilde{\mathbb{F}}_2(\mathfrak{e})}(\mathbf{x}), \mathcal{T}_{\tilde{\mathbb{F}}_2(\mathfrak{e})}(\mathbf{x})\rangle\}$$

So,

$$(\tilde{\mathbb{F}}_1,\mathcal{E})^c \cup (\tilde{\mathbb{F}}_2,\mathcal{E})^c = \{\langle \mathbf{x}, \max\{\mathcal{F}_{\tilde{\mathbb{F}}_1(\mathfrak{e})}(\mathbf{x}), \mathcal{F}_{\tilde{\mathbb{F}}_2(\mathfrak{e})}(\mathbf{x})\}, \max\{\mathcal{RF}_{\tilde{\mathbb{F}}_1(\mathfrak{e})}(\mathbf{x}), \mathcal{RF}_{\tilde{\mathbb{F}}_2(\mathfrak{e})}(\mathbf{x})\},$$
$$\min\{\mathcal{RT}_{\tilde{\mathbb{F}}_1(\mathfrak{e})}(\mathbf{x}), \mathcal{RT}_{\tilde{\mathbb{F}}_2(\mathfrak{e})}(\mathbf{x})\}, \min\{\mathcal{T}_{\tilde{\mathbb{F}}_1(\mathfrak{e})}(\mathbf{x}), \mathcal{T}_{\tilde{\mathbb{F}}_2(\mathfrak{e})}(\mathbf{x})\}\rangle\}$$

Hence, $[(\tilde{\mathbb{F}}_1,\mathcal{E}) \cap (\tilde{\mathbb{F}}_2,\mathcal{E})]^c = (\tilde{\mathbb{F}}_1,\mathcal{E})^c \cup (\tilde{\mathbb{F}}_2,\mathcal{E})^c$.

Proposition 3. *Consider* $(\tilde{\mathbb{F}}_1,\mathcal{E})$ *and* $(\tilde{\mathbb{F}}_2,\mathcal{E})$ *be two CDVNS sets over the universe set* $\mathbf{X}$. *So,*

(i) $[(\tilde{\mathbb{F}}_1,\mathcal{E}) \vee (\tilde{\mathbb{F}}_2,\mathcal{E})]^c = (\tilde{\mathbb{F}}_1,\mathcal{E})^c \wedge (\tilde{\mathbb{F}}_2,\mathcal{E})^c$

(ii) $[(\tilde{\mathbb{F}}_1,\mathcal{E}) \wedge (\tilde{\mathbb{F}}_2,\mathcal{E})]^c = (\tilde{\mathbb{F}}_1,\mathcal{E})^c \vee (\tilde{\mathbb{F}}_2,\mathcal{E})^c$

Proof. (i) $\forall\ \mathfrak{e} \in \mathcal{E}$ *and* $\mathbf{x} \in \mathbf{X}$,

$$(\tilde{\mathbb{F}}_1,\mathcal{E}) \vee (\tilde{\mathbb{F}}_2,\mathcal{E}) = \{\langle \mathbf{x}, \max\{\mathcal{T}_{\tilde{\mathbb{F}}_1(\mathfrak{e})}(\mathbf{x}), \mathcal{T}_{\tilde{\mathbb{F}}_2(\mathfrak{e})}(\mathbf{x})\}, \max\{\mathcal{RT}_{\tilde{\mathbb{F}}_1(\mathfrak{e})}(\mathbf{x}), \mathcal{RT}_{\tilde{\mathbb{F}}_2(\mathfrak{e})}(\mathbf{x})\},$$
$$\min\{\mathcal{RF}_{\tilde{\mathbb{F}}_1(\mathfrak{e})}(\mathbf{x}), \mathcal{RF}_{\tilde{\mathbb{F}}_2(\mathfrak{e})}(\mathbf{x})\}, \min\{\mathcal{F}_{\tilde{\mathbb{F}}_1(\mathfrak{e})}(\mathbf{x}), \mathcal{F}_{\tilde{\mathbb{F}}_2(\mathfrak{e})}(\mathbf{x})\}\rangle\},$$
$$[(\tilde{\mathbb{F}}_1,\mathcal{E}) \vee (\tilde{\mathbb{F}}_2,\mathcal{E})]^c = \{\langle \mathbf{x}, \min\{\mathcal{F}_{\tilde{\mathbb{F}}_1(\mathfrak{e})}(\mathbf{x}), \mathcal{F}_{\tilde{\mathbb{F}}_2(\mathfrak{e})}(\mathbf{x})\}, \min\{\mathcal{RF}_{\tilde{\mathbb{F}}_1(\mathfrak{e})}(\mathbf{x}), \mathcal{RF}_{\tilde{\mathbb{F}}_2(\mathfrak{e})}(\mathbf{x})\},$$
$$\max\{\mathcal{RT}_{\tilde{\mathbb{F}}_1(\mathfrak{e})}(\mathbf{x}), \mathcal{RT}_{\tilde{\mathbb{F}}_2(\mathfrak{e})}(\mathbf{x})\}, \max\{\mathcal{T}_{\tilde{\mathbb{F}}_1(\mathfrak{e})}(\mathbf{x}), \mathcal{T}_{\tilde{\mathbb{F}}_2(\mathfrak{e})}(\mathbf{x})\}\rangle\},$$

Presently,

$$(\tilde{\mathbb{F}}_1,\mathcal{E})^c = \{\langle \mathbf{x}, \mathcal{F}_{\tilde{\mathbb{F}}_1(\mathfrak{e})}(\mathbf{x}), \mathcal{RF}_{\tilde{\mathbb{F}}_1(\mathfrak{e})}(\mathbf{x}), \mathcal{RT}_{\tilde{\mathbb{F}}_1(\mathfrak{e})}(\mathbf{x}), \mathcal{T}_{\tilde{\mathbb{F}}_1(\mathfrak{e})}(\mathbf{x})\rangle\}$$
$$(\tilde{\mathbb{F}}_2,\mathcal{E})^c = \{\langle \mathbf{x}, \mathcal{F}_{\tilde{\mathbb{F}}_2(\mathfrak{e})}(\mathbf{x}), \mathcal{RF}_{\tilde{\mathbb{F}}_2(\mathfrak{e})}(\mathbf{x}), \mathcal{RT}_{\tilde{\mathbb{F}}_2(\mathfrak{e})}(\mathbf{x}), \mathcal{T}_{\tilde{\mathbb{F}}_2(\mathfrak{e})}(\mathbf{x})\rangle\}$$

So,

$$(\tilde{\mathbb{F}}_1,\mathcal{E})^c \wedge (\tilde{\mathbb{F}}_2,\mathcal{E})^c = \{\langle \mathbf{x}, \min\{\mathcal{F}_{\tilde{\mathbb{F}}_1(\mathfrak{e})}(\mathbf{x}), \mathcal{F}_{\tilde{\mathbb{F}}_2(\mathfrak{e})}(\mathbf{x})\}, \min\{\mathcal{RF}_{\tilde{\mathbb{F}}_1(\mathfrak{e})}(\mathbf{x}), \mathcal{RF}_{\tilde{\mathbb{F}}_2(\mathfrak{e})}(\mathbf{x})\},$$
$$\max\{\mathcal{RT}_{\tilde{\mathbb{F}}_1(\mathfrak{e})}(\mathbf{x}), \mathcal{RT}_{\tilde{\mathbb{F}}_2(\mathfrak{e})}(\mathbf{x})\}, \max\{\mathcal{T}_{\tilde{\mathbb{F}}_1(\mathfrak{e})}(\mathbf{x}), \mathcal{T}_{\tilde{\mathbb{F}}_2(\mathfrak{e})}(\mathbf{x})\}\rangle\}$$

Hence, $[(\tilde{\mathbb{F}}_1,\mathcal{E})\vee(\tilde{\mathbb{F}}_2,\mathcal{E})]^c=(\tilde{\mathbb{F}}_1,\mathcal{E})^c\wedge(\tilde{\mathbb{F}}_2,\mathcal{E})^c$.
(ii) In a similar way, $\forall\ \mathfrak{e}\in\mathcal{E}$ *and* $\mathbf{x}\in\mathbf{X}$,

$$\begin{aligned}(\tilde{\mathbb{F}}_1,\mathcal{E})\wedge(\tilde{\mathbb{F}}_2,\mathcal{E})&=\{\langle\mathbf{x},\min\{\mathcal{T}_{\tilde{\mathbb{F}}_1(\mathfrak{e})}(\mathbf{x}),\mathcal{T}_{\tilde{\mathbb{F}}_2(\mathfrak{e})}(\mathbf{x})\},\min\{\mathcal{RT}_{\tilde{\mathbb{F}}_1(\mathfrak{e})}(\mathbf{x}),\mathcal{RT}_{\tilde{\mathbb{F}}_2(\mathfrak{e})}(\mathbf{x})\},\\&\qquad\max\{\mathcal{RF}_{\tilde{\mathbb{F}}_1(\mathfrak{e})}(\mathbf{x}),\mathcal{RF}_{\tilde{\mathbb{F}}_2(\mathfrak{e})}(\mathbf{x})\},\max\{\mathcal{F}_{\tilde{\mathbb{F}}_1(\mathfrak{e})}(\mathbf{x}),\mathcal{F}_{\tilde{\mathbb{F}}_2(\mathfrak{e})}(\mathbf{x})\}\rangle\},\\[(\tilde{\mathbb{F}}_1,\mathcal{E})\wedge(\tilde{\mathbb{F}}_2,\mathcal{E})]^c&=\{\langle\mathbf{x},\max\{\mathcal{F}_{\tilde{\mathbb{F}}_1(\mathfrak{e})}(\mathbf{x}),\mathcal{F}_{\tilde{\mathbb{F}}_2(\mathfrak{e})}(\mathbf{x})\},\max\{\mathcal{RF}_{\tilde{\mathbb{F}}_1(\mathfrak{e})}(\mathbf{x}),\mathcal{RF}_{\tilde{\mathbb{F}}_2(\mathfrak{e})}(\mathbf{x})\},\\&\qquad\min\{\mathcal{RT}_{\tilde{\mathbb{F}}_1(\mathfrak{e})}(\mathbf{x}),\mathcal{RT}_{\tilde{\mathbb{F}}_2(\mathfrak{e})}(\mathbf{x})\},\min\{\mathcal{T}_{\tilde{\mathbb{F}}_1(\mathfrak{e})}(\mathbf{x}),\mathcal{T}_{\tilde{\mathbb{F}}_2(\mathfrak{e})}(\mathbf{x})\}\rangle\},\end{aligned}$$

Now,

$$\begin{aligned}(\tilde{\mathbb{F}}_1,\mathcal{E})^c&=\{\langle\mathbf{x},\mathcal{F}_{\tilde{\mathbb{F}}_1(\mathfrak{e})}(\mathbf{x}),\mathcal{RF}_{\tilde{\mathbb{F}}_1(\mathfrak{e})}(\mathbf{x}),\mathcal{RT}_{\tilde{\mathbb{F}}_1(\mathfrak{e})}(\mathbf{x}),\mathcal{T}_{\tilde{\mathbb{F}}_1(\mathfrak{e})}(\mathbf{x})\rangle\}\\(\tilde{\mathbb{F}}_2,\mathcal{E})^c&=\{\langle\mathbf{x},\mathcal{F}_{\tilde{\mathbb{F}}_2(\mathfrak{e})}(\mathbf{x}),\mathcal{RF}_{\tilde{\mathbb{F}}_2(\mathfrak{e})}(\mathbf{x}),\mathcal{RT}_{\tilde{\mathbb{F}}_2(\mathfrak{e})}(\mathbf{x}),\mathcal{T}_{\tilde{\mathbb{F}}_2(\mathfrak{e})}(\mathbf{x})\rangle\}\end{aligned}$$

So,

$$\begin{aligned}(\tilde{\mathbb{F}}_1,\mathcal{E})^c\vee(\tilde{\mathbb{F}}_2,\mathcal{E})^c&=\{\langle\mathbf{x},\max\{\mathcal{F}_{\tilde{\mathbb{F}}_1(\mathfrak{e})}(\mathbf{x}),\mathcal{F}_{\tilde{\mathbb{F}}_2(\mathfrak{e})}(\mathbf{x})\},\max\{\mathcal{RF}_{\tilde{\mathbb{F}}_1(\mathfrak{e})}(\mathbf{x}),\mathcal{RF}_{\tilde{\mathbb{F}}_2(\mathfrak{e})}(\mathbf{x})\},\\&\qquad\min\{\mathcal{RT}_{\tilde{\mathbb{F}}_1(\mathfrak{e})}(\mathbf{x}),\mathcal{RT}_{\tilde{\mathbb{F}}_2(\mathfrak{e})}(\mathbf{x})\},\min\{\mathcal{T}_{\tilde{\mathbb{F}}_1(\mathfrak{e})}(\mathbf{x}),\mathcal{T}_{\tilde{\mathbb{F}}_2(\mathfrak{e})}(\mathbf{x})\}\rangle\}\end{aligned}$$

Hence, $[(\tilde{\mathbb{F}}_1,\mathcal{E})\wedge(\tilde{\mathbb{F}}_2,\mathcal{E})]^c=(\tilde{\mathbb{F}}_1,\mathcal{E})^c\vee(\tilde{\mathbb{F}}_2,\mathcal{E})^c$.

Example 1. *Assume that* $\mathbf{X}$ *is the universe set, which is* $\mathbf{X}=\{\mathbf{x}_1,\mathbf{x}_2,\mathbf{x}_3,\mathbf{x}_4\}$*, and that* $\mathcal{E}=\{\mathfrak{e}_1,\mathfrak{e}_2\}$ *is the set of parameters. Over the universe set* $\mathbf{X}$*, let's examine CDVNS sets* $(\tilde{\mathbb{F}}_1,\mathcal{E})$ *and* $(\tilde{\mathbb{F}}_2,\mathcal{E})$ *as follows.*

$$(\tilde{\mathbb{F}}_1,\mathcal{E})=\begin{bmatrix}\mathfrak{e}_1=\langle\mathbf{x}_1,0.3e^{\iota\pi(0.2)},0.4e^{\iota\pi(0.3)},0.3e^{\iota\pi(0.2)},0.6e^{\iota\pi(0.5)}\rangle,\\\langle\mathbf{x}_2,0.4e^{\iota\pi(0.3)},0.2e^{\iota\pi(0.1)},0.1e^{\iota\pi(0.1)},0.8e^{\iota\pi(0.7)}\rangle,\\\langle\mathbf{x}_3,0.6e^{\iota\pi(0.5)},0.2e^{\iota\pi(0.1)},0.2e^{\iota\pi(0.1)},0.5e^{\iota\pi(0.4)}\rangle,\\\langle\mathbf{x}_4,0.2e^{\iota\pi(0.1)},0.3e^{\iota\pi(0.2)},0.2e^{\iota\pi(0.1)},0.4e^{\iota\pi(0.3)}\rangle\\\mathfrak{e}_2=\langle\mathbf{x}_1,0.4e^{\iota\pi(0.3)},0.3e^{\iota\pi(0.2)},0.3e^{\iota\pi(0.2)},0.8e^{\iota\pi(0.7)}\rangle,\\\langle\mathbf{x}_2,0.3e^{\iota\pi(0.2)},0.4e^{\iota\pi(0.3)},0.3e^{\iota\pi(0.2)},0.2e^{\iota\pi(0.1)}\rangle,\\\langle\mathbf{x}_3,0.3e^{\iota\pi(0.2)},0.2e^{\iota\pi(0.1)},0.1e^{\iota\pi(0.1)},0.7e^{\iota\pi(0.6)}\rangle,\\\langle\mathbf{x}_4,0.1e^{\iota\pi(0.1)},0.2e^{\iota\pi(0.1)},0.2e^{\iota\pi(0.1)},0.9e^{\iota\pi(0.8)}\rangle\end{bmatrix}$$

$$(\tilde{\mathbb{F}}_2,\mathcal{E})=\begin{bmatrix}\mathfrak{e}_1=\langle\mathbf{x}_1,0.6e^{\iota\pi(0.5)},0.3e^{\iota\pi(0.2)},0.3e^{\iota\pi(0.2)},0.8e^{\iota\pi(0.7)}\rangle,\\\langle\mathbf{x}_2,0.2e^{\iota\pi(0.1)},0.5e^{\iota\pi(0.4)},0.4e^{\iota\pi(0.3)},0.8e^{\iota\pi(0.7)}\rangle,\\\langle\mathbf{x}_3,0.1e^{\iota\pi(0.1)},0.1e^{\iota\pi(0.1)},0.1e^{\iota\pi(0.1)},0.4e^{\iota\pi(0.3)}\rangle,\\\langle\mathbf{x}_4,0.5e^{\iota\pi(0.4)},0.2e^{\iota\pi(0.1)},0.2e^{\iota\pi(0.1)},0.3e^{\iota\pi(0.2)}\rangle\\\mathfrak{e}_2=\langle\mathbf{x}_1,0.7e^{\iota\pi(0.6)},0.5e^{\iota\pi(0.4)},0.4e^{\iota\pi(0.3)},0.6e^{\iota\pi(0.5)}\rangle,\\\langle\mathbf{x}_2,0.4e^{\iota\pi(0.3)},0.2e^{\iota\pi(0.1)},0.2e^{\iota\pi(0.1)},0.3e^{\iota\pi(0.2)}\rangle,\\\langle\mathbf{x}_3,0.5e^{\iota\pi(0.4)},0.3e^{\iota\pi(0.2)},0.2e^{\iota\pi(0.1)},0.4e^{\iota\pi(0.3)}\rangle,\\\langle\mathbf{x}_4,0.4e^{\iota\pi(0.3)},0.2e^{\iota\pi(0.1)},0.1e^{\iota\pi(0.1)},0.6e^{\iota\pi(0.5)}\rangle\end{bmatrix}$$

The following are their AND, OR, union, and intersection operations:

$$(\tilde{\mathbb{F}}_1,\mathcal{E})\cup(\tilde{\mathbb{F}}_2,\mathcal{E})=\begin{bmatrix}\mathfrak{e}_1=\langle\mathbf{x}_1,0.6e^{\iota\pi(0.5)},0.4e^{\iota\pi(0.3)},0.3e^{\iota\pi(0.2)},0.6e^{\iota\pi(0.5)}\rangle,\\\langle\mathbf{x}_2,0.4e^{\iota\pi(0.3)},0.5e^{\iota\pi(0.4)},0.1e^{\iota\pi(0.1)},0.8e^{\iota\pi(0.7)}\rangle,\\\langle\mathbf{x}_3,0.6e^{\iota\pi(0.5)},0.2e^{\iota\pi(0.1)},0.1e^{\iota\pi(0.1)},0.4e^{\iota\pi(0.3)}\rangle,\\\langle\mathbf{x}_4,0.5e^{\iota\pi(0.4)},0.3e^{\iota\pi(0.2)},0.2e^{\iota\pi(0.1)},0.3e^{\iota\pi(0.2)}\rangle\\\mathfrak{e}_2=\langle\mathbf{x}_1,0.7e^{\iota\pi(0.6)},0.5e^{\iota\pi(0.4)},0.3e^{\iota\pi(0.2)},0.6e^{\iota\pi(0.5)}\rangle,\\\langle\mathbf{x}_2,0.4e^{\iota\pi(0.3)},0.4e^{\iota\pi(0.3)},0.2e^{\iota\pi(0.1)},0.2e^{\iota\pi(0.1)}\rangle,\\\langle\mathbf{x}_3,0.5e^{\iota\pi(0.4)},0.3e^{\iota\pi(0.2)},0.1e^{\iota\pi(0.1)},0.4e^{\iota\pi(0.3)}\rangle,\\\langle\mathbf{x}_4,0.4e^{\iota\pi(0.3)},0.2e^{\iota\pi(0.1)},0.1e^{\iota\pi(0.1)},0.6e^{\iota\pi(0.5)}\rangle\end{bmatrix}$$

$$(\tilde{\mathbb{F}}_1,\mathcal{E})\cap(\tilde{\mathbb{F}}_2,\mathcal{E})=\begin{bmatrix}\mathfrak{e}_1=\langle \mathbf{x}_1,0.3e^{\iota\pi(0.2)},0.3e^{\iota\pi(0.3)},0.3e^{\iota\pi(0.2)},0.8e^{\iota\pi(0.7)}\rangle,\\ \langle \mathbf{x}_2,0.2e^{\iota\pi(0.1)},0.2e^{\iota\pi(0.1)},0.4e^{\iota\pi(0.3)},0.8e^{\iota\pi(0.7)}\rangle,\\ \langle \mathbf{x}_3,0.1e^{\iota\pi(0.1)},0.1e^{\iota\pi(0.1)},0.2e^{\iota\pi(0.1)},0.5e^{\iota\pi(0.4)}\rangle,\\ \langle \mathbf{x}_4,0.2e^{\iota\pi(0.1)},0.2e^{\iota\pi(0.2)},0.2e^{\iota\pi(0.1)},0.4e^{\iota\pi(0.4)}\rangle\\ \mathfrak{e}_2=\langle \mathbf{x}_1,0.3e^{\iota\pi(0.2)},0.3e^{\iota\pi(0.3)},0.3e^{\iota\pi(0.2)},0.8e^{\iota\pi(0.7)}\rangle,\\ \langle \mathbf{x}_2,0.2e^{\iota\pi(0.1)},0.2e^{\iota\pi(0.1)},0.4e^{\iota\pi(0.3)},0.8e^{\iota\pi(0.7)}\rangle,\\ \langle \mathbf{x}_3,0.1e^{\iota\pi(0.1)},0.1e^{\iota\pi(0.1)},0.2e^{\iota\pi(0.1)},0.5e^{\iota\pi(0.4)}\rangle,\\ \langle \mathbf{x}_4,0.2e^{\iota\pi(0.1)},0.2e^{\iota\pi(0.2)},0.2e^{\iota\pi(0.1)},0.4e^{\iota\pi(0.3)}\rangle\end{bmatrix}$$

$$(\tilde{\mathbb{F}}_1,\mathcal{E})\setminus(\tilde{\mathbb{F}}_2,\mathcal{E})=\begin{bmatrix}\mathfrak{e}_1=\langle \mathbf{x}_1,0.3e^{\iota\pi(0.2)},0.3e^{\iota\pi(0.2)},0.3e^{\iota\pi(0.2)},0.6e^{\iota\pi(0.5)}\rangle,\\ \langle \mathbf{x}_2,0.4e^{\iota\pi(0.3)},0.2e^{\iota\pi(0.1)},0.5e^{\iota\pi(0.4)},0.8e^{\iota\pi(0.7)}\rangle,\\ \langle \mathbf{x}_3,0.4e^{\iota\pi(0.3)},0.1e^{\iota\pi(0.1)},0.2e^{\iota\pi(0.1)},0.5e^{\iota\pi(0.4)}\rangle,\\ \langle \mathbf{x}_4,0.2e^{\iota\pi(0.1)},0.2e^{\iota\pi(0.1)},0.2e^{\iota\pi(0.1)},0.5e^{\iota\pi(0.4)}\rangle\\ \mathfrak{e}_2=\langle \mathbf{x}_1,0.4e^{\iota\pi(0.3)},0.3e^{\iota\pi(0.2)},0.5e^{\iota\pi(0.4)},0.8e^{\iota\pi(0.7)}\rangle,\\ \langle \mathbf{x}_2,0.3e^{\iota\pi(0.2)},0.2e^{\iota\pi(0.1)},0.3e^{\iota\pi(0.2)},0.4e^{\iota\pi(0.3)}\rangle,\\ \langle \mathbf{x}_3,0.3e^{\iota\pi(0.2)},0.2e^{\iota\pi(0.1)},0.3e^{\iota\pi(0.2)},0.7e^{\iota\pi(0.6)}\rangle,\\ \langle \mathbf{x}_4,0.1e^{\iota\pi(0.1)},0.1e^{\iota\pi(0.1)},0.2e^{\iota\pi(0.1)},0.9e^{\iota\pi(0.8)}\rangle\end{bmatrix}$$

$$(\tilde{\mathbb{F}}_1,\mathcal{E})\wedge(\tilde{\mathbb{F}}_2,\mathcal{E})=\begin{bmatrix}(\mathfrak{e}_1,\mathfrak{e}_1)=\langle \mathbf{x}_1,0.3e^{\iota\pi(0.2)},0.3e^{\iota\pi(0.2)},0.3e^{\iota\pi(0.2)},0.8e^{\iota\pi(0.7)}\rangle,\\ \langle \mathbf{x}_2,0.2e^{\iota\pi(0.1)},0.2e^{\iota\pi(0.1)},0.4e^{\iota\pi(0.3)},0.8e^{\iota\pi(0.7)}\rangle,\\ \langle \mathbf{x}_3,0.1e^{\iota\pi(0.1)},0.1e^{\iota\pi(0.1)},0.2e^{\iota\pi(0.1)},0.5e^{\iota\pi(0.4)}\rangle,\\ \langle \mathbf{x}_4,0.2e^{\iota\pi(0.1)},0.2e^{\iota\pi(0.1)},0.2e^{\iota\pi(0.1)},0.4e^{\iota\pi(0.3)}\rangle\\ (\mathfrak{e}_1,\mathfrak{e}_2)=\langle \mathbf{x}_1,0.3e^{\iota\pi(0.2)},0.4e^{\iota\pi(0.3)},0.4e^{\iota\pi(0.3)},0.6e^{\iota\pi(0.5)}\rangle,\\ \langle \mathbf{x}_2,0.4e^{\iota\pi(0.3)},0.2e^{\iota\pi(0.1)},0.2e^{\iota\pi(0.1)},0.8e^{\iota\pi(0.7)}\rangle,\\ \langle \mathbf{x}_3,0.5e^{\iota\pi(0.4)},0.2e^{\iota\pi(0.1)},0.2e^{\iota\pi(0.1)},0.5e^{\iota\pi(0.4)}\rangle,\\ \langle \mathbf{x}_4,0.2e^{\iota\pi(0.1)},0.2e^{\iota\pi(0.1)},0.2e^{\iota\pi(0.1)},0.6e^{\iota\pi(0.5)}\rangle\\ (\mathfrak{e}_2,\mathfrak{e}_1)=\langle \mathbf{x}_1,0.4e^{\iota\pi(0.3)},0.3e^{\iota\pi(0.2)},0.3e^{\iota\pi(0.2)},0.8e^{\iota\pi(0.7)}\rangle,\\ \langle \mathbf{x}_2,0.2e^{\iota\pi(0.1)},0.4e^{\iota\pi(0.3)},0.4e^{\iota\pi(0.3)},0.8e^{\iota\pi(0.7)}\rangle,\\ \langle \mathbf{x}_3,0.1e^{\iota\pi(0.1)},0.1e^{\iota\pi(0.1)},0.1e^{\iota\pi(0.1)},0.7e^{\iota\pi(0.6)}\rangle,\\ \langle \mathbf{x}_4,0.1e^{\iota\pi(0.1)},0.2e^{\iota\pi(0.1)},0.2e^{\iota\pi(0.1)},0.9e^{\iota\pi(0.8)}\rangle\\ (\mathfrak{e}_2,\mathfrak{e}_2)=\langle \mathbf{x}_1,0.3e^{\iota\pi(0.2)},0.3e^{\iota\pi(0.2)},0.3e^{\iota\pi(0.2)},0.8e^{\iota\pi(0.7)}\rangle,\\ \langle \mathbf{x}_2,0.2e^{\iota\pi(0.1)},0.2e^{\iota\pi(0.1)},0.4e^{\iota\pi(0.3)},0.8e^{\iota\pi(0.7)}\rangle,\\ \langle \mathbf{x}_3,0.1e^{\iota\pi(0.1)},0.1e^{\iota\pi(0.1)},0.2e^{\iota\pi(0.1)},0.5e^{\iota\pi(0.4)}\rangle,\\ \langle \mathbf{x}_4,0.2e^{\iota\pi(0.1)},0.2e^{\iota\pi(0.1)},0.2e^{\iota\pi(0.1)},0.4e^{\iota\pi(0.3)}\rangle\end{bmatrix}$$

$$(\tilde{\mathbb{F}}_1,\mathcal{E})\vee(\tilde{\mathbb{F}}_2,\mathcal{E})=\begin{bmatrix}(\mathfrak{e}_1,\mathfrak{e}_1)=\langle \mathbf{x}_1,0.6e^{\iota\pi(0.5)},0.4e^{\iota\pi(0.3)},0.3e^{\iota\pi(0.2)},0.6e^{\iota\pi(0.5)}\rangle,\\ \langle \mathbf{x}_2,0.4e^{\iota\pi(0.3)},0.5e^{\iota\pi(0.4)},0.1e^{\iota\pi(0.1)},0.8e^{\iota\pi(0.7)}\rangle,\\ \langle \mathbf{x}_3,0.6e^{\iota\pi(0.5)},0.2e^{\iota\pi(0.1)},0.1e^{\iota\pi(0.1)},0.4e^{\iota\pi(0.3)}\rangle,\\ \langle \mathbf{x}_4,0.5e^{\iota\pi(0.4)},0.3e^{\iota\pi(0.2)},0.2e^{\iota\pi(0.1)},0.3e^{\iota\pi(0.2)}\rangle\\ (\mathfrak{e}_1,\mathfrak{e}_2)=\langle \mathbf{x}_1,0.7e^{\iota\pi(0.6)},0.5e^{\iota\pi(0.4)},0.3e^{\iota\pi(0.2)},0.8e^{\iota\pi(0.7)}\rangle,\\ \langle \mathbf{x}_2,0.4e^{\iota\pi(0.3)},0.2e^{\iota\pi(0.1)},0.1e^{\iota\pi(0.1)},0.3e^{\iota\pi(0.2)}\rangle,\\ \langle \mathbf{x}_3,0.6e^{\iota\pi(0.5)},0.3e^{\iota\pi(0.2)},0.2e^{\iota\pi(0.1)},0.4e^{\iota\pi(0.3)}\rangle,\\ \langle \mathbf{x}_4,0.4e^{\iota\pi(0.3)},0.3e^{\iota\pi(0.2)},0.1e^{\iota\pi(0.1)},0.4e^{\iota\pi(0.3)}\rangle\\ (\mathfrak{e}_2,\mathfrak{e}_1)=\langle \mathbf{x}_1,0.6e^{\iota\pi(0.5)},0.3e^{\iota\pi(0.2)},0.3e^{\iota\pi(0.2)},0.8e^{\iota\pi(0.7)}\rangle,\\ \langle \mathbf{x}_2,0.3e^{\iota\pi(0.2)},0.5e^{\iota\pi(0.4)},0.3e^{\iota\pi(0.2)},0.2e^{\iota\pi(0.1)}\rangle,\\ \langle \mathbf{x}_3,0.3e^{\iota\pi(0.2)},0.2e^{\iota\pi(0.1)},0.1e^{\iota\pi(0.1)},0.4e^{\iota\pi(0.3)}\rangle,\\ \langle \mathbf{x}_4,0.5e^{\iota\pi(0.4)},0.2e^{\iota\pi(0.1)},0.2e^{\iota\pi(0.1)},0.3e^{\iota\pi(0.2)}\rangle\\ (\mathfrak{e}_2,\mathfrak{e}_2)=\langle \mathbf{x}_1,0.7e^{\iota\pi(0.6)},0.5e^{\iota\pi(0.4)},0.3e^{\iota\pi(0.2)},0.6e^{\iota\pi(0.5)}\rangle,\\ \langle \mathbf{x}_2,0.4e^{\iota\pi(0.3)},0.4e^{\iota\pi(0.3)},0.2e^{\iota\pi(0.1)},0.2e^{\iota\pi(0.1)}\rangle,\\ \langle \mathbf{x}_3,0.5e^{\iota\pi(0.4)},0.3e^{\iota\pi(0.2)},0.1e^{\iota\pi(0.1)},0.4e^{\iota\pi(0.3)}\rangle,\\ \langle \mathbf{x}_4,0.4e^{\iota\pi(0.3)},0.2e^{\iota\pi(0.1)},0.1e^{\iota\pi(0.1)},0.6e^{\iota\pi(0.5)}\rangle\end{bmatrix}$$

4. Complex Double-Valued Neutrosophic Soft Topological Spaces

Based on the established operations of the CDVNS union, intersection, neutrosophic soft null, and absolute sets, we presented the CDVNS topology in this part. To help you grasp the ideas, a few examples are provided.

Definition 21. *The family of all CDVNS sets over the universe set* $\mathbf{X}$ *and* $\tau \subset CDVNSS(\mathbf{X}, \mathcal{E})$ *is denoted by* $CDVNSS(\mathbf{X}, \mathcal{E})$*. The CDVNS topology on* $\mathbf{X}$ *is thus defined as* τ *if*

(i) $0_{(\mathbf{X},\mathcal{E})}$ *and* $1_{(\mathbf{X},\mathcal{E})} \in \tau$*,*

(ii) The union of any number of CDVNS sets in $\tau \in \tau$*,*

(iii) The intersection of a finite number of CDVNS sets in $\tau \in \tau$*.*

It is then claimed that $(\mathbf{X}, \tau, \mathcal{E})$ *is a CDVNS topological space (CDVNSTS) over* $\mathbf{X}$*. It is said that every member of* τ *is a CDVNS open set.*

Definition 22. *The CDVNS topological space* $(\mathbf{X}, \tau, \mathcal{E})$ *and the CDVNS set* $(\tilde{\mathbb{F}}, \mathcal{E})$ *over* $\mathbf{X}$ *are considered. If the complement of* $(\tilde{\mathbb{F}}, \mathcal{E})$ *is a CDVNS open set, then* $(\tilde{\mathbb{F}}, \mathcal{E})$ *is a CDVNS closed set.*

Proposition 4. *Consider the CDVNS topological space* $(\mathbf{X}, \tau, \mathcal{E})$ *over the universe set* $\mathbf{X}$*. Next,*

(i) $0_{(\mathbf{X},\mathcal{E})}$ *and* $1_{(\mathbf{X},\mathcal{E})}$ *are CDVNS closed sets over* $\mathbf{X}$*,*

(ii) The union of any number of CDVNS sets is a CDVNS closed sets over $\mathbf{X}$*,*

(iii) The intersection of a finite number of CDVNS sets is a CDVNS closed sets over $\mathbf{X}$*.*

Definition 23. *Suppose that the family of all CDVNS sets over the universe set* $\mathbf{X}$ *is* $CDVNSS(\mathbf{X}, \mathcal{E})$*.*

(i) The CDVNS indiscrete topology is τ*, and the CDVNS indiscrete topological space over* $\mathbf{X}$ *is* $(\mathbf{X}, \tau, \mathcal{E})$*, if* $\tau = \{0_{(\mathbf{X},\mathcal{E})}, 1_{(\mathbf{X},\mathcal{E})}\}$*.*

(ii) $(\mathbf{X}, \tau, \mathcal{E})$ *is a CDVNS discrete topological space over* $\mathbf{X}$*, and* $\tau = CDVNSS(\mathbf{X}, \mathcal{E})$ *is a CDVNS discrete topology.*

Proposition 5. *For the same universe set* $\mathbf{X}$*, suppose* $(\mathbf{X}, \tau_1, \mathcal{E})$ *and* $(\mathbf{X}, \tau_2, \mathcal{E})$ *be two CDVNS topological spaces. The CDVNS topological space over* $\mathbf{X}$ *is then* $(\mathbf{X}, \tau_1 \cap \tau_2, \mathcal{E})$*.*

Proof. (i). Given that $0_{(\mathbf{X},\mathcal{E})}$*,* $1_{(\mathbf{X},\mathcal{E})} \in \tau_1$ *and* $0_{(\mathbf{X},\mathcal{E})}$*,* $1_{(\mathbf{X},\mathcal{E})} \in \tau_2$*, then* $0_{(\mathbf{X},\mathcal{E})}$*,* $1_{(\mathbf{X},\mathcal{E})} \in \tau_1 \cap \tau_2$*. (ii). Suppose that* $\{(\tilde{\mathbb{F}}_{\mathfrak{i}}, \mathcal{E}) | \mathfrak{i} \in \mathrm{I}\}$ *be a family of CDVNS sets in* $\tau_1 \cap \tau_2$*. Then* $(\tilde{\mathbb{F}}_{\mathfrak{i}}, \mathcal{E}) \in \tau_1$ *and* $(\tilde{\mathbb{F}}_{\mathfrak{i}}, \mathcal{E}) \in \tau_2 \ \forall \ \mathfrak{i} \in \mathrm{I}$*, so* $\cup_{\mathfrak{i}\in\mathrm{I}}(\tilde{\mathbb{F}}_{\mathfrak{i}}, \mathcal{E}) \in \tau_1$ *and* $\cup_{\mathfrak{i}\in\mathrm{I}}(\tilde{\mathbb{F}}_{\mathfrak{i}}, \mathcal{E}) \in \tau_2$*. Hence* $\cup_{\mathfrak{i}\in\mathrm{I}}(\tilde{\mathbb{F}}_{\mathfrak{i}}, \mathcal{E}) \in \tau_1 \cap \tau_2$*. (iii). Let* $\{(\tilde{\mathbb{F}}_{\mathfrak{i}}, \mathcal{E}) | i = \overline{1, n}\}$ *be a family of finite number of CDVNS sets in* $\tau_1 \cap \tau_2$*. So,* $(\tilde{\mathbb{F}}_{\mathfrak{i}}, \mathcal{E}) \in \tau_1$ *and* $(\tilde{\mathbb{F}}_{\mathfrak{i}}, \mathcal{E}) \in \tau_2 \ \forall \ i = \overline{1, n}$*, so* $\bigcap_{\mathfrak{i}=I}^{n}(\tilde{\mathbb{F}}_{\mathfrak{i}}, \mathcal{E}) \in \tau_1$ *and* $\bigcap_{\mathfrak{i}=I}^{n}(\tilde{\mathbb{F}}_{\mathfrak{i}}, \mathcal{E}) \in \tau_2$*. Thus* $\bigcap_{\mathfrak{i}=I}^{n}(\tilde{\mathbb{F}}_{\mathfrak{i}}, \mathcal{E}) \in \tau_1 \cap \tau_2$*.*

Remark 1. *A CDVNS topology over* $\mathbf{X}$ *might not be the union of two CDVNS topologies over* $\mathbf{X}$*.*

Example 2. *Suppose* $\mathcal{E} = \{\mathfrak{e}_1, \mathfrak{e}_2\}$ *be a parameters collection, and* $\mathbf{X} = \{\mathbf{x}_1, \mathbf{x}_2, \mathbf{x}_3\}$ *be an initial universe set, and:*

$$\tau_1 = \{0_{(\mathbf{X},\mathcal{E})}, 1_{(\mathbf{X},\mathcal{E})}, (\tilde{\mathbb{F}}_1, \mathcal{E}), (\tilde{\mathbb{F}}_2, \mathcal{E}), (\tilde{\mathbb{F}}_3, \mathcal{E})\},$$
$$\tau_2 = \{0_{(\mathbf{X},\mathcal{E})}, 1_{(\mathbf{X},\mathcal{E})}, (\tilde{\mathbb{F}}_2, \mathcal{E}), (\tilde{\mathbb{F}}_4, \mathcal{E})\}.$$

be two topologies of CDVNS over $\mathbf{X}$. *Here,* $(\tilde{\mathbb{F}}_1, \mathcal{E})$, $(\tilde{\mathbb{F}}_2, \mathcal{E})$, $(\tilde{\mathbb{F}}_3, \mathcal{E})$, *as well as* $(\tilde{\mathbb{F}}_4, \mathcal{E})$ *are established by the CDVNS described as follows:*

$$(\tilde{\mathbb{F}}_1, \mathcal{E}) = \begin{bmatrix} \mathfrak{e}_1 = \langle \mathbf{x}_1, 0.9e^{\iota\pi(0.9)}, 0.6e^{\iota\pi(0.8)}, 0.2e^{\iota\pi(0.4)}, 0.3e^{\iota\pi(0.5)} \rangle, \\ \langle \mathbf{x}_2, 0.7e^{\iota\pi(0.7)}, 0.6e^{\iota\pi(0.5)}, 0.3e^{\iota\pi(0.3)}, 0.5e^{\iota\pi(0.4)} \rangle \\ \langle \mathbf{x}_3, 0.4e^{\iota\pi(0.3)}, 0.5e^{\iota\pi(0.2)}, 0.3e^{\iota\pi(0.4)}, 0.4e^{\iota\pi(0.2)} \rangle; \\ \mathfrak{e}_2 = \langle \mathbf{x}_1, 0.7e^{\iota\pi(0.9)}, 0.3e^{\iota\pi(0.8)}, 0.3e^{\iota\pi(0.1)}, 0.4e^{\iota\pi(0.7)} \rangle, \\ \langle \mathbf{x}_2, 0.6e^{\iota\pi(0.5)}, 0.5e^{\iota\pi(0.7)}, 0.3e^{\iota\pi(0.3)}, 0.4e^{\iota\pi(0.2)} \rangle, \\ \langle \mathbf{x}_3, 0.7e^{\iota\pi(0.8)}, 0.4e^{\iota\pi(0.4)}, 0.2e^{\iota\pi(0.3)}, 0.3e^{\iota\pi(0.4)} \rangle. \end{bmatrix}$$

$$(\tilde{\mathbb{F}}_2, \mathcal{E}) = \begin{bmatrix} \mathfrak{e}_1 = \langle \mathbf{x}_1, 0.7e^{\iota\pi(0.8)}, 0.5e^{\iota\pi(0.4)}, 0.4e^{\iota\pi(0.4)}, 0.5e^{\iota\pi(0.5)} \rangle, \\ \langle \mathbf{x}_2, 0.6e^{\iota\pi(0.4)}, 0.5e^{\iota\pi(0.5)}, 0.4e^{\iota\pi(0.4)}, 0.7e^{\iota\pi(0.6)} \rangle \\ \langle \mathbf{x}_3, 0.3e^{\iota\pi(0.2)}, 0.4e^{\iota\pi(0.2)}, 0.5e^{\iota\pi(0.7)}, 0.6e^{\iota\pi(0.8)} \rangle; \\ \mathfrak{e}_2 = \langle \mathbf{x}_1, 0.6e^{\iota\pi(0.6)}, 0.2e^{\iota\pi(0.6)}, 0.4e^{\iota\pi(0.3)}, 0.5e^{\iota\pi(0.7)} \rangle, \\ \langle \mathbf{x}_2, 0.5e^{\iota\pi(0.4)}, 0.4e^{\iota\pi(0.1)}, 0.4e^{\iota\pi(0.5)}, 0.6e^{\iota\pi(0.7)} \rangle, \\ \langle \mathbf{x}_3, 0.4e^{\iota\pi(0.3)}, 0.3e^{\iota\pi(0.3)}, 0.6e^{\iota\pi(0.7)}, 0.5e^{\iota\pi(0.4)} \rangle. \end{bmatrix}$$

$$(\tilde{\mathbb{F}}_3, \mathcal{E}) = \begin{bmatrix} \mathfrak{e}_1 = \langle \mathbf{x}_1, 0.5e^{\iota\pi(0.6)}, 0.4e^{\iota\pi(0.2)}, 0.5e^{\iota\pi(0.4)}, 0.6e^{\iota\pi(0.5)} \rangle, \\ \langle \mathbf{x}_2, 0.4e^{\iota\pi(0.2)}, 0.3e^{\iota\pi(0.1)}, 0.5e^{\iota\pi(0.6)}, 0.7e^{\iota\pi(0.7)} \rangle \\ \langle \mathbf{x}_3, 0.2e^{\iota\pi(0.1)}, 0.3e^{\iota\pi(0.2)}, 0.6e^{\iota\pi(0.8)}, 0.8e^{\iota\pi(0.9)} \rangle; \\ \mathfrak{e}_2 = \langle \mathbf{x}_1, 0.4e^{\iota\pi(0.3)}, 0.2e^{\iota\pi(0.1)}, 0.5e^{\iota\pi(0.4)}, 0.6e^{\iota\pi(0.8)} \rangle, \\ \langle \mathbf{x}_2, 0.4e^{\iota\pi(0.3)}, 0.2e^{\iota\pi(0.1)}, 0.5e^{\iota\pi(0.6)}, 0.8e^{\iota\pi(0.9)} \rangle, \\ \langle \mathbf{x}_3, 0.3e^{\iota\pi(0.2)}, 0.3e^{\iota\pi(0.1)}, 0.7e^{\iota\pi(0.9)}, 0.6e^{\iota\pi(0.5)} \rangle. \end{bmatrix}$$

$$(\tilde{\mathbb{F}}_4, \mathcal{E}) = \begin{bmatrix} \mathfrak{e}_1 = \langle \mathbf{x}_1, 0.6e^{\iota\pi(0.7)}, 0.3e^{\iota\pi(0.2)}, 0.1e^{\iota\pi(0.1)}, 0.2e^{\iota\pi(0.1)} \rangle, \\ \langle \mathbf{x}_2, 0.5e^{\iota\pi(0.4)}, 0.3e^{\iota\pi(0.3)}, 0.6e^{\iota\pi(0.6)}, 0.8e^{\iota\pi(0.9)} \rangle \\ \langle \mathbf{x}_3, 0.2e^{\iota\pi(0.2)}, 0.3e^{\iota\pi(0.1)}, 0.7e^{\iota\pi(0.8)}, 0.9e^{\iota\pi(0.9)} \rangle; \\ \mathfrak{e}_2 = \langle \mathbf{x}_1, 0.3e^{\iota\pi(0.3)}, 0.2e^{\iota\pi(0.1)}, 0.6e^{\iota\pi(0.5)}, 0.7e^{\iota\pi(0.8)} \rangle, \\ \langle \mathbf{x}_2, 0.4e^{\iota\pi(0.2)}, 0.1e^{\iota\pi(0.1)}, 0.7e^{\iota\pi(0.8)}, 0.9e^{\iota\pi(0.9)} \rangle, \\ \langle \mathbf{x}_3, 0.2e^{\iota\pi(0.2)}, 0.2e^{\iota\pi(0.1)}, 0.8e^{\iota\pi(0.9)}, 0.7e^{\iota\pi(0.8)} \rangle. \end{bmatrix}$$

Since $(\tilde{\mathbb{F}}_1, \mathcal{E}) \cup (\tilde{\mathbb{F}}_4, \mathcal{E}) \notin \tau_1 \cup \tau_2$, *then* $\tau_1 \cup \tau_2$ *is not a CDVNS topology over* $\mathbf{X}$.

Proposition 6. *Let* $(\mathbf{X}, \tau, \mathcal{E})$ *be a CDVNS topological space over* $\mathbf{X}$ *and*

$$\tau = \{(\tilde{\mathbb{F}}_{\mathrm{i}}, \mathcal{E}) : (\tilde{\mathbb{F}}_{\mathrm{i}}, \mathcal{E}) \in CDVNSS(\mathbf{X}, \mathcal{E})\} = \{[e, \tilde{\mathbb{F}}_{\mathrm{i}}(\mathfrak{e})]_{\mathfrak{e} \in \mathcal{E}} : (\tilde{\mathbb{F}}_{\mathrm{i}}, \mathcal{E}) \in CDVNSS(\mathbf{X}, \mathcal{E})\}$$

where $\tilde{\mathbb{F}}_{\mathrm{i}}(\mathfrak{e}) = \{\langle \mathbf{x}, \mathcal{T}_{\tilde{\mathbb{F}}_{\mathrm{i}}(\mathfrak{e})}(\mathbf{x}), \mathcal{RT}_{\tilde{\mathbb{F}}_{\mathrm{i}}(\mathfrak{e})}(\mathbf{x}), \mathcal{RF}_{\tilde{\mathbb{F}}_{\mathrm{i}}(\mathfrak{e})}(\mathbf{x}), \mathcal{F}_{\tilde{\mathbb{F}}_{\mathrm{i}}(\mathfrak{e})}(\mathbf{x}) \rangle : \mathbf{x} \in \mathbf{X}\}$. *Then*

$$\begin{aligned} \tau_1 &= \{[\mathcal{T}_{\tilde{\mathbb{F}}_{\mathrm{i}}(\mathfrak{e})}(\mathbf{X})]_{\mathfrak{e} \in \mathcal{E}}\} \\ \tau_2 &= \{[\mathcal{RT}_{\tilde{\mathbb{F}}_{\mathrm{i}}(\mathfrak{e})}(\mathbf{X})]_{\mathfrak{e} \in \mathcal{E}}\} \\ \tau_3 &= \{[\mathcal{RF}_{\tilde{\mathbb{F}}_{\mathrm{i}}(\mathfrak{e})}(\mathbf{X})]_{\mathfrak{e} \in \mathcal{E}}\} \\ \tau_4 &= \{[\mathcal{F}_{\tilde{\mathbb{F}}_{\mathrm{i}}(\mathfrak{e})}(\mathbf{X})]_{\mathfrak{e} \in \mathcal{E}}\} \end{aligned}$$

define complex fuzzy soft topologies on $\mathbf{X}$.

Proof. (i). $0_{(\mathbf{X},\mathcal{E})}, 1_{(\mathbf{X},\mathcal{E})} \in \tau \Rightarrow 0,1 \in \tau_1, 0,1 \in \tau_2, 0,1 \in \tau_3 and 0,1 \in \tau_4$. *(ii). Suppose that* $(\tilde{\mathbb{F}}_{\mathfrak{i}}, \mathcal{E})|i \in I$ *be a family of CDVNS sets in* τ. *Then* $\{[\mathcal{T}_{\tilde{\mathbb{F}}_{\mathfrak{i}}(\mathfrak{e})}(\mathbf{X})]_{\mathfrak{e}\in\mathcal{E}}\}_{\mathfrak{i}\in\mathrm{I}}$ *is a collection of complex fuzzy soft sets in* τ_1, $\{[\mathcal{RT}_{\tilde{\mathbb{F}}_{\mathfrak{i}}(\mathfrak{e})}(\mathbf{X})]_{\mathfrak{e}\in\mathcal{E}}\}_{\mathfrak{i}\in\mathrm{I}}$ *is a collection of complex fuzzy soft sets in* τ_2, $\{[\mathcal{RF}_{\tilde{\mathbb{F}}_{\mathfrak{i}}(\mathfrak{e})}(\mathbf{X})]_{\mathfrak{e}\in\mathcal{E}}\}_{\mathfrak{i}\in\mathrm{I}}$ *is a family of complex fuzzy soft sets in* τ_3, $\{[\mathcal{F}_{\tilde{\mathbb{F}}_{\mathfrak{i}}(\mathfrak{e})}(\mathbf{X})]_{\mathfrak{e}\in\mathcal{E}}\}_{\mathfrak{i}\in\mathrm{I}}$ *is a family of complex fuzzy soft sets in* τ_4. *Since* τ *is a CDVNS topology, so* $\cup_{\mathfrak{i}\in\mathrm{I}}(\tilde{\mathbb{F}}_{\mathfrak{i}}, \mathcal{E}) \in \tau_1$. *Which is,*

$$\cup_{\mathfrak{i}\in\mathrm{I}}(\tilde{\mathbb{F}}_{\mathfrak{i}}, \mathcal{E}) = \{\langle sup[\mathcal{T}_{\tilde{\mathbb{F}}_{\mathfrak{i}}(\mathfrak{e})}(\mathbf{X})]_{\mathfrak{e}\in\mathcal{E}}, sup[\mathcal{RT}_{\tilde{\mathbb{F}}_{\mathfrak{i}}(\mathfrak{e})}(\mathbf{X})]_{\mathfrak{e}\in\mathcal{E}}, inf[\mathcal{RF}_{\tilde{\mathbb{F}}_{\mathfrak{i}}(\mathfrak{e})}(\mathbf{X})]_{\mathfrak{e}\in\mathcal{E}}, inf[\mathcal{F}_{\tilde{\mathbb{F}}_{\mathfrak{i}}(\mathfrak{e})}(\mathbf{X})]_{\mathfrak{e}\in\mathcal{E}}\rangle\}_{\mathfrak{i}\in I} \in \tau.$$

Hence,

$$\begin{aligned}
\{sup[\mathcal{T}_{\tilde{\mathbb{F}}_{\mathfrak{i}}(\mathfrak{e})}(\mathbf{X})]_{\mathfrak{e}\in\mathcal{E}}\}_{\mathfrak{i}\in\mathrm{I}} &\in \tau_1\\
\{sup[\mathcal{RT}_{\tilde{\mathbb{F}}_{\mathfrak{i}}(\mathfrak{e})}(\mathbf{X})]_{\mathfrak{e}\in\mathcal{E}}\}_{\mathfrak{i}\in\mathrm{I}} &\in \tau_2\\
\{inf[\mathcal{RF}_{\tilde{\mathbb{F}}_{\mathfrak{i}}(\mathfrak{e})}(\mathbf{X})]_{\mathfrak{e}\in\mathcal{E}}\}_{\mathfrak{i}\in\mathrm{I}} &\in \tau_3\\
\{inf[\mathcal{F}_{\tilde{\mathbb{F}}_{\mathfrak{i}}(\mathfrak{e})}(\mathbf{X})]_{\mathfrak{e}\in\mathcal{E}}\}_{\mathfrak{i}\in\mathrm{I}} &\in \tau_4.
\end{aligned}$$

(iii). Suppose that $\{(\tilde{\mathbb{F}}_{\mathfrak{i}}, \mathcal{E})|i = \overline{1,n}\}$ *be a collection of finite number of CDVNS sets in* τ. *Then* $\{[\mathcal{T}_{\tilde{\mathbb{F}}_{\mathfrak{i}}(\mathfrak{e})}(\mathbf{X})]_{\mathfrak{e}\in\mathcal{E}}\}_{\mathfrak{i}=\overline{1,n}}$ *is a family of complex fuzzy soft sets in* τ_1, $\{[\mathcal{RT}_{\tilde{\mathbb{F}}_{\mathfrak{i}}(\mathfrak{e})}(\mathbf{X})]_{\mathfrak{e}\in\mathcal{E}}\}_{\mathfrak{i}=\overline{1,n}}$ *is a family of complex fuzzy soft sets in* τ_2, $\{[\mathcal{RF}_{\tilde{\mathbb{F}}_{\mathfrak{i}}(\mathfrak{e})}(\mathbf{X})]_{\mathfrak{e}\in\mathcal{E}}\}_{\mathfrak{i}=\overline{1,n}}$ *is a family of complex fuzzy soft sets in* τ_3, $\{[\mathcal{F}_{\tilde{\mathbb{F}}_{\mathfrak{i}}(\mathfrak{e})}(\mathbf{X})]_{\mathfrak{e}\in\mathcal{E}}\}_{\mathfrak{i}=\overline{1,n}}$ *is a family of complex fuzzy soft sets in* τ_4. *Since* τ *is a CDVNS topology, then* $\cap_{\mathfrak{i}=1}^{n}(\tilde{\mathbb{F}}_{\mathfrak{i}}, \mathcal{E}) \in \tau_1$. *That is,*

$$\cap_{\mathfrak{i}=1}^{n}(\tilde{\mathbb{F}}_{\mathfrak{i}}, \mathcal{E}) = \{\langle \min[\mathcal{T}_{\tilde{\mathbb{F}}_{\mathfrak{i}}(\mathfrak{e})}(\mathbf{X})]_{\mathfrak{e}\in\mathcal{E}}, \min[\mathcal{RT}_{\tilde{\mathbb{F}}_{\mathfrak{i}}(\mathfrak{e})}(\mathbf{X})]_{\mathfrak{e}\in\mathcal{E}}, \max[\mathcal{RF}_{\tilde{\mathbb{F}}_{\mathfrak{i}}(\mathfrak{e})}(\mathbf{X})]_{\mathfrak{e}\in\mathcal{E}}, \max[\mathcal{F}_{\tilde{\mathbb{F}}_{\mathfrak{i}}(\mathfrak{e})}(\mathbf{X})]_{\mathfrak{e}\in\mathcal{E}}\rangle\}_{\mathfrak{i}=\overline{1,n}} \in \tau.$$

hence,

$$\begin{aligned}
\{\min[\mathcal{T}_{\tilde{\mathbb{F}}_{\mathfrak{i}}(\mathfrak{e})}(\mathbf{X})]_{\mathfrak{e}\in\mathcal{E}}\}_{\mathfrak{i}\in\mathrm{I}} &\in \tau_1\\
\{\min[\mathcal{RT}_{\tilde{\mathbb{F}}_{\mathfrak{i}}(\mathfrak{e})}(\mathbf{X})]_{\mathfrak{e}\in\mathcal{E}}\}_{\mathfrak{i}\in\mathrm{I}} &\in \tau_2\\
\{\min[\mathcal{RF}_{\tilde{\mathbb{F}}_{\mathfrak{i}}(\mathfrak{e})}(\mathbf{X})]^{c}_{\mathfrak{e}\in\mathcal{E}}\}_{\mathfrak{i}\in\mathrm{I}} &\in \tau_3\\
\{\min[\mathcal{F}_{\tilde{\mathbb{F}}_{\mathfrak{i}}(\mathfrak{e})}(\mathbf{X})]^{c}_{\mathfrak{e}\in\mathcal{E}}\}_{\mathfrak{i}\in\mathrm{I}} &\in \tau_4.
\end{aligned}$$

Remark 2. *The above proposition's converse is typically untrue.*

Example 3. *Consider* $\mathcal{E} = \{\mathfrak{e}_1, \mathfrak{e}_2\}$ *be a collection of parameters, and* $\mathbf{X} = \{\mathbf{x}_1, \mathbf{x}_2, \mathbf{x}_3\}$ *be an initial universe set, and:*

$$\tau_1 = \{0_{(\mathbf{X},\mathcal{E})}, 1_{(\mathbf{X},\mathcal{E})}, (\tilde{\mathbb{F}}_1, \mathcal{E}), (\tilde{\mathbb{F}}_2, \mathcal{E}), (\tilde{\mathbb{F}}_3, \mathcal{E})\}$$

be a CDVNS set family over $\mathbf{X}$. *Here,* $(\tilde{\mathbb{F}}_1, \mathcal{E})$, $(\tilde{\mathbb{F}}_2, \mathcal{E})$ *and* $(\tilde{\mathbb{F}}_3, \mathcal{E})$ *are the CDVNS sets, described as follows:*

$$(\tilde{\mathbb{F}}_1, \mathcal{E}) = \begin{bmatrix}
\mathfrak{e}_1 = \langle \mathbf{x}_1, 0.9e^{\iota\pi(0.9)}, 0.6e^{\iota\pi(0.8)}, 0.2e^{\iota\pi(0.4)}, 0.3e^{\iota\pi(0.7)}\rangle,\\
\quad \langle \mathbf{x}_2, 0.7e^{\iota\pi(0.7)}, 0.6e^{\iota\pi(0.5)}, 0.3e^{\iota\pi(0.3)}, 0.5e^{\iota\pi(0.4)}\rangle\\
\quad \langle \mathbf{x}_3, 0.4e^{\iota\pi(0.3)}, 0.5e^{\iota\pi(0.2)}, 0.3e^{\iota\pi(0.4)}, 0.4e^{\iota\pi(0.2)}\rangle;\\
\mathfrak{e}_2 = \langle \mathbf{x}_1, 0.7e^{\iota\pi(0.9)}, 0.3e^{\iota\pi(0.8)}, 0.3e^{\iota\pi(0.1)}, 0.4e^{\iota\pi(0.7)}\rangle,\\
\quad \langle \mathbf{x}_2, 0.6e^{\iota\pi(0.5)}, 0.5e^{\iota\pi(0.7)}, 0.3e^{\iota\pi(0.3)}, 0.4e^{\iota\pi(0.2)}\rangle,\\
\quad \langle \mathbf{x}_3, 0.7e^{\iota\pi(0.8)}, 0.4e^{\iota\pi(0.4)}, 0.2e^{\iota\pi(0.3)}, 0.3e^{\iota\pi(0.4)}\rangle.
\end{bmatrix}$$

$$(\tilde{\mathbb{F}}_2,\mathcal{E}) = \begin{bmatrix} \mathfrak{e}_1 = \langle \mathbf{x}_1, 0.7e^{\iota\pi(0.8)}, 0.5e^{\iota\pi(0.4)}, 0.4e^{\iota\pi(0.4)}, 0.5e^{\iota\pi(0.8)}\rangle, \\ \quad \langle \mathbf{x}_2, 0.6e^{\iota\pi(0.4)}, 0.5e^{\iota\pi(0.5)}, 0.4e^{\iota\pi(0.4)}, 0.7e^{\iota\pi(0.6)}\rangle \\ \quad \langle \mathbf{x}_3, 0.3e^{\iota\pi(0.2)}, 0.4e^{\iota\pi(0.2)}, 0.5e^{\iota\pi(0.7)}, 0.6e^{\iota\pi(0.8)}\rangle; \\ \mathfrak{e}_2 = \langle \mathbf{x}_1, 0.6e^{\iota\pi(0.6)}, 0.2e^{\iota\pi(0.6)}, 0.4e^{\iota\pi(0.3)}, 0.5e^{\iota\pi(0.8)}\rangle, \\ \quad \langle \mathbf{x}_2, 0.5e^{\iota\pi(0.4)}, 0.4e^{\iota\pi(0.1)}, 0.4e^{\iota\pi(0.5)}, 0.6e^{\iota\pi(0.7)}\rangle, \\ \quad \langle \mathbf{x}_3, 0.4e^{\iota\pi(0.3)}, 0.3e^{\iota\pi(0.3)}, 0.6e^{\iota\pi(0.7)}, 0.5e^{\iota\pi(0.4)}\rangle. \end{bmatrix}$$

$$(\tilde{\mathbb{F}}_3,\mathcal{E}) = \begin{bmatrix} \mathfrak{e}_1 = \langle \mathbf{x}_1, 0.8e^{\iota\pi(0.8)}, 0.4e^{\iota\pi(0.2)}, 0.5e^{\iota\pi(0.4)}, 0.6e^{\iota\pi(0.8)}\rangle, \\ \quad \langle \mathbf{x}_2, 0.4e^{\iota\pi(0.2)}, 0.3e^{\iota\pi(0.1)}, 0.5e^{\iota\pi(0.6)}, 0.7e^{\iota\pi(0.7)}\rangle \\ \quad \langle \mathbf{x}_3, 0.2e^{\iota\pi(0.1)}, 0.3e^{\iota\pi(0.2)}, 0.6e^{\iota\pi(0.8)}, 0.8e^{\iota\pi(0.9)}\rangle; \\ \mathfrak{e}_2 = \langle \mathbf{x}_1, 0.4e^{\iota\pi(0.3)}, 0.2e^{\iota\pi(0.1)}, 0.5e^{\iota\pi(0.4)}, 0.6e^{\iota\pi(0.8)}\rangle, \\ \quad \langle \mathbf{x}_2, 0.4e^{\iota\pi(0.3)}, 0.2e^{\iota\pi(0.1)}, 0.5e^{\iota\pi(0.6)}, 0.8e^{\iota\pi(0.9)}\rangle, \\ \quad \langle \mathbf{x}_3, 0.3e^{\iota\pi(0.2)}, 0.3e^{\iota\pi(0.1)}, 0.7e^{\iota\pi(0.9)}, 0.6e^{\iota\pi(0.5)}\rangle. \end{bmatrix}$$

Then,

$$\begin{aligned}
\tau_1 &= \{\langle \mathcal{T}_{\tilde{\mathbb{F}}_{0_{(\mathbf{X},\mathcal{E})^{(\mathfrak{e})}}}}(\mathbf{X}), \mathcal{T}_{\tilde{\mathbb{F}}_{1_{(\mathbf{X},\mathcal{E})^{(\mathfrak{e})}}}}(\mathbf{X}), \mathcal{T}_{\tilde{\mathbb{F}}_{1(\mathfrak{e})}}(\mathbf{X}), \mathcal{T}_{\tilde{\mathbb{F}}_{2(\mathfrak{e})}}(\mathbf{X}), \mathcal{T}_{\tilde{\mathbb{F}}_{3(\mathfrak{e})}}(\mathbf{X})\rangle_{\mathfrak{e}\in\mathcal{E}}\}, \\
\tau_2 &= \{\langle \mathcal{RT}_{\tilde{\mathbb{F}}_{0_{(\mathbf{X},\mathcal{E})^{(\mathfrak{e})}}}}(\mathbf{X}), \mathcal{RT}_{\tilde{\mathbb{F}}_{1_{(\mathbf{X},\mathcal{E})^{(\mathfrak{e})}}}}(\mathbf{X}), \mathcal{RT}_{\tilde{\mathbb{F}}_{1(\mathfrak{e})}}(\mathbf{X}), \mathcal{RT}_{\tilde{\mathbb{F}}_{2(\mathfrak{e})}}(\mathbf{X}), \mathcal{RT}_{\tilde{\mathbb{F}}_{3(\mathfrak{e})}}(\mathbf{X})\rangle_{\mathfrak{e}\in\mathcal{E}}\}, \\
\tau_3 &= \{\langle \mathcal{RF}_{\tilde{\mathbb{F}}_{0_{(\mathbf{X},\mathcal{E})^{(\mathfrak{e})}}}}(\mathbf{X}), \mathcal{RF}_{\tilde{\mathbb{F}}_{1_{(\mathbf{X},\mathcal{E})^{(\mathfrak{e})}}}}(\mathbf{X}), \mathcal{RF}_{\tilde{\mathbb{F}}_{1(\mathfrak{e})}}(\mathbf{X}), \mathcal{RF}_{\tilde{\mathbb{F}}_{2(\mathfrak{e})}}(\mathbf{X}), \mathcal{RF}_{\tilde{\mathbb{F}}_{3(\mathfrak{e})}}(\mathbf{X})\rangle_{\mathfrak{e}\in\mathcal{E}}\}, \\
\tau_4 &= \{\langle \mathcal{F}_{\tilde{\mathbb{F}}_{0_{(\mathbf{X},\mathcal{E})^{(\mathfrak{e})}}}}(\mathbf{X}), \mathcal{F}_{\tilde{\mathbb{F}}_{1_{(\mathbf{X},\mathcal{E})^{(\mathfrak{e})}}}}(\mathbf{X}), \mathcal{F}_{\tilde{\mathbb{F}}_{1(\mathfrak{e})}}(\mathbf{X}), \mathcal{F}_{\tilde{\mathbb{F}}_{2(\mathfrak{e})}}(\mathbf{X}), \mathcal{F}_{\tilde{\mathbb{F}}_{3(\mathfrak{e})}}(\mathbf{X})\rangle_{\mathfrak{e}\in\mathcal{E}}\}.
\end{aligned}$$

are complex fuzzy soft topologies on $\mathbf{X}$*. For example,*

$$\begin{aligned}
\tau_1 = \{&\langle (0,0,0),(1,1,1),(0.9e^{\iota\pi(0.9)},0.7e^{\iota\pi(0.7)},0.4e^{\iota\pi(0.3)}), \\
&(0.7e^{\iota\pi(0.8)},0.6e^{\iota\pi(0.4)},0.3e^{\iota\pi(0.2)}),(0.8e^{\iota\pi(0.8)},0.4e^{\iota\pi(0.2)},0.2e^{\iota\pi(0.1)})\rangle_{\mathfrak{e}_1}, \\
&\langle (0,0,0),(1,1,1),(0.7e^{\iota\pi(0.9)},0.6e^{\iota\pi(0.5)},0.7e^{\iota\pi(0.8)}), \\
&(0.6e^{\iota\pi(0.6)},0.5e^{\iota\pi(0.4)},0.4e^{\iota\pi(0.3)}),(0.4e^{\iota\pi(0.3)},0.4e^{\iota\pi(0.3)},0.3e^{\iota\pi(0.2)})\rangle_{\mathfrak{e}_2}\}
\end{aligned}$$

$$\begin{aligned}
\tau_2 = \{&\langle (0,0,0),(1,1,1),(0.6e^{\iota\pi(0.8)},0.6e^{\iota\pi(0.5)},0.5e^{\iota\pi(0.2)}), \\
&(0.5e^{\iota\pi(0.4)},0.5e^{\iota\pi(0.5)},0.4e^{\iota\pi(0.2)}),(0.4e^{\iota\pi(0.2)},0.3e^{\iota\pi(0.1)},0.3e^{\iota\pi(0.2)})\rangle_{\mathfrak{e}_1}, \\
&\langle (0,0,0),(1,1,1),(0.3e^{\iota\pi(0.8)},0.5e^{\iota\pi(0.7)},0.4e^{\iota\pi(0.4)}), \\
&(0.2e^{\iota\pi(0.6)},0.4e^{\iota\pi(0.1)},0.3e^{\iota\pi(0.3)}),(0.2e^{\iota\pi(0.1)},0.2e^{\iota\pi(0.1)},0.3e^{\iota\pi(0.1)})\rangle_{\mathfrak{e}_2}\}
\end{aligned}$$

$$\begin{aligned}
\tau_3 = \{&\langle (0,0,0),(1,1,1),(0.2e^{\iota\pi(0.4)},0.3e^{\iota\pi(0.3)},0.3e^{\iota\pi(0.4)}), \\
&(0.4e^{\iota\pi(0.4)},0.4e^{\iota\pi(0.4)},0.5e^{\iota\pi(0.7)}),(0.5e^{\iota\pi(0.3)},0.5e^{\iota\pi(0.6)},0.6e^{\iota\pi(0.8)})\rangle_{\mathfrak{e}_1}, \\
&\langle (0,0,0),(1,1,1),(0.3e^{\iota\pi(0.1)},0.3e^{\iota\pi(0.3)},0.2e^{\iota\pi(0.3)}), \\
&(0.4e^{\iota\pi(0.3)},0.4e^{\iota\pi(0.5)},0.6e^{\iota\pi(0.7)}),(0.5e^{\iota\pi(0.4)},0.5e^{\iota\pi(0.6)},0.7e^{\iota\pi(0.9)})\rangle_{\mathfrak{e}_2}\}
\end{aligned}$$

$$\begin{aligned}
\tau_4 = \{&\langle (0,0,0),(1,1,1),(0.3e^{\iota\pi(0.7)},0.5e^{\iota\pi(0.4)},0.4e^{\iota\pi(0.2)}),
\end{aligned}$$

$$(0.5e^{\iota\pi(0.8)}, 0.7e^{\iota\pi(0.6)}, 0.6e^{\iota\pi(0.8)}), (0.6e^{\iota\pi(0.8)}, 0.7e^{\iota\pi(0.7)}, 0.8e^{\iota\pi(0.9)})\rangle_{\mathfrak{e}_1},$$
$$\langle(0,0,0),(1,1,1),(0.4e^{\iota\pi(0.7)}, 0.4e^{\iota\pi(0.2)}, 0.3e^{\iota\pi(0.4)}),$$
$$(0.5e^{\iota\pi(0.8)}, 0.6e^{\iota\pi(0.7)}, 0.5e^{\iota\pi(0.4)}), (0.6e^{\iota\pi(0.8)}, 0.8e^{\iota\pi(0.9)}, 0.6e^{\iota\pi(0.5)})\rangle_{\mathfrak{e}_2}\}$$

Given that $(\tilde{\mathbb{F}}_2, \mathcal{E}) \cap (\tilde{\mathbb{F}}_3, \mathcal{E}) \notin \tau$, τ *is not a CDVNS topology on* $\mathbf{X}$.

Proposition 7. *Consider that* $(\mathbf{X}, \tau, \mathcal{E})$ *be a CDVNS topological space over* $\mathbf{X}$. *Then*

$$\tau_{1_\mathfrak{e}} = \{[\mathcal{T}_{\tilde{\mathbb{F}}(\mathfrak{e})}(\mathbf{X})] : (\tilde{\mathbb{F}}, \mathcal{E}) \in \tau\}$$
$$\tau_{2_\mathfrak{e}} = \{[\mathcal{RT}_{\tilde{\mathbb{F}}(\mathfrak{e})}(\mathbf{X})] : (\tilde{\mathbb{F}}, \mathcal{E}) \in \tau\}$$
$$\tau_{3_\mathfrak{e}} = \{[\mathcal{RF}_{\tilde{\mathbb{F}}(\mathfrak{e})}(\mathbf{X})] : (\tilde{\mathbb{F}}, \mathcal{E}) \in \tau\}$$
$$\tau_{4_\mathfrak{e}} = \{[\mathcal{F}_{\tilde{\mathbb{F}}(\mathfrak{e})}(\mathbf{X})] : (\tilde{\mathbb{F}}, \mathcal{E}) \in \tau\}$$

$\forall\ \mathfrak{e} \in \mathcal{E}$ *define complex fuzzy topologies on* $\mathbf{X}$.

Remark 3. *In general, the opposite of the aforementioned statement is untrue.*

Example 4. *Consider the Example* 3. *So,*

$$\tau_{1_{\mathfrak{e}_1}} = \{\langle \mathcal{T}_{\tilde{\mathbb{F}}_{0_{(\mathbf{X},\mathcal{E})^{(\mathfrak{e}_1)}}}}(\mathbf{X}), \mathcal{T}_{\tilde{\mathbb{F}}_{1_{(\mathbf{X},\mathcal{E})^{(\mathfrak{e}_1)}}}}(\mathbf{X}), \mathcal{T}_{\tilde{\mathbb{F}}_{1(\mathfrak{e}_1)}}(\mathbf{X}), \mathcal{T}_{\tilde{\mathbb{F}}_{2(\mathfrak{e}_1)}}(\mathbf{X}), \mathcal{T}_{\tilde{\mathbb{F}}_{3(\mathfrak{e}_1)}}(\mathbf{X})\rangle\},$$
$$\tau_{2_{\mathfrak{e}_1}} = \{\langle \mathcal{RT}_{\tilde{\mathbb{F}}_{0_{(\mathbf{X},\mathcal{E})^{(\mathfrak{e}_1)}}}}(\mathbf{X}), \mathcal{RT}_{\tilde{\mathbb{F}}_{1_{(\mathbf{X},\mathcal{E})^{(\mathfrak{e}_1)}}}}(\mathbf{X}), \mathcal{RT}_{\tilde{\mathbb{F}}_{1(\mathfrak{e}_1)}}(\mathbf{X}), \mathcal{RT}_{\tilde{\mathbb{F}}_{2(\mathfrak{e}_1)}}(\mathbf{X}), \mathcal{RT}_{\tilde{\mathbb{F}}_{3(\mathfrak{e}_1)}}(\mathbf{X})\rangle\},$$
$$\tau_{3_{\mathfrak{e}_1}} = \{\langle \mathcal{RF}_{\tilde{\mathbb{F}}_{0_{(\mathbf{X},\mathcal{E})^{(\mathfrak{e}_1)}}}}(\mathbf{X}), \mathcal{RF}_{\tilde{\mathbb{F}}_{1_{(\mathbf{X},\mathcal{E})^{(\mathfrak{e}_1)}}}}(\mathbf{X}), \mathcal{RF}_{\tilde{\mathbb{F}}_{1(\mathfrak{e}_1)}}(\mathbf{X}), \mathcal{RF}_{\tilde{\mathbb{F}}_{2(\mathfrak{e}_1)}}(\mathbf{X}), \mathcal{RF}_{\tilde{\mathbb{F}}_{3(\mathfrak{e}_1)}}(\mathbf{X})\rangle\},$$
$$\tau_{4_{\mathfrak{e}_1}} = \{\langle \mathcal{F}_{\tilde{\mathbb{F}}_{0_{(\mathbf{X},\mathcal{E})^{(\mathfrak{e}_1)}}}}(\mathbf{X}), \mathcal{F}_{\tilde{\mathbb{F}}_{1_{(\mathbf{X},\mathcal{E})^{(\mathfrak{e}_1)}}}}(\mathbf{X}), \mathcal{F}_{\tilde{\mathbb{F}}_{1(\mathfrak{e}_1)}}(\mathbf{X}), \mathcal{F}_{\tilde{\mathbb{F}}_{2(\mathfrak{e}_1)}}(\mathbf{X}), \mathcal{F}_{\tilde{\mathbb{F}}_{3(\mathfrak{e}_1)}}(\mathbf{X})\rangle\}.$$

are complex fuzzy soft topologies on $\mathbf{X}$. *For example,*

$$\tau_{1_{\mathfrak{e}_1}} = \{\langle(0,0,0),(1,1,1),(0.9e^{\iota\pi(0.9)}, 0.7e^{\iota\pi(0.7)}, 0.4e^{\iota\pi(0.3)}),$$
$$(0.7e^{\iota\pi(0.8)}, 0.6e^{\iota\pi(0.4)}, 0.3e^{\iota\pi(0.2)}), (0.8e^{\iota\pi(0.8)}, 0.4e^{\iota\pi(0.2)}, 0.2e^{\iota\pi(0.1)})\rangle\}$$

$$\tau_{2_{\mathfrak{e}_1}} = \{\langle(0,0,0),(1,1,1),(0.6e^{\iota\pi(0.8)}, 0.6e^{\iota\pi(0.5)}, 0.5e^{\iota\pi(0.2)}),$$
$$(0.5e^{\iota\pi(0.4)}, 0.5e^{\iota\pi(0.5)}, 0.4e^{\iota\pi(0.2)}), (0.4e^{\iota\pi(0.2)}, 0.3e^{\iota\pi(0.1)}, 0.3e^{\iota\pi(0.2)})\rangle\}$$

$$\tau_{3_{\mathfrak{e}_1}} = \{\langle(0,0,0),(1,1,1),(0.2e^{\iota\pi(0.4)}, 0.3e^{\iota\pi(0.3)}, 0.3e^{\iota\pi(0.4)}),$$
$$(0.4e^{\iota\pi(0.4)}, 0.4e^{\iota\pi(0.4)}, 0.5e^{\iota\pi(0.7)}), (0.5e^{\iota\pi(0.3)}, 0.5e^{\iota\pi(0.6)}, 0.6e^{\iota\pi(0.8)})\rangle\}$$

$$\tau_{4_{\mathfrak{e}_1}} = \{\langle(0,0,0),(1,1,1),(0.3e^{\iota\pi(0.7)}, 0.5e^{\iota\pi(0.4)}, 0.4e^{\iota\pi(0.2)}),$$
$$(0.5e^{\iota\pi(0.8)}, 0.7e^{\iota\pi(0.6)}, 0.6e^{\iota\pi(0.8)}), (0.6e^{\iota\pi(0.8)}, 0.7e^{\iota\pi(0.7)}, 0.8e^{\iota\pi(0.9)})\rangle\}$$

Here, $\{\tau_{1_{\mathfrak{e}_1}}, \tau_{2_{\mathfrak{e}_1}}, \tau_{3_{\mathfrak{e}_1}}, \tau_{4_{\mathfrak{e}_1}}\}$ *and* $\{\tau_{1_{\mathfrak{e}_2}}, \tau_{2_{\mathfrak{e}_2}}, \tau_{3_{\mathfrak{e}_2}}, \tau_{4_{\mathfrak{e}_2}}\}$ *are complex fuzzy quadri-topology on* $\mathbf{X}$. *But* τ *is not a CDVNS topology on* $\mathbf{X}$.

Definition 24. *Consider a CDVNS topological space* $(\mathbf{X}, \tau, \mathcal{E})$ *over* $\mathbf{X}$ *and a CDVNS set* $(\tilde{\mathbb{F}}, \mathcal{E}) \in CDVNSS(\mathbf{X}, \mathcal{E})$. *Next,* $(\tilde{\mathbb{F}}, \mathcal{E})$*'s CDVNS interior, represented as* $(\tilde{\mathbb{F}}, \mathcal{E})^\circ$ *is defined as the CDVNS union of all of* $(\tilde{\mathbb{F}}, \mathcal{E})$*'s CDVNS open subsets.* $(\tilde{\mathbb{F}}, \mathcal{E})^\circ$ *is evident.* $(\tilde{\mathbb{F}}, \mathcal{E})$ *contains, the largest CDVNS open set.*

Example 5. *The CDVNS topology τ_1, as shown in Example 2, will be examined. Assume the following definition of any $(\tilde{\mathbb{F}},\mathcal{E}) \in CDVNSS(\mathbf{X},\mathcal{E})$:*

$$(\tilde{\mathbb{F}},\mathcal{E}) = \begin{bmatrix} \mathfrak{e}_1 = \langle \mathbf{x}_1, 0.9e^{\iota\pi(0.9)}, 0.7e^{\iota\pi(0.8)}, 0.2e^{\iota\pi(0.1)}, 0.3e^{\iota\pi(0.1)}\rangle, \\ \quad \langle \mathbf{x}_2, 0.8e^{\iota\pi(0.9)}, 0.9e^{\iota\pi(0.7)}, 0.3e^{\iota\pi(0.1)}, 0.3e^{\iota\pi(0.2)}\rangle \\ \quad \langle \mathbf{x}_3, 0.5e^{\iota\pi(0.5)}, 0.6e^{\iota\pi(0.4)}, 0.2e^{\iota\pi(0.1)}, 0.3e^{\iota\pi(0.2)}\rangle; \\ \mathfrak{e}_2 = \langle \mathbf{x}_1, 0.8e^{\iota\pi(0.8)}, 0.5e^{\iota\pi(0.7)}, 0.2e^{\iota\pi(0.1)}, 0.1e^{\iota\pi(0.1)}\rangle, \\ \quad \langle \mathbf{x}_2, 0.7e^{\iota\pi(0.6)}, 0.6e^{\iota\pi(0.8)}, 0.2e^{\iota\pi(0.2)}, 0.2e^{\iota\pi(0.1)}\rangle, \\ \quad \langle \mathbf{x}_3, 0.8e^{\iota\pi(0.7)}, 0.5e^{\iota\pi(0.6)}, 0.1e^{\iota\pi(0.1)}, 0.2e^{\iota\pi(0.3)}\rangle. \end{bmatrix}$$

Then $0_{(\mathbf{X},\mathcal{E})}, (\tilde{\mathbb{F}}_2,\mathcal{E}), (\tilde{\mathbb{F}}_3,\mathcal{E}) \subseteq (\tilde{\mathbb{F}},\mathcal{E})$. Therefore, $(\tilde{\mathbb{F}},\mathcal{E})^\circ = 0_{(\mathbf{X},\mathcal{E})} \cup (\tilde{\mathbb{F}}_2,\mathcal{E}) \cup (\tilde{\mathbb{F}}_3,\mathcal{E}) = (\tilde{\mathbb{F}},\mathcal{E})$.

Theorem 1. *Consider that $(\mathbf{X},\tau,\mathcal{E})$ be a CDVNS topological space over $\mathbf{X}$ and $(\tilde{\mathbb{F}},\mathcal{E}) \in CDVNSS(\mathbf{X},\mathcal{E})$. $(\tilde{\mathbb{F}},\mathcal{E})$ is a CDVNS open set and if and only if $(\tilde{\mathbb{F}},\mathcal{E}) = (\tilde{\mathbb{F}},\mathcal{E})^\circ$.*

Proof. Consider the CDVNS open set $(\tilde{\mathbb{F}},\mathcal{E})$. Then $(\tilde{\mathbb{F}},\mathcal{E})$ equals $(\tilde{\mathbb{F}},\mathcal{E})$, which is the largest CDVNS open set contained by $(\tilde{\mathbb{F}},\mathcal{E})$. It follows that $(\tilde{\mathbb{F}},\mathcal{E}) = (\tilde{\mathbb{F}},\mathcal{E})^\circ$.
If, on the other hand, $(\tilde{\mathbb{F}},\mathcal{E}) = (\tilde{\mathbb{F}},\mathcal{E})^\circ$, then $(\tilde{\mathbb{F}},\mathcal{E})$ is a CDVNS open set, then $(\tilde{\mathbb{F}},\mathcal{E})^\circ$ is a CDVNS open set.

Theorem 2. *The CDVNS topological space over $\mathbf{X}$ is $(\mathbf{X},\tau,\mathcal{E})$. Then $(\tilde{\mathbb{F}}_1,\mathcal{E}), (\tilde{\mathbb{F}}_2,\mathcal{E}) \in CDVNSS(\mathbf{X},\mathcal{E})$. Next,*

(i) $[(\tilde{\mathbb{F}},\mathcal{E})^\circ]^\circ = (\tilde{\mathbb{F}},\mathcal{E})^\circ$,

(ii) $(0_{(\mathbf{X},\mathcal{E})})^\circ = 0_{(\mathbf{X},\mathcal{E})}$ *and* $(1_{(\mathbf{X},\mathcal{E})})^\circ = 1_{(\mathbf{X},\mathcal{E})}$,

(iii) $(\tilde{\mathbb{F}}_1,\mathcal{E}) \subseteq (\tilde{\mathbb{F}}_2,\mathcal{E}) \Rightarrow (\tilde{F}_1,\mathcal{E})^\circ \subseteq (\tilde{\mathbb{F}}_2,\mathcal{E})^\circ$,

(iv) $[(\tilde{\mathbb{F}}_1,\mathcal{E}) \cap (\tilde{\mathbb{F}}_2,\mathcal{E})]^\circ = (\tilde{\mathbb{F}}_1,\mathcal{E})^\circ \cap (\tilde{\mathbb{F}}_2,\mathcal{E})^\circ$,

(v) $(\tilde{\mathbb{F}}_1,\mathcal{E})^\circ \cup (\tilde{\mathbb{F}}_2,\mathcal{E})^\circ \subseteq [(\tilde{\mathbb{F}}_1,\mathcal{E}) \cup (\tilde{\mathbb{F}}_2,\mathcal{E})]^\circ$.

Proof.

(i) Let $(\tilde{\mathbb{F}}_1,\mathcal{E})^\circ = (\tilde{\mathbb{F}}_2,\mathcal{E})$ Then $(\tilde{\mathbb{F}}_2,\mathcal{E}) \in \tau iff (\tilde{\mathbb{F}}_2,\mathcal{E}) = (\tilde{\mathbb{F}}_2,\mathcal{E})^\circ$. So $[(\tilde{\mathbb{F}}_1,\mathcal{E})^\circ]^\circ = (\tilde{\mathbb{F}}_1,\mathcal{E})^\circ$.

(ii) Since $0_{(\mathbf{X},\mathcal{E})}$ and $1_{(\mathbf{X},\mathcal{E})}$ are always CDVNS open sets, we have:

$$(0_{(\mathbf{X},\mathcal{E})})^\circ = 0_{(\mathbf{X},\mathcal{E})}, \quad \text{and} \quad (1_{(\mathbf{X},\mathcal{E})})^\circ = 1_{(\mathbf{X},\mathcal{E})}.$$

(iii) As is well known,$(\tilde{\mathbb{F}}_1,\mathcal{E})^\circ \subseteq (\tilde{\mathbb{F}}_1,\mathcal{E}) \subseteq (\tilde{\mathbb{F}}_2,\mathcal{E})$ and $(\tilde{\mathbb{F}}_2,\mathcal{E})^\circ \subseteq (\tilde{\mathbb{F}}_2,\mathcal{E})$. Since $(\tilde{\mathbb{F}}_2,\mathcal{E})^\circ$ is the biggest CDVNS open set contained in $(\tilde{\mathbb{F}}_2,\mathcal{E})$ and so $(\tilde{\mathbb{F}}_1,\mathcal{E})^\circ \subseteq (\tilde{\mathbb{F}}_2,\mathcal{E})^\circ$.

(iv) Since $(\tilde{\mathbb{F}}_1,\mathcal{E}) \cap (\tilde{\mathbb{F}}_2,\mathcal{E}) \subseteq (\tilde{\mathbb{F}}_1,\mathcal{E})$ and $(\tilde{\mathbb{F}}_1,\mathcal{E}) \cap (\tilde{\mathbb{F}}_2,\mathcal{E}) \subseteq (\tilde{\mathbb{F}}_2,\mathcal{E})$, then $[(\tilde{\mathbb{F}}_1,\mathcal{E}) \cap (\tilde{\mathbb{F}}_2,\mathcal{E})]^\circ \subseteq (\tilde{\mathbb{F}}_1,\mathcal{E})^\circ$ and $[(\tilde{\mathbb{F}}_1,\mathcal{E}) \cap (\tilde{\mathbb{F}}_2,\mathcal{E})]^\circ \subseteq (\tilde{\mathbb{F}}_2,\mathcal{E})^\circ$ and so,

$$[(\tilde{\mathbb{F}}_1,\mathcal{E}) \cap (\tilde{\mathbb{F}}_2,\mathcal{E})]^\circ \subseteq (\tilde{\mathbb{F}}_1,\mathcal{E})^\circ \cap (\tilde{\mathbb{F}}_2,\mathcal{E})^\circ.$$

However, given that $(\tilde{\mathbb{F}}_1,\mathcal{E})^\circ \subseteq (\tilde{\mathbb{F}}_1,\mathcal{E})$ and $(\tilde{\mathbb{F}}_2,\mathcal{E})^\circ \subseteq (\tilde{\mathbb{F}}_2,\mathcal{E})$, then:

$$(\tilde{\mathbb{F}}_1,\mathcal{E})^\circ \cap (\tilde{\mathbb{F}}_2,\mathcal{E})^\circ \subseteq (\tilde{\mathbb{F}}_1,\mathcal{E}) \cap (\tilde{\mathbb{F}}_2,\mathcal{E}).$$

Besides,$[(\tilde{\mathbb{F}}_1,\mathcal{E}) \cap (\tilde{\mathbb{F}}_2,\mathcal{E})]^\circ \subseteq (\tilde{\mathbb{F}}_1,\mathcal{E}) \cap (\tilde{\mathbb{F}}_2,\mathcal{E})$ and is the biggest CDVNS open set. Therefore, $(\tilde{\mathbb{F}}_1,\mathcal{E})^\circ \cap (\tilde{\mathbb{F}}_2,\mathcal{E})^\circ \subseteq [(\tilde{\mathbb{F}}_1,\mathcal{E}) \cap (\tilde{\mathbb{F}}_2,\mathcal{E})]^\circ$. Thus, $[(\tilde{\mathbb{F}}_1,\mathcal{E}) \cap (\tilde{\mathbb{F}}_2,\mathcal{E})]^\circ = (\tilde{\mathbb{F}}_1,\mathcal{E})^\circ \cap (\tilde{\mathbb{F}}_2,\mathcal{E})^\circ$.

(v) Since $(\tilde{\mathbb{F}}_1,\mathcal{E}) \subseteq (\tilde{\mathbb{F}}_1,\mathcal{E}) \cup (\tilde{\mathbb{F}}_2,\mathcal{E})$ and $(\tilde{\mathbb{F}}_2,\mathcal{E}) \subseteq (\tilde{\mathbb{F}}_1,\mathcal{E}) \cup (\tilde{\mathbb{F}}_2,\mathcal{E})$, then:

$$(\tilde{\mathbb{F}}_1,\mathcal{E})^\circ \subseteq [(\tilde{\mathbb{F}}_1,\mathcal{E}) \cup (\tilde{\mathbb{F}}_2,\mathcal{E})]^\circ, \quad \text{and} \quad (\tilde{\mathbb{F}}_2,\mathcal{E})^\circ \subseteq [(\tilde{\mathbb{F}}_1,\mathcal{E}) \cup (\tilde{\mathbb{F}}_2,\mathcal{E})]^\circ.$$

Therefore,

$$(\tilde{\mathbb{F}}_1,\mathcal{E})^\circ \cup (\tilde{\mathbb{F}}_2,\mathcal{E})^\circ \subseteq [(\tilde{\mathbb{F}}_1,\mathcal{E}) \cup (\tilde{\mathbb{F}}_2,\mathcal{E})]^\circ.$$

Definition 25. *Consider a CDVNS topological space $(\mathbf{X},\tau,\mathcal{E})$ over $\mathbf{X}$ and a CDVNS set $(\tilde{\mathbb{F}},\mathcal{E}) \in CDVNSS(\mathbf{X},\mathcal{E})$. The CDVNS intersection of all the CDVNS closed supersets of $(\tilde{\mathbb{F}},\mathcal{E})$ is then the CDVNS closure of $(\tilde{\mathbb{F}},\mathcal{E})$, represented by $\overline{(\tilde{\mathbb{F}},\mathcal{E})}$. It is evident that the smallest CDVNS closed set that contains $(\tilde{\mathbb{F}},\mathcal{E})$ is $\overline{(\tilde{\mathbb{F}},\mathcal{E})}$.*

Example 6. *The CDVNS topology τ_1, as shown in Example 2, will be examined. Assume the following definition of any $(\tilde{\mathbb{F}},\mathcal{E}) \in CDVNSS(\mathbf{X},\mathcal{E})$:*

$$(\tilde{\mathbb{F}},\mathcal{E}) = \begin{bmatrix} \mathfrak{e}_1 = \langle \mathbf{x}_1, 0.2e^{\iota\pi(0.1)}, 0.1e^{\iota\pi(0.1)}, 0.7e^{\iota\pi(0.9)}, 0.9e^{\iota\pi(0.9)}\rangle, \\ \quad \langle \mathbf{x}_2, 0.4e^{\iota\pi(0.2)}, 0.2e^{\iota\pi(0.1)}, 0.7e^{\iota\pi(0.8)}, 0.8e^{\iota\pi(0.9)}\rangle \\ \quad \langle \mathbf{x}_3, 0.1e^{\iota\pi(0.1)}, 0.2e^{\iota\pi(0.1)}, 0.6e^{\iota\pi(0.7)}, 0.8e^{\iota\pi(0.8)}\rangle; \\ \mathfrak{e}_2 = \langle \mathbf{x}_1, 0.1e^{\iota\pi(0.1)}, 0.2e^{\iota\pi(0.1)}, 0.4e^{\iota\pi(0.6)}, 0.8e^{\iota\pi(0.9)}\rangle, \\ \quad \langle \mathbf{x}_2, 0.1e^{\iota\pi(0.1)}, 0.2e^{\iota\pi(0.1)}, 0.6e^{\iota\pi(0.7)}, 0.7e^{\iota\pi(0.6)}\rangle, \\ \quad \langle \mathbf{x}_3, 0.2e^{\iota\pi(0.3)}, 0.1e^{\iota\pi(0.2)}, 0.5e^{\iota\pi(0.8)}, 0.8e^{\iota\pi(0.8)}\rangle. \end{bmatrix}$$

Evidently, $(0_{(\mathbf{X},\mathcal{E})})^c, (1_{(\mathbf{X},\mathcal{E})})^c, (\tilde{\mathbb{F}}_1,\mathcal{E})^c, (\tilde{\mathbb{F}}_2,\mathcal{E})^c, and (\tilde{\mathbb{F}}_3,\mathcal{E})^c$ are all CDVNS closed sets over $(\mathbf{X},\tau_1,\mathcal{E})$. They are given as following:

$$(0_{(\mathbf{X},\mathcal{E})})^c = 1_{(\mathbf{X},\mathcal{E})}, \quad (1_{(\mathbf{X},\mathcal{E})})^c = 0_{(\mathbf{X},\mathcal{E})}$$

$$(\tilde{\mathbb{F}}_1,\mathcal{E})^c = \begin{bmatrix} \mathfrak{e}_1 = \langle \mathbf{x}_1, 0.3e^{\iota\pi(0.5)}, 0.2e^{\iota\pi(0.4)}, 0.6e^{\iota\pi(0.8)}, 0.9e^{\iota\pi(0.9)}\rangle, \\ \quad \langle \mathbf{x}_2, 0.5e^{\iota\pi(0.4)}, 0.3e^{\iota\pi(0.3)}, 0.6e^{\iota\pi(0.5)}, 0.7e^{\iota\pi(0.7)}\rangle \\ \quad \langle \mathbf{x}_3, 0.4e^{\iota\pi(0.2)}, 0.3e^{\iota\pi(0.4)}, 0.5e^{\iota\pi(0.2)}, 0.4e^{\iota\pi(0.3)}\rangle; \\ \mathfrak{e}_2 = \langle \mathbf{x}_1, 0.4e^{\iota\pi(0.7)}, 0.3e^{\iota\pi(0.1)}, 0.3e^{\iota\pi(0.8)}, 0.7e^{\iota\pi(0.9)}\rangle, \\ \quad \langle \mathbf{x}_2, 0.4e^{\iota\pi(0.2)}, 0.3e^{\iota\pi(0.3)}, 0.5e^{\iota\pi(0.7)}, 0.6e^{\iota\pi(0.5)}\rangle, \\ \quad \langle \mathbf{x}_3, 0.3e^{\iota\pi(0.4)}, 0.2e^{\iota\pi(0.3)}, 0.4e^{\iota\pi(0.4)}, 0.7e^{\iota\pi(0.8)}\rangle. \end{bmatrix}$$

$$(\tilde{\mathbb{F}}_2,\mathcal{E})^c = \begin{bmatrix} \mathfrak{e}_1 = \langle \mathbf{x}_1, 0.5e^{\iota\pi(0.5)}, 0.4e^{\iota\pi(0.4)}, 0.5e^{\iota\pi(0.4)}, 0.7e^{\iota\pi(0.8)}\rangle, \\ \quad \langle \mathbf{x}_2, 0.7e^{\iota\pi(0.6)}, 0.4e^{\iota\pi(0.4)}, 0.5e^{\iota\pi(0.5)}, 0.6e^{\iota\pi(0.4)}\rangle \\ \quad \langle \mathbf{x}_3, 0.6e^{\iota\pi(0.8)}, 0.5e^{\iota\pi(0.7)}, 0.4e^{\iota\pi(0.2)}, 0.3e^{\iota\pi(0.2)}\rangle; \\ \mathfrak{e}_2 = \langle \mathbf{x}_1, 0.5e^{\iota\pi(0.7)}, 0.4e^{\iota\pi(0.3)}, 0.2e^{\iota\pi(0.6)}, 0.6e^{\iota\pi(0.6)}\rangle, \\ \quad \langle \mathbf{x}_2, 0.6e^{\iota\pi(0.7)}, 0.4e^{\iota\pi(0.5)}, 0.4e^{\iota\pi(0.1)}, 0.5e^{\iota\pi(0.4)}\rangle, \\ \quad \langle \mathbf{x}_3, 0.5e^{\iota\pi(0.4)}, 0.6e^{\iota\pi(0.7)}, 0.3e^{\iota\pi(0.3)}, 0.4e^{\iota\pi(0.3)}\rangle. \end{bmatrix}$$

$$(\tilde{\mathbb{F}}_3,\mathcal{E})^c = \begin{bmatrix} \mathfrak{e}_1 = \langle \mathbf{x}_1, 0.6e^{\iota\pi(0.5)}, 0.5e^{\iota\pi(0.4)}, 0.4e^{\iota\pi(0.2)}, 0.5e^{\iota\pi(0.6)}\rangle, \\ \quad \langle \mathbf{x}_2, 0.7e^{\iota\pi(0.7)}, 0.5e^{\iota\pi(0.6)}, 0.3e^{\iota\pi(0.1)}, 0.4e^{\iota\pi(0.2)}\rangle \\ \quad \langle \mathbf{x}_3, 0.8e^{\iota\pi(0.9)}, 0.6e^{\iota\pi(0.8)}, 0.3e^{\iota\pi(0.2)}, 0.2e^{\iota\pi(0.1)}\rangle; \\ \mathfrak{e}_2 = \langle \mathbf{x}_1, 0.6e^{\iota\pi(0.8)}, 0.5e^{\iota\pi(0.4)}, 0.2e^{\iota\pi(0.1)}, 0.4e^{\iota\pi(0.3)}\rangle, \\ \quad \langle \mathbf{x}_2, 0.8e^{\iota\pi(0.9)}, 0.5e^{\iota\pi(0.6)}, 0.2e^{\iota\pi(0.1)}, 0.4e^{\iota\pi(0.3)}\rangle, \\ \quad \langle \mathbf{x}_3, 0.6e^{\iota\pi(0.5)}, 0.7e^{\iota\pi(0.9)}, 0.3e^{\iota\pi(0.1)}, 0.3e^{\iota\pi(0.2)}\rangle. \end{bmatrix}$$

Then $(1_{(\mathbf{X},\mathcal{E})})^c, (\tilde{\mathbb{F}}_1,\mathcal{E})^c, (\tilde{\mathbb{F}}_2,\mathcal{E})^c, (\tilde{\mathbb{F}}_3,\mathcal{E})^c \supseteq (\tilde{\mathbb{F}},\mathcal{E})$. *Therefore,*

$$\overline{(\tilde{\mathbb{F}},\mathcal{E})} = (1_{(\mathbf{X},\mathcal{E})})^c \cap (\tilde{\mathbb{F}}_1,\mathcal{E})^c \cap (\tilde{\mathbb{F}}_3,\mathcal{E})^c \cap (\tilde{\mathbb{F}}_2,\mathcal{E})^c = (\tilde{\mathbb{F}}_1,\mathcal{E})^c$$

.

Theorem 3. *Consider* $(\mathbf{X},\tau,\mathcal{E})$ *be a CDVNS topological space over* $\mathbf{X}$ *and* $(\tilde{\mathbb{F}},\mathcal{E}) \in CDVNSS(\mathbf{X},\mathcal{E})$. $(\tilde{\mathbb{F}},\mathcal{E})$ *is a CDVNS closed set and if and only if* $(\tilde{\mathbb{F}},\mathcal{E}) = \overline{(\tilde{\mathbb{F}},\mathcal{E})}$.

Proof. Consider that $(\tilde{\mathbb{F}},\mathcal{E})$ be a CDVNS closed set. Then the smallest CDVNS open set that containing $(\tilde{\mathbb{F}},\mathcal{E})$ is equal to $(\tilde{\mathbb{F}},\mathcal{E})$. Hence, $(\tilde{\mathbb{F}},\mathcal{E}) = \overline{(\tilde{\mathbb{F}},\mathcal{E})}$
On the other hand, it is recognized that $\overline{(\tilde{\mathbb{F}},\mathcal{E})}$ is a CDVNS closed set and if $(\tilde{\mathbb{F}},\mathcal{E}) = \overline{(\tilde{\mathbb{F}},\mathcal{E})}$, so $(\tilde{\mathbb{F}},\mathcal{E})$ is a CDVNS closed set.

Theorem 4. *The CDVNS topological space over* $\mathbf{X}$ *is* $(\mathbf{X},\tau,\mathcal{E})$. *Then* $(\tilde{\mathbb{F}}_1,\mathcal{E}), (\tilde{\mathbb{F}}_2,\mathcal{E}) \in CDVNSS(\mathbf{X},\mathcal{E})$. *So,*

(i) $\overline{[\overline{(\tilde{\mathbb{F}},\mathcal{E})}]} = \overline{(\tilde{\mathbb{F}},\mathcal{E})}$,

(ii) $\overline{(0_{(\mathbf{X},\mathcal{E})})} = 0_{(\mathbf{X},\mathcal{E})}$ *and* $\overline{(1_{(\mathbf{X},\mathcal{E})})} = 1_{(\mathbf{X},\mathcal{E})}$,

(iii) $(\tilde{\mathbb{F}}_1,\mathcal{E}) \subseteq (\tilde{\mathbb{F}}_2,\mathcal{E}) \Rightarrow \overline{(\tilde{\mathbb{F}}_1,\mathcal{E})} \subseteq \overline{(\tilde{\mathbb{F}}_2,\mathcal{E})}$,

(iv) $\overline{[(\tilde{\mathbb{F}}_1,\mathcal{E}) \cup (\tilde{\mathbb{F}}_2,\mathcal{E})]} = \overline{(\tilde{\mathbb{F}}_1,\mathcal{E})} \cup \overline{(\tilde{\mathbb{F}}_2,\mathcal{E})}$,

(v) $\overline{(\tilde{\mathbb{F}}_1,\mathcal{E})} \cap \overline{(\tilde{\mathbb{F}}_2,\mathcal{E})} \subseteq \overline{[(\tilde{\mathbb{F}}_1,\mathcal{E}) \cap (\tilde{\mathbb{F}}_2,\mathcal{E})]}$.

Proof.

(i) Let $\overline{(\tilde{\mathbb{F}}_1,\mathcal{E})} = (\tilde{\mathbb{F}}_2,\mathcal{E})$ Then $(\tilde{\mathbb{F}}_2,\mathcal{E})$ a CDVNS closed set.Hence $(\tilde{\mathbb{F}}_2,\mathcal{E})$ and $\overline{(\tilde{\mathbb{F}}_2,\mathcal{E})}$ are equal. Therefore $\overline{[\overline{(\tilde{\mathbb{F}}_1,\mathcal{E})}]} = \overline{(\tilde{\mathbb{F}}_1,\mathcal{E})}$.

(ii) Since $0_{(\mathbf{X},\mathcal{E})}$ and $1_{(\mathbf{X},\mathcal{E})}$ are always CDVNS closed sets, we have:

$$\overline{(0_{(\mathbf{X},\mathcal{E})})} = 0_{(\mathbf{X},\mathcal{E})}, \quad \text{and} \quad \overline{(1_{(\mathbf{X},\mathcal{E})})} = 1_{(\mathbf{X},\mathcal{E})}.$$

(iii) It is known that $(\tilde{\mathbb{F}}_1,\mathcal{E}) \subseteq \overline{(\tilde{\mathbb{F}}_1,\mathcal{E})}$ and $(\tilde{\mathbb{F}}_2,\mathcal{E}) \subseteq \overline{(\tilde{\mathbb{F}}_2,\mathcal{E})}$, so $(\tilde{\mathbb{F}}_1,\mathcal{E}) \subseteq (\tilde{\mathbb{F}}_2,\mathcal{E}) \subseteq \overline{(\tilde{\mathbb{F}}_2,\mathcal{E})}$. Since $\overline{(\tilde{\mathbb{F}}_2,\mathcal{E})}$ is the smallest CDVNS closed set containing $(\tilde{\mathbb{F}}_1,\mathcal{E})$, then $\overline{(\tilde{\mathbb{F}}_1,\mathcal{E})} \subseteq \overline{(\tilde{\mathbb{F}}_2,\mathcal{E})}$.

(iv) Since $(\tilde{\mathbb{F}}_1,\mathcal{E}) \subseteq (\tilde{\mathbb{F}}_1,\mathcal{E}) \cup (\tilde{\mathbb{F}}_2,\mathcal{E})$ and $(\tilde{\mathbb{F}}_2,\mathcal{E}) \subseteq (\tilde{\mathbb{F}}_1,\mathcal{E}) \cup (\tilde{\mathbb{F}}_2,\mathcal{E})$, then $\overline{(\tilde{\mathbb{F}}_1,\mathcal{E})} \subseteq \overline{[(\tilde{\mathbb{F}}_1,\mathcal{E}) \cup (\tilde{\mathbb{F}}_2,\mathcal{E})]}$ and $\overline{(\tilde{\mathbb{F}}_2,\mathcal{E})} \subseteq \overline{[(\tilde{\mathbb{F}}_1,\mathcal{E}) \cup (\tilde{\mathbb{F}}_2,\mathcal{E})]}$ and so,

$$\overline{(\tilde{\mathbb{F}}_1,\mathcal{E})} \cup \overline{(\tilde{\mathbb{F}}_2,\mathcal{E})} \subseteq \overline{[(\tilde{\mathbb{F}}_1,\mathcal{E}) \cup (\tilde{\mathbb{F}}_2,\mathcal{E})]}.$$

Conversely, since $(\tilde{\mathbb{F}}_1,\mathcal{E}) \subseteq \overline{(\tilde{\mathbb{F}}_1,\mathcal{E})}$ and $(\tilde{\mathbb{F}}_2,\mathcal{E}) \subseteq \overline{(\tilde{\mathbb{F}}_2,\mathcal{E})}$, then:

$$(\tilde{\mathbb{F}}_1,\mathcal{E}) \cup (\tilde{\mathbb{F}}_2,\mathcal{E}) \subseteq \overline{(\tilde{\mathbb{F}}_1,\mathcal{E})} \cup \overline{(\tilde{\mathbb{F}}_2,\mathcal{E})}.$$

Besides,$\overline{[(\tilde{\mathbb{F}}_1,\mathcal{E}) \cup (\tilde{\mathbb{F}}_2,\mathcal{E})]}$ and is the smallest CDVNS closed set that containing $(\tilde{\mathbb{F}}_1,\mathcal{E}) \cup (\tilde{\mathbb{F}}_2,\mathcal{E})$. Therefore, $\overline{[(\tilde{\mathbb{F}}_1,\mathcal{E}) \cup (\tilde{\mathbb{F}}_2,\mathcal{E})]} \subseteq \overline{(\tilde{\mathbb{F}}_1,\mathcal{E})} \cup \overline{(\tilde{\mathbb{F}}_2,\mathcal{E})}$. Thus, $\overline{[(\tilde{\mathbb{F}}_1,\mathcal{E}) \cup (\tilde{\mathbb{F}}_2,\mathcal{E})]} = \overline{(\tilde{\mathbb{F}}_1,\mathcal{E})} \cup \overline{(\tilde{\mathbb{F}}_2,\mathcal{E})}$.

(v) Since

$$(\tilde{\mathbb{F}}_1,\mathcal{E})\cap(\tilde{\mathbb{F}}_2,\mathcal{E})\subseteq\overline{[(\tilde{\mathbb{F}}_1,\mathcal{E})\cap(\tilde{\mathbb{F}}_2,\mathcal{E})]},\quad\text{and}\quad\overline{[(\tilde{\mathbb{F}}_1,\mathcal{E})\cap(\tilde{\mathbb{F}}_2,\mathcal{E})]}.$$

is the smallest CDVNS closed set that containing $(\tilde{\mathbb{F}}_1,\mathcal{E})\cap(\tilde{\mathbb{F}}_2,\mathcal{E})$. Then,

$$\overline{[(\tilde{\mathbb{F}}_1,\mathcal{E})\cap(\tilde{\mathbb{F}}_2,\mathcal{E})]}\subseteq\overline{(\tilde{\mathbb{F}}_1,\mathcal{E})}\cap\overline{(\tilde{\mathbb{F}}_2,\mathcal{E})}.$$

Theorem 5. *The CDVNS topological space over* $\mathbf{X}$ *is* $(\mathbf{X},\tau,\mathcal{E})$. *Then,* $(\tilde{\mathbb{F}},\mathcal{E})\in CDVNSS(\mathbf{X},\mathcal{E})$. *So:*

(i) $\overline{[(\tilde{\mathbb{F}},\mathcal{E})]^c}=[(\tilde{\mathbb{F}},\mathcal{E})^c]^\circ$,

(ii) $[(\tilde{\mathbb{F}},\mathcal{E})^\circ]^c=\overline{[(\tilde{\mathbb{F}},\mathcal{E})^c]}$.

Proof.

(i)

$$\begin{aligned}\overline{(\tilde{\mathbb{F}},\mathcal{E})}&=\cap\{(\tilde{\mathbb{G}},\mathcal{E})\in\tau^c:(\tilde{\mathbb{G}},\mathcal{E})\supseteq(\tilde{\mathbb{F}},\mathcal{E})\}\\&\Rightarrow[\overline{(\tilde{\mathbb{F}},\mathcal{E})}]^c=\Big[\cap\{(\tilde{\mathbb{G}},\mathcal{E})\in\tau^c:(\tilde{\mathbb{G}},\mathcal{E})\supseteq(\tilde{\mathbb{F}},\mathcal{E})\}\Big]^c\\&=\cup\{(\tilde{\mathbb{G}},\mathcal{E})^c\in\tau:(\tilde{\mathbb{G}},\mathcal{E})^c\subseteq(\tilde{\mathbb{F}},\mathcal{E})^c\}\\&=[(\tilde{\mathbb{F}},\mathcal{E})^c]^\circ.\end{aligned}$$

(ii)

$$\begin{aligned}(\tilde{\mathbb{F}},\mathcal{E})^\circ&=\cup\{(\tilde{\mathbb{G}},\mathcal{E})\in\tau:(\tilde{\mathbb{G}},\mathcal{E})\subseteq(\tilde{\mathbb{F}},\mathcal{E})\}\\&\Rightarrow[(\tilde{\mathbb{F}},\mathcal{E})^\circ]^c=\Big[\cap\{(\tilde{\mathbb{G}},\mathcal{E})\in\tau:(\tilde{\mathbb{G}},\mathcal{E})\subseteq(\tilde{\mathbb{F}},\mathcal{E})\}\Big]^c\\&=\cap\{(\tilde{\mathbb{G}},\mathcal{E})^c\in\tau^c:(\tilde{\mathbb{G}},\mathcal{E})^c\supseteq(\tilde{\mathbb{F}},\mathcal{E})^c\}\\&=\overline{[(\tilde{\mathbb{F}},\mathcal{E})^c]}.\end{aligned}$$

5. Methodology and Analytical Framework

Consider a framework for emotional analysis where the set $T=\{T_1,T_2,T_3,T_4\}$ represents individuals who are the recipients of emotional energy. The expression of this energy is captured through the set $S=\{S_1,S_2,S_3,S_4\}$, which encompasses a range of communicative channels including gestures, tone of voice, verbal communication, and digital interactions. These observed signals are then classified into distinct emotional categories defined by the set $C=\{C_1,C_2,C_3,C_4\}$, which correspond to the states of admiration, attachment, infatuation, and genuine love. The objective of this model is to systematically evaluate the signals from set S, as directed toward targets in set T, to accurately assign them to the most appropriate emotional category in set C, thereby identifying the true nature of the affective relationship. The cotangent similarity measures between T_i and C_j is defined as:
$Cotangent_{DNSS}(T_i,C_j)=$

$$\frac{1}{n}\sum_{k=1}^{n}\{\cot[\frac{\pi}{4}+\frac{\pi}{12}(|\mathcal{T}_{ik}-\mathcal{T}_{jk}|+|\mathcal{RT}_{ik}-\mathcal{RT}_{jk}|+|\mathcal{RF}_{ik}-\mathcal{RF}_{jk}|+|\mathcal{F}_{ik}-\mathcal{F}_{jk}|)]\}$$

Table 1: Emotional Affinity Feature Matrix for Signal-Based Interaction Analysis ($T \times S$)

	S_1	S_2	...	S_n
T_1	$\mathcal{T}_{11}, \mathcal{RT}_{11}, \mathcal{RF}_{11}, \mathcal{F}_{11}$	$\mathcal{T}_{12}, \mathcal{RT}_{12}, \mathcal{RF}_{12}, \mathcal{F}_{12}$	...	$\mathcal{T}_{1n}, \mathcal{RT}_{1n}, \mathcal{RF}_{1n}, \mathcal{F}_{1n}$
T_2	$\mathcal{T}_{21}, \mathcal{RT}_{21}, \mathcal{RF}_{21}, \mathcal{F}_{21}$	$\mathcal{T}_{22}, \mathcal{RT}_{22}, \mathcal{RF}_{22}, \mathcal{F}_{22}$	...	$\mathcal{T}_{2n}, \mathcal{RT}_{2n}, \mathcal{RF}_{2n}, \mathcal{F}_{2n}$
...	...	...	...	...
T_m	$\mathcal{T}_{m1}, \mathcal{RT}_{m1}, \mathcal{RF}_{m1}, \mathcal{F}_{m1}$	$\mathcal{T}_{m2}, \mathcal{RT}_{m2}, \mathcal{RF}_{m2}, \mathcal{F}_{m2}$	...	$\mathcal{T}_{mn}, \mathcal{RT}_{mn}, \mathcal{RF}_{mn}, \mathcal{F}_{mn}$

Table 2: Emotional Classification Matrix for Signal-Based Affectional Mapping ($T \times S \to C$)

Row-I	S_1	S_2	S_3	S_4	**Row-II**	C_1	C_2	C_3	C_4
T_1	$\begin{pmatrix} 0.6e^{\iota\pi(0.4)} \\ 0.5e^{\iota\pi(0.5)} \\ 0.7e^{\iota\pi(0.6)} \\ 0.3e^{\iota\pi(0.4)} \end{pmatrix}$	$\begin{pmatrix} 0.7e^{\iota\pi(0.4)} \\ 0.2e^{\iota\pi(0.5)} \\ 0.8e^{\iota\pi(0.8)} \\ 0.5e^{\iota\pi(0.7)} \end{pmatrix}$	$\begin{pmatrix} 0.4e^{\iota\pi(0.4)} \\ 0.6e^{\iota\pi(0.8)} \\ 0.3e^{\iota\pi(0.6)} \\ 0.2e^{\iota\pi(0.4)} \end{pmatrix}$	$\begin{pmatrix} 0.7e^{\iota\pi(0.9)} \\ 0.6e^{\iota\pi(0.2)} \\ 0.5e^{\iota\pi(0.6)} \\ 0.4e^{\iota\pi(0.6)} \end{pmatrix}$	S_1	$\begin{pmatrix} 0.9e^{\iota\pi(0.9)} \\ 0.4e^{\iota\pi(0.2)} \\ 0.3e^{\iota\pi(0.6)} \\ 0.5e^{\iota\pi(0.9)} \end{pmatrix}$	$\begin{pmatrix} 0.2e^{\iota\pi(0.3)} \\ 0.1e^{\iota\pi(0.2)} \\ 0.6e^{\iota\pi(0.2)} \\ 0.3e^{\iota\pi(0.6)} \end{pmatrix}$	$\begin{pmatrix} 0.2e^{\iota\pi(0.5)} \\ 0.5e^{\iota\pi(0.2)} \\ 0.3e^{\iota\pi(0.6)} \\ 0.7e^{\iota\pi(0.6)} \end{pmatrix}$	$\begin{pmatrix} 0.4e^{\iota\pi(0.3)} \\ 0.5e^{\iota\pi(0.2)} \\ 0.7e^{\iota\pi(0.6)} \\ 0.8e^{\iota\pi(0.7)} \end{pmatrix}$
T_2	$\begin{pmatrix} 0.5e^{\iota\pi(0.6)} \\ 0.7e^{\iota\pi(0.6)} \\ 0.8e^{\iota\pi(0.9)} \\ 0.4e^{\iota\pi(0.4)} \end{pmatrix}$	$\begin{pmatrix} 0.6e^{\iota\pi(0.6)} \\ 0.9e^{\iota\pi(0.6)} \\ 0.5e^{\iota\pi(0.7)} \\ 0.7e^{\iota\pi(0.4)} \end{pmatrix}$	$\begin{pmatrix} 0.2e^{\iota\pi(0.1)} \\ 0.9e^{\iota\pi(0.3)} \\ 0.2e^{\iota\pi(0.3)} \\ 0.6e^{\iota\pi(0.5)} \end{pmatrix}$	$\begin{pmatrix} 0.1e^{\iota\pi(0.4)} \\ 0.5e^{\iota\pi(0.9)} \\ 0.7e^{\iota\pi(0.7)} \\ 0.3e^{\iota\pi(0.3)} \end{pmatrix}$	S_2	$\begin{pmatrix} 0.2e^{\iota\pi(0.2)} \\ 0.5e^{\iota\pi(0.4)} \\ 0.8e^{\iota\pi(0.8)} \\ 0.9e^{\iota\pi(0.4)} \end{pmatrix}$	$\begin{pmatrix} 0.3e^{\iota\pi(0.3)} \\ 0.4e^{\iota\pi(0.9)} \\ 0.2e^{\iota\pi(0.1)} \\ 0.7e^{\iota\pi(0.1)} \end{pmatrix}$	$\begin{pmatrix} 0.4e^{\iota\pi(0.6)} \\ 0.7e^{\iota\pi(0.5)} \\ 0.2e^{\iota\pi(0.5)} \\ 0.6e^{\iota\pi(0.1)} \end{pmatrix}$	$\begin{pmatrix} 0.5e^{\iota\pi(0.2)} \\ 0.8e^{\iota\pi(0.2)} \\ 0.9e^{\iota\pi(0.4)} \\ 0.2e^{\iota\pi(0.4)} \end{pmatrix}$
T_3	$\begin{pmatrix} 0.3e^{\iota\pi(0.4)} \\ 0.9e^{\iota\pi(0.2)} \\ 0.6e^{\iota\pi(0.6)} \\ 0.3e^{\iota\pi(0.3)} \end{pmatrix}$	$\begin{pmatrix} 0.8e^{\iota\pi(0.9)} \\ 0.6e^{\iota\pi(0.1)} \\ 0.7e^{\iota\pi(0.8)} \\ 0.5e^{\iota\pi(0.5)} \end{pmatrix}$	$\begin{pmatrix} 0.6e^{\iota\pi(0.5)} \\ 0.4e^{\iota\pi(0.4)} \\ 0.7e^{\iota\pi(0.9)} \\ 0.3e^{\iota\pi(0.3)} \end{pmatrix}$	$\begin{pmatrix} 0.2e^{\iota\pi(0.2)} \\ 0.4e^{\iota\pi(0.5)} \\ 0.8e^{\iota\pi(0.6)} \\ 0.5e^{\iota\pi(0.4)} \end{pmatrix}$	S_3	$\begin{pmatrix} 0.1e^{\iota\pi(0.1)} \\ 0.7e^{\iota\pi(0.5)} \\ 0.6e^{\iota\pi(0.2)} \\ 0.4e^{\iota\pi(0.9)} \end{pmatrix}$	$\begin{pmatrix} 0.7e^{\iota\pi(0.4)} \\ 0.8e^{\iota\pi(0.5)} \\ 0.7e^{\iota\pi(0.6)} \\ 0.1e^{\iota\pi(0.4)} \end{pmatrix}$	$\begin{pmatrix} 0.6e^{\iota\pi(0.7)} \\ 0.9e^{\iota\pi(0.5)} \\ 0.6e^{\iota\pi(0.4)} \\ 0.3e^{\iota\pi(0.2)} \end{pmatrix}$	$\begin{pmatrix} 0.6e^{\iota\pi(0.4)} \\ 0.7e^{\iota\pi(0.5)} \\ 0.4e^{\iota\pi(0.6)} \\ 0.2e^{\iota\pi(0.4)} \end{pmatrix}$
T_4	$\begin{pmatrix} 0.7e^{\iota\pi(0.7)} \\ 0.4e^{\iota\pi(0.4)} \\ 0.2e^{\iota\pi(0.9)} \\ 0.8e^{\iota\pi(0.8)} \end{pmatrix}$	$\begin{pmatrix} 0.9e^{\iota\pi(0.1)} \\ 0.3e^{\iota\pi(0.2)} \\ 0.6e^{\iota\pi(0.6)} \\ 0.3e^{\iota\pi(0.3)} \end{pmatrix}$	$\begin{pmatrix} 0.8e^{\iota\pi(0.7)} \\ 0.5e^{\iota\pi(0.9)} \\ 0.8e^{\iota\pi(0.6)} \\ 0.6e^{\iota\pi(0.5)} \end{pmatrix}$	$\begin{pmatrix} 0.6e^{\iota\pi(0.7)} \\ 0.1e^{\iota\pi(0.2)} \\ 0.6e^{\iota\pi(0.9)} \\ 0.2e^{\iota\pi(0.2)} \end{pmatrix}$	S_4	$\begin{pmatrix} 0.7e^{\iota\pi(0.4)} \\ 0.6e^{\iota\pi(0.5)} \\ 0.4e^{\iota\pi(0.6)} \\ 0.6e^{\iota\pi(0.5)} \end{pmatrix}$	$\begin{pmatrix} 0.6e^{\iota\pi(0.6)} \\ 0.2e^{\iota\pi(0.1)} \\ 0.9e^{\iota\pi(0.8)} \\ 0.8e^{\iota\pi(0.4)} \end{pmatrix}$	$\begin{pmatrix} 0.3e^{\iota\pi(0.3)} \\ 0.8e^{\iota\pi(0.9)} \\ 0.7e^{\iota\pi(0.7)} \\ 0.1e^{\iota\pi(0.4)} \end{pmatrix}$	$\begin{pmatrix} 0.9e^{\iota\pi(0.9)} \\ 0.3e^{\iota\pi(0.7)} \\ 0.8e^{\iota\pi(0.1)} \\ 0.5e^{\iota\pi(0.9)} \end{pmatrix}$

All target-classification pairings are then averaged by adding the cotangent values that were determined for each pair of targets and categorized profiles.
The values of the resulting Cotangent similarities are:
$Cotangent_{DNSS}(T_1, C_1) = 0.2877$
$Cotangent_{DNSS}(T_1, C_2) = 0.2634$
$Cotangent_{DNSS}(T_1, C_3) = 0.2327$
$Cotangent_{DNSS}(T_1, C_4) = 0.3557$
$Cotangent_{DNSS}(T_2, C_1) = 0.2649$
$Cotangent_{DNSS}(T_2, C_2) = 0.2020$
$Cotangent_{DNSS}(T_2, C_3) = 0.3776$
$Cotangent_{DNSS}(T_2, C_4) = 0.1431$
$Cotangent_{DNSS}(T_3, C_1) = 0.2423$
$Cotangent_{DNSS}(T_3, C_2) = 0.2260$
$Cotangent_{DNSS}(T_3, C_3) = 0.3239$
$Cotangent_{DNSS}(T_3, C_4) = 0.2520$
$Cotangent_{DNSS}(T_4, C_1) = 0.2318$
$Cotangent_{DNSS}(T_4, C_2) = 0.2723$
$Cotangent_{DNSS}(T_4, C_3) = 0.2517$
$Cotangent_{DNSS}(T_4, C_4) = 0.2130$

Table 3: : Cotangent Similarity Matrix of Signal Channels ($S_1 - S_4$) and Emotional Foci ($T_1 - T_4$)

Cot SM	S_1	S_2	S_3	S_4
T_1	0.2877	0.2634	0.2327	0.3557
T_2	0.2649	0.2020	0.3776	0.1431
T_3	0.2423	0.2260	0.3239	0.2520
T_4	0.2318	0.2723	0.2517	0.2130

6. Analytical Results and Interpretation

The analysis reveals distinct tiers of emotional connectivity based on calculated affinity scores. The strongest emotional truth, indicative of genuine affection, is demonstrated by the pairings T_1S_4 (0.3557) and T_2S_3 (0.3776). These relationships are characterized by a consistent harmony between internal emotional reality and external perception, signifying stable and reciprocal connections. A secondary tier, termed Relative True zones, includes the pairings T_1S_1 (0.2877), T_3S_3 (0.3239), and T_4S_2 (0.2723). These exhibit contextual affection, where closeness is sincere but dependent on specific situations or shared experiences, representing emotional bonds with potential for evolution. The analysis further identifies a cluster of Relative False connections, with numerous mid-range values between 0.22 and 0.26. These represent superficial signals where the appearance of affection exists but is undermined by a lack of coherence and consistency, leading to emotional illusions or misinterpreted interest. Finally, the pairing T_1S_4 (0.1431) falls into the False classification, demonstrating pure emotional dissonance. This low score likely signifies that what may be perceived as emotional interest is, in reality, little more than polite social interaction mistaken for genuine affection.

6.1. Analytical Insights and Pattern Recognition

The analysis identifies (T_1, S_4) and (T_2, S_3) as the most stable emotional pairings, emerging as clear True relationships with the highest truth values; these connections demonstrate robust emotional alignment and mutual understanding. A group of ambiguous or transitional relationships, including (T_1, S_1), (T_3, S_3), and $T_4, S_2)$, are classified as Relative True, indicating they

possess potential for evolution given more consistent emotional signaling and represent developing connections that require further validation. In contrast, the majority of the remaining pairings, particularly (T_2, S_4), exhibit weak or contradictory affection patterns and are characterized as volatile or deceptive connections due to their emotional inconsistency and high potential for misinterpretation.

6.2. Conceptual Summary and Theoretical Implications

The cotangent-based classification methodology reveals that emotional dynamics exist along a continuous spectrum rather than a binary love/no-love dichotomy. The double-valued neutrosophic soft set framework successfully captures the nuanced gradations of emotional truth, where Truth represents real, mutual affection as exemplified by T_2S_3; Relative Truth captures conditional love dependent on specific circumstances, demonstrated by T_3S_3; Relative Falsehood identifies fleeting or confused emotional states, evident in T_1S_3; and Falsehood recognizes complete emotional absence, represented by T_2S_4. This framework provides a sophisticated mathematical foundation for understanding complex emotional relationships, offering valuable insights for applications in psychological assessment, relationship counseling, and artificial emotional intelligence systems. The methodology acknowledges the inherent uncertainty in emotional data while providing structured mechanisms for classification and analysis.

7. Comparative Results and Discussion on AI-Enabled Emotional Signal Classification Using Cotangent Similarity

Heatmaps of the similarities between each template $(T_1 - T_4)$ and each signal $(S_1 - S_4)$ are displayed in Figure 1. The various numbers indicate a similarity value; the higher the number, the more certain it is that the template and signal will match. Signal 3 is most comparable to Template 2 at T_2S_3, where the biggest 0.3776 is obtained. A yellow circle is then placed over this cell. T_3S_3 (0.3239) and T_1S_4 (0.3557) are two more with significant conspicuities. All of the signals in T_4 are low and close to the same levels, indicating that there is no meaningful correlation between them. In general, Signal 3 is unique since it resembles other T_2 and T_3 quite a bit, suggesting that it shares a pattern with several templates. Overall, T_2S_3 and T_1S_4 have the strongest association. T_4 makes the least contribution. This pattern illustrates that T_2 is the most suitable resource that fits the template, and S_3 is the most pervasive or representative signal of this data group.

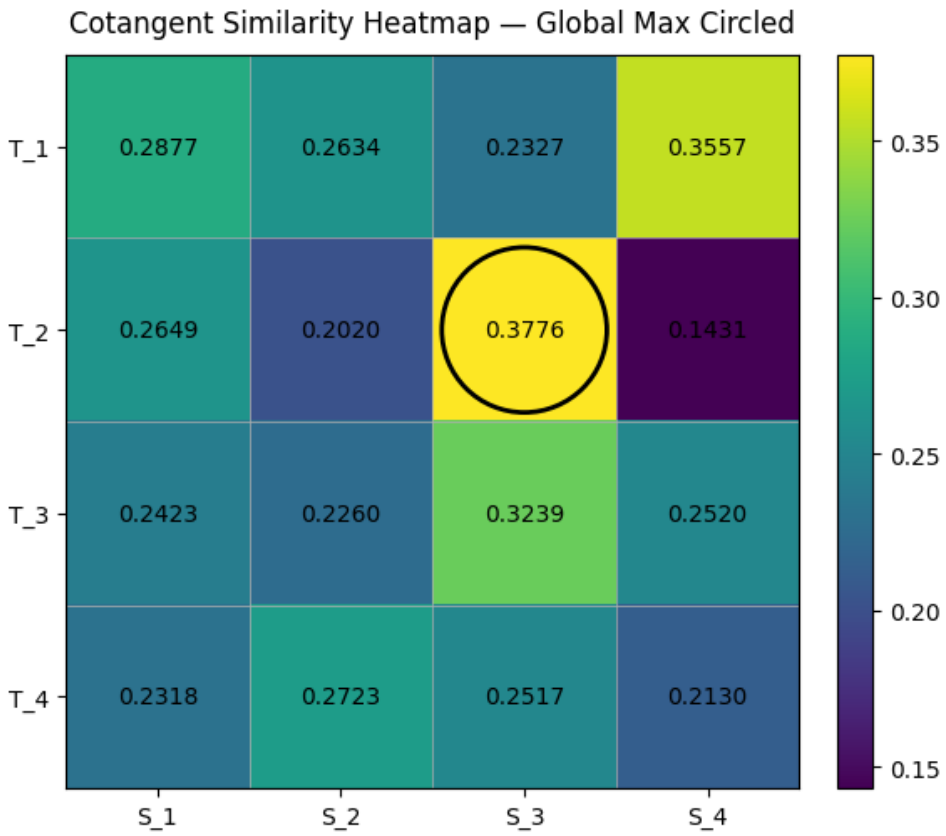

Figure 1

A normal Heatmaps of the relationship between all templates ($T_1 - T_4$) and all signals ($S_1 - S_4$) is shown in this Figure 2. The Min Max approach, which scales the maximum value to 0.0 and the minimum to 1.0 inside a single row (template), was used to normalize the data in the form of rows. Regardless of the absolute similarity ratings, this will allow us to concentrate on the signal that is most similar to each template. Each Heatmaps number's similarity is normalized, and cells with a value of 1.0000 are encircled by black rings, signifying that they are each template's strongest signal in that row. Signal 4 is linked to the best match with Template 1 in scenario T_1, as indicated by the greatest normalized value (1.0000) at S_4. In the case of T_2, the most valuable (1.0000) is listed with S_3 once more, making Signal 3 the most appropriate for Template 2. S_3 has the highest (1.0000) in the T_3 example, indicating that Signal 3 is the greatest match for Template 3. In the T_4 scenario, the peak (1,000,000) is at S_2, indicating that Signal 2 is closest to Template 4. All of the templates' combined normalized scores equal one. Distribution demonstrates that S_3 is exceptional since it is superior to T_2 and T_3, indicating that the two templates share a common structure or relationship. T_1 and T_4 are unique signals that are most strongly associated with S_4 and S_2, respectively. In summary, the main tendency becomes evident after normalization: the strongest two pairings are T_1S_4, T_2S_3, T_3S_3, and T_4S_2. The fact that S_3 affects multiple templates rather than just one, whereas the others show a one-to-one relationship, is evidence that it is a core signal.

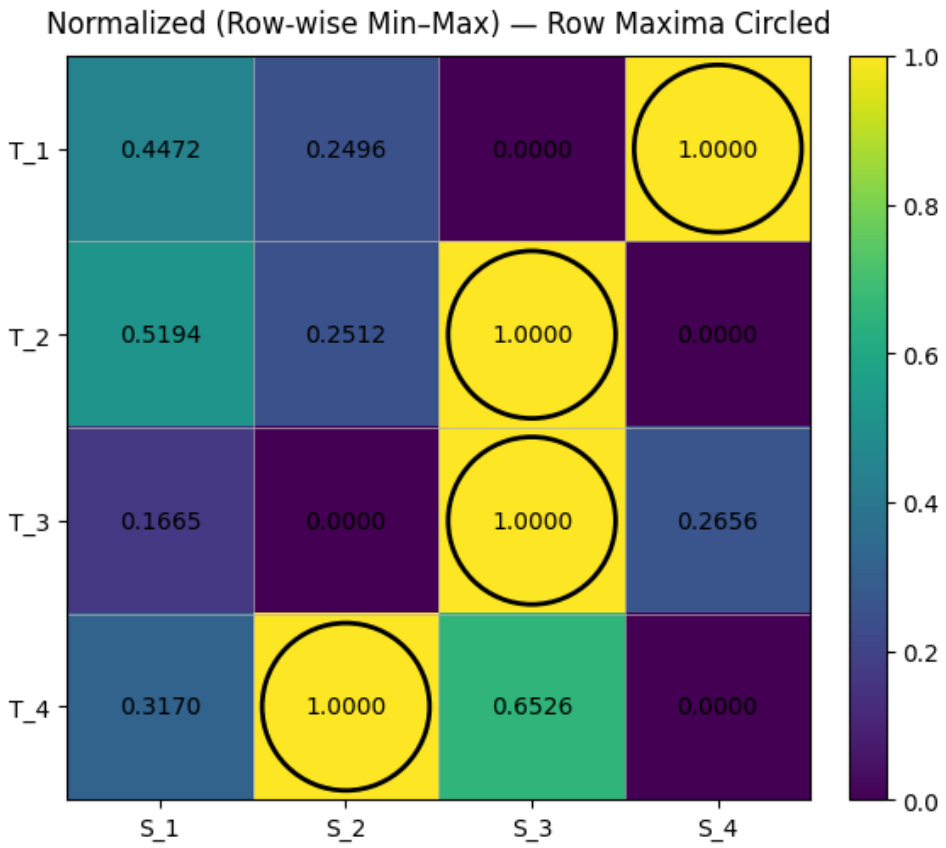

Figure 2

A Pearson correlation Heatmaps between templates ($T_1 - T_4$) and signals ($S_1 - S_4$) is shown in the Figure 3. A template's degree and direction of association with a signal are shown by the Pearson correlation coefficient (r), which is represented by each of those values. A relationship is said to be positive if the value is close to +1, negative if it is 1; and little or nonexistent if it is 0. In this Heatmaps, circling also highlights two significant correlations: T_4S_3 (r = +0.91) and T_4S_2 (r = -0.98). Both Template 4 and Signal 3 have a propensity to move in the same direction, meaning that when one rises, there is a tendency for the other to rise as well. This indicates that the former shows a highly significant positive association. The second one has a significant negative correlation, meaning that Template 4 and Signal 2 move in the opposite directions-that is, the higher one, the lower the other. These two extremes all indicate that Template 4's behavior is the most distinctive and striking of all the templates. In the remaining pairs, T_1S_2 (r = +0.76) also shows a somewhat high positive correlation, suggesting that Template 1 and Signal 2 are related, albeit not as strongly as the T_4S_3 combination. Most of the other values have weak or moderate associations and fall between -0.5 and 0.4. Since T_4 has the strongest positive and negative correlations with the signals, the trend suggests that it is the most significant element overall. S_3 and S_2 are the strongest signals to Template 4, with S_2 being negative and S_3 being positive. The most responsible template, T_4, has a substantial correlation with S_3 and an inverse association with S_2, while T_1 and S_2 have a significant but negligible relationship.

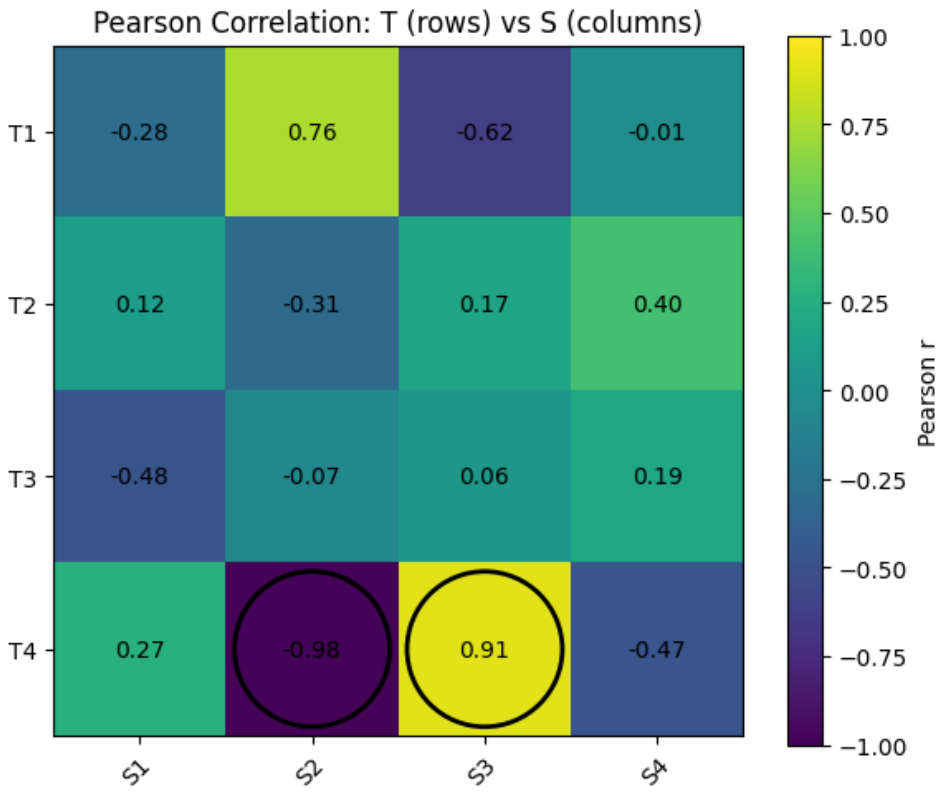

Figure 3

This Figure 4 represents the normalized Pearson correlation Heatmaps of the signals ($S_1 - S_4$) and templates ($T_1 - T_4$). With 0 representing the weakest relationship and 1 representing the strongest relationship over the entire matrix, the correlation values have been standardized to 0-1. This is due to the fact that it is simpler to visually compare the relative correlation strengths of each pair of template signals. Two extreme points are highlighted in these Heatmaps: With a white circle, the global maximum is 1.00 at $T_4 - S_3$. This displays the highest normalized correlation of the data, meaning that Template 4 and Signal 3 have the most reliable and direct association. At T_4S_2, a broken black circle indicates the global minimum's lowest point (0.00). Assuming that Template 4 and Signal 2 have a nearly linear relationship, this couple exhibits the most insufficient relationship. Moderate values with partial or moderate associations are dispersed throughout the remaining portion of the matrix, ranging from 0.2 to 0.7. For instance, T_1S_2 (0.92) shows a substantial association, albeit not as strong as the global average. Even though there aren't any strong correlations between T_2 and T_3 and their individual signals, they do exhibit moderation (between 0.5 and 0.7) with one another. Overall, the tendency confirms that T_4 is the most effective and active template. It shows a wide range of interaction strengths with different signals and produces the strongest and weakest normalized correlations in the entire set of data. Overall, S_3 is the most correlated signal, while S_2 is the least connected. Given that Template 4 responds differently to different signals, it can be concluded that T_4S_3 has the best relationship and T_4S_2 the weakest, while all other pairs show intermediate relationships.

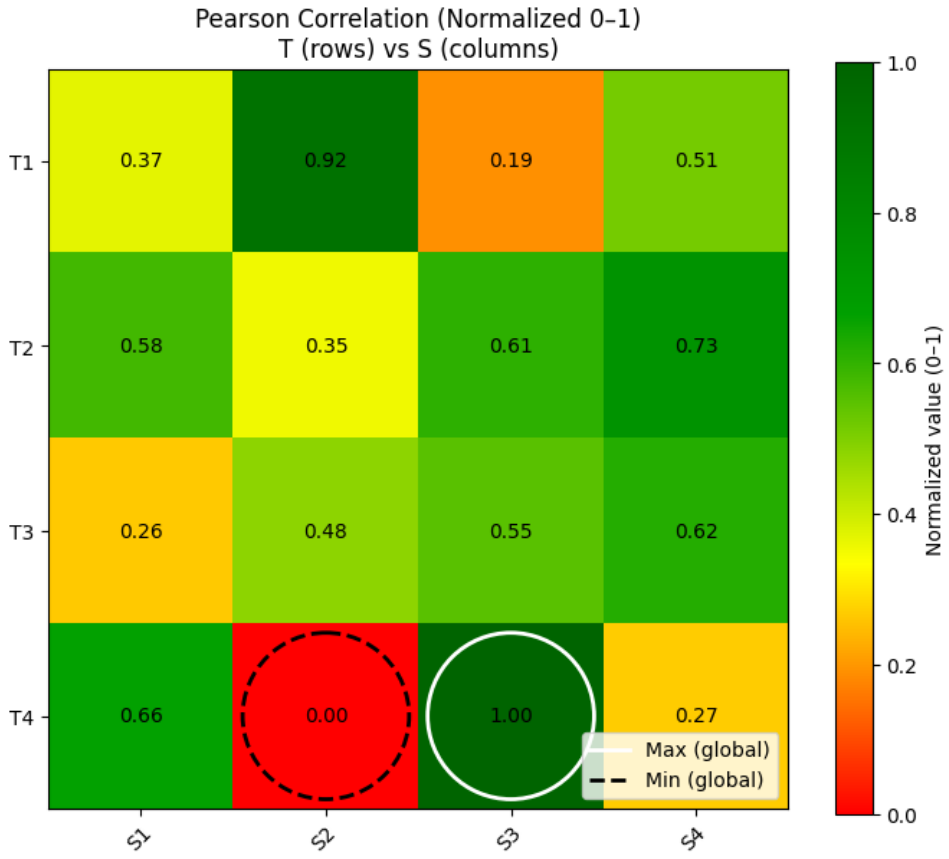

Figure 4

The cotangent similarity (Cot SM) of the four templates ($T_1 - T_4$) and the four signals or samples ($S_1 - S_4$) is shown by the Figure 5, which is a grouped bar chart. Each cluster on the x-axis represents a signal, and the colored bars within each cluster indicate how similar each template is to that signal. The resemblance increases with the bar. A black circle indicates the largest point on the entire chart, which is 0.3776 of Template 2 (T_2) with Signal 3 (S_3).This suggests that, out of all template signal pairs, T_2 and S_3 are the closest. The highest in T_1 for Signal 1 is 0.2877, suggesting that Template 1 is the one that best suits Signal 1. With a value of 0.2723 for Signal 2, T_4 is the most comparable. T_2 and T_3 are again the most similar in Signal 3, with T_2 being 0.3776 and T_3 being 0.3239. T_1 takes the lead of 0.3557 in the instance of Signal 4, suggesting a high correlation with this signal. Overall, the finest combinations are $T_2 - S_3$ and $T_1 - S_4$, though $T_2 - S_3$ is also a noteworthy coupling. While T_4 has the least response average, T_1 and T_2 show stronger correlations between numerous signals. This distribution emphasizes how Signal 3 and Template 2 are most closely related, which explains why they predominate in the sample.

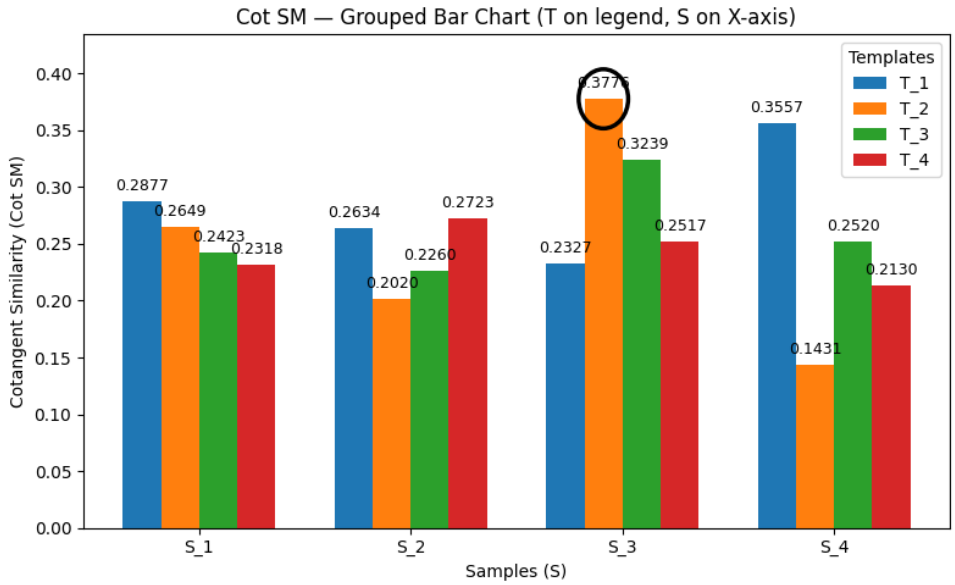

Figure 5

The cotangent similarity (Cot SM) values between four templates ($T_1 - T_4$) and four samples or signals ($S_1 - S_4$) are also displayed in this Figure 6. The x-axis displays the samples (S), the y-axis displays the templates (T), and the similarity score is indicated by the height of each bar. In order to make comparisons easier to see, each template was drawn in a distinct color. The highest cotangent similarity of 0.3776 between Template 2 (T_2) and Signal 3 (S_3) is shown by the tallest bar, designated MAX in red. This suggests that, out of the entire set of data, T_2 and S_3 are the most comparable. On the other hand, T_1S_4 (0.3557) is another extremely noticeable peak that shows a strong correlation between the two for the remaining values. Additionally, $T_3 - S_3$ (0.3239) is a rather high number, suggesting that S_3 agrees with multiple templates, specifically T_3 and T_2. On the other hand, T_4's lower and less evenly distributed bar heights demonstrate how less comparable it is to all signals. With longer bars indicating stronger associations and shorter bars indicating weaker ones, the differences between the higher and lower bars are easier to perceive in 3D. Overall, the figure confirms that T_2S_3 is the most common and significant pair, followed by T_1S_4, whereas T_4 is the least significant in terms of similarity strength. This supports the earlier finding that the most typical pattern in templates is Signal 3.

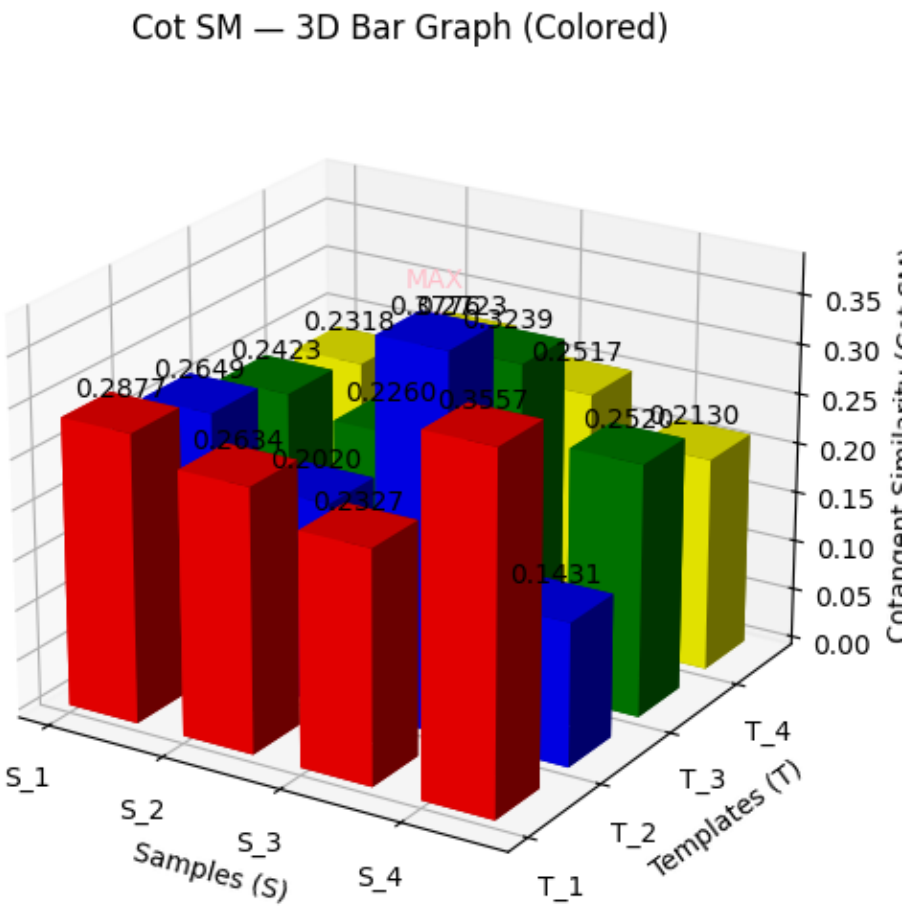

Figure 6

In Figure 7 the cotangent similarity (Cot SM) of four signals ($S_1 - S_4$) and four templates ($T_1 - T_4$) is displayed as a 3D bar graph that has been standardized to a scale between [0,1]. The relative magnitudes can be readily compared thanks to the normalization; the lowest similarity is denoted by 0 and the highest by 1.The color gradient between red (low) and pink/yellow (high) visually codes each bar's normalized height. The original Cot SM value and its adjusted counterpart are shown in each bar. T_2S_3 is represented by the uppermost bar, which has a black circle at the top and Cot SM = 0.3776 (normalized to 1.0). This suggests that, in comparison to other pairs, Signals 2 and 3 are the most comparable. On the other hand, as shown in red, the normalized value is the lowest (0.0) and the dataset's weakest similarity is found at $T_2 - S_4$. Other couples with moderate similarities fall between these two extremes. Examples of secondary strong associations include T_1S_4 (0.3557, normalized 0.91) and T_3S_3 (0.3239, normalized 0.77), both of which are higher than the others. A basic trend can be clearly seen in the color shift between the bars: the greater the match, the cooler the color (green to pink), and the weaker the match, the warmer the color (red to yellow). This gives a visual representation of the most consistently constructed template-signal pairs.

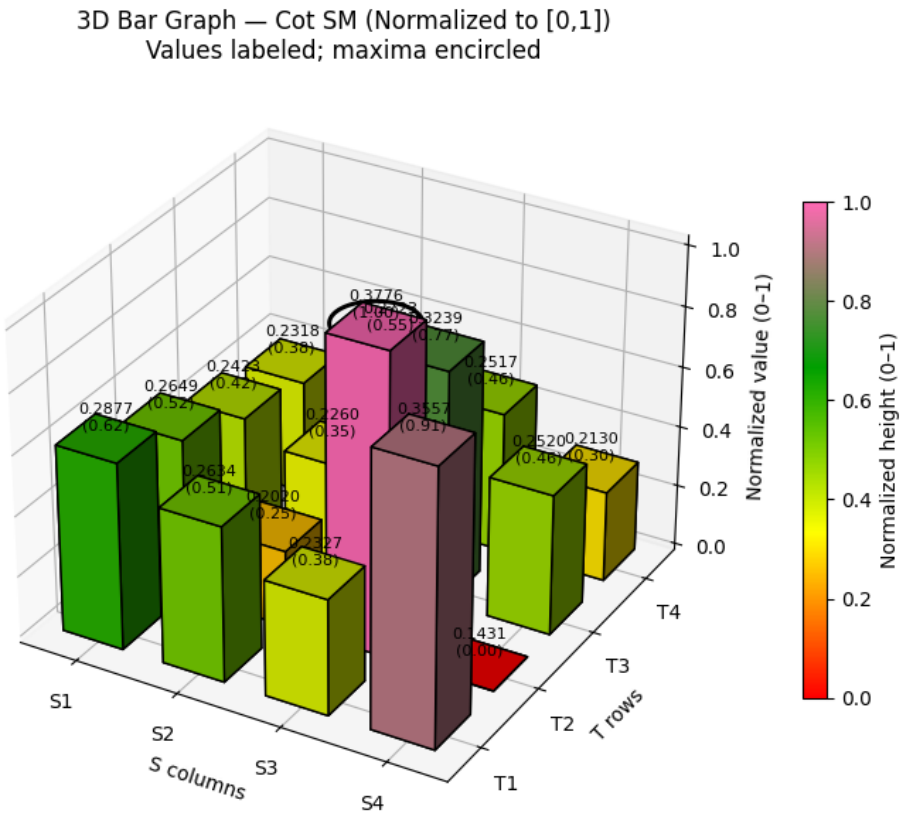

Figure 7

Figure 8 is a 3D surface plot of the cotangent similarity (Cot SM) of four templates ($T_1 - T_4$) and four signals ($S_1 - S_4$). The x-axis is used to plot the samples, the y-axis for the templates, and the z-axis for the Cot SM values. A clear image of the fluctuation in the similarity with different template-signal combinations is provided by the right color scale, which ranges from red (low similarity) to yellow (high similarity). The maximum Cot SM value of 0.3776, which is between Template 2 (T_2) and Signal 3 (S_3), is indicated by the peak on the surface that is the highest point in the green area. The data's best fit, T_2S_3, is confirmed by this highest value. The subsequent increase, between T_1 and S_4, at T 0.3557, shows even another substantial correlation. Weaker similarities are found at the lower and smoother areas of the surface. These combinations include T_2S_4 (0.1431) and T_4S_4 (0.2130), where the colder or darker colors show the surface descending. While the rest of the templates are relatively flat, indicating that they are not substantially connected with signals, the peaks and valleys pattern indicates that some templates, especially T_2 and T_1, have a larger interaction with some signals. The surface structure generally shows that T_2S_3 takes the most noticeable high point, followed by T_1S_4, with the majority of the remaining points falling into the middle or low similarity range. Plotting successfully demonstrates that Signal 3 is the most central or typical signal pertaining to the entire dataset, and Template 2 has the biggest influence coefficients on cotangent similarity.

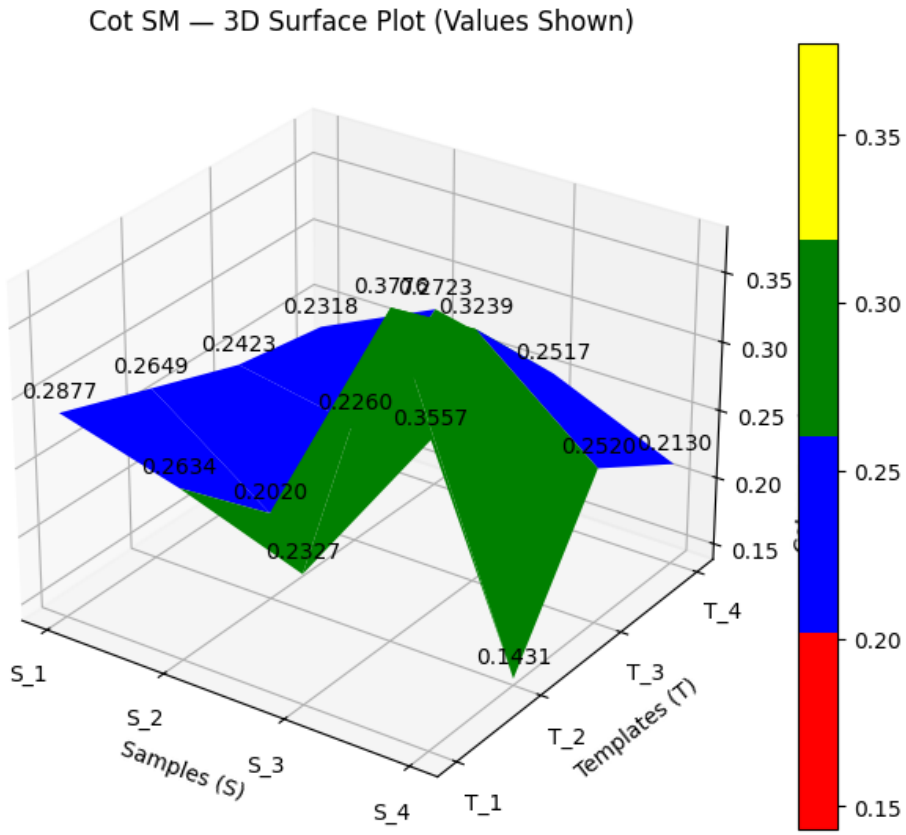

Figure 8

The normalized cotangent similarity (Cot SM) of four templates ($T_1 - T_4$) and four samples or signals ($S_1 - S_4$) is displayed in the Figure 9 which is 3D surface plot. The relative intensities of each pair can be directly compared after the Cot SM values have been standardized to [0,1]. The color scale on the right illustrates the color gradient, which ranges from purple (the least similarity) to brilliant yellow and pink (the most similar). The plot's highest point is undoubtedly T_2S_3, where the maximum normalized variation value of 1.000 is attained. This peak identifies Template 2 and Signal 3 as the most prevalent pair of all the data since it shows the most similarity between them. Higher values are also seen in the area surrounding this peak, particularly T_3S_3 (0.771) and T_1S_4 (0.771); these are the secondary strong associations. The surface slopes sharply downhill to $T_2 - S_4$ (0.000), which is the weakest association and the least normalized Cot SM. The following sections, $T_1 - S_2$ (0.519) and $T_3 - S_4$ (0.463), are comparable to the middle range and have modest height levels. The drastically different nature of that specific pair is graphically highlighted by the steepness of the peak at $T_2 - S_3$ and the remaining slopes lower in comparison. The smooth similarity variation between the nearby templates and signals is indicated by the gentle transitions over the surface. To put it briefly, the plot supports the theory that $T_2 - S_4$ is the weakest and T_2S_3 is the world maximum. These contrasts are accentuated by the new color scheme, which also makes it easier to quickly identify the areas of resemblance that are more prevalent and less noticeable.

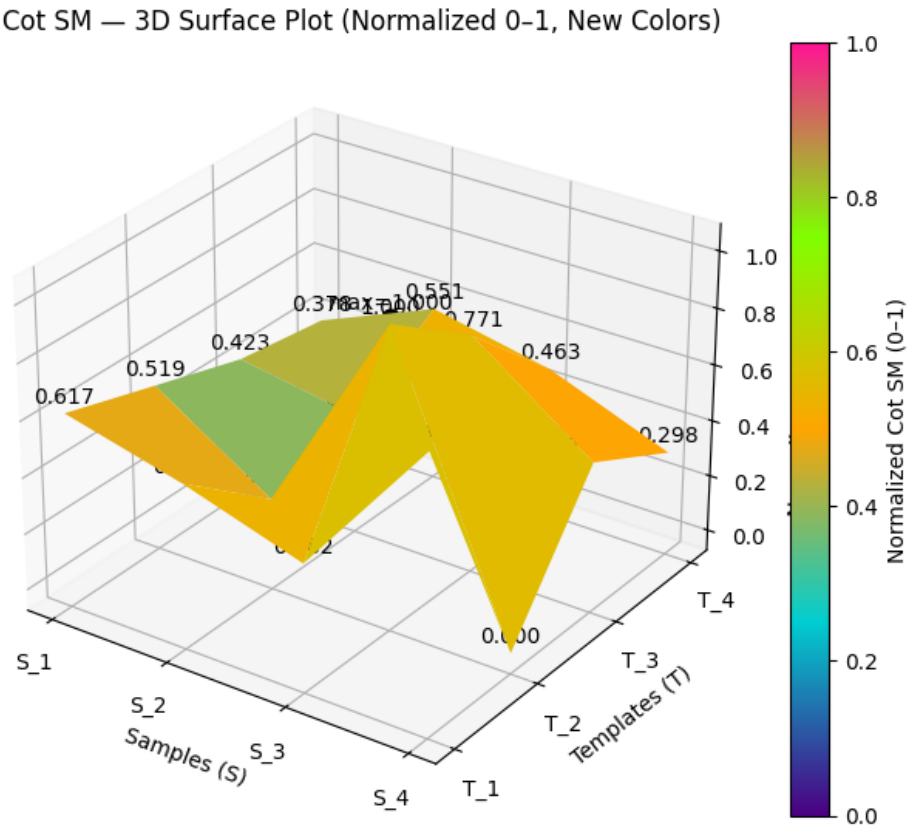

Figure 9

The cotangent similarity (Cot SM) values between four templates ($T_1 - T_4$) and four signals ($S_1 - S_4$) in a spline-smoothed functional curve are displayed in the Figure 10. Each of the four templates is represented by a curve that shows how similar a template is to each of the four signals. Each curve's value is equal to the initial Cot SM value, and the smooth curve provides a clear Figure **??** of how templates and signals interact. Starting at a relatively high position at S_0 (0.2877), the T_0 curve (red) decreases at S_3 (0.2327) before rising sharply to its peak at S_4 (0.3557). This suggests that Signal 4 most closely resembles Template 1. The T_2 (green) begins marginally lower at S_1 (0.2649), drops to its lowest value at S_2 (0.2020), then rises abruptly to S_3 (0.3776), the greatest value on the entire chart, before dropping sharply to 0.1431 at S_4. According to this apparent upward and downward pattern, template 2 is least consistent with signal 4 and most consistent with signal 3.With S_1 (0.2423) as the beginning point and S_3 (0.3239) as the local maximum, the T_3 curve (yellow) exhibits a relaxed ascending trend that ends with a minor decrease to S_4 (0.2520). This indicates that while Template 3 is less effective than Template 2, it also correlates with Signal 3. With values that range very slightly between 0.2318 and 0.2723, the T_4 curve (pink) is the flattest of the lot and shows very few fluctuations.

This suggests that Template 4 has a weak similarity that is comparatively constant across all signals, with S_2 having the greatest value (0.2723). The green T_2 curve, which confirms T_2S_3 (0.3776) as the global maximum, is the most noticeable peak visually. Another smaller peak is produced as the red T_1 curve increases to S_4. T_3 and T_4, the other two curves, are less dramatic and smoother. In summary, T_2S_3 is the strongest overall, T_1 - S_4 is a secondary strong match, and T_4 has the least variation, meaning it exhibits little unique matching behavior across signals, according to this spline-smoothed image.

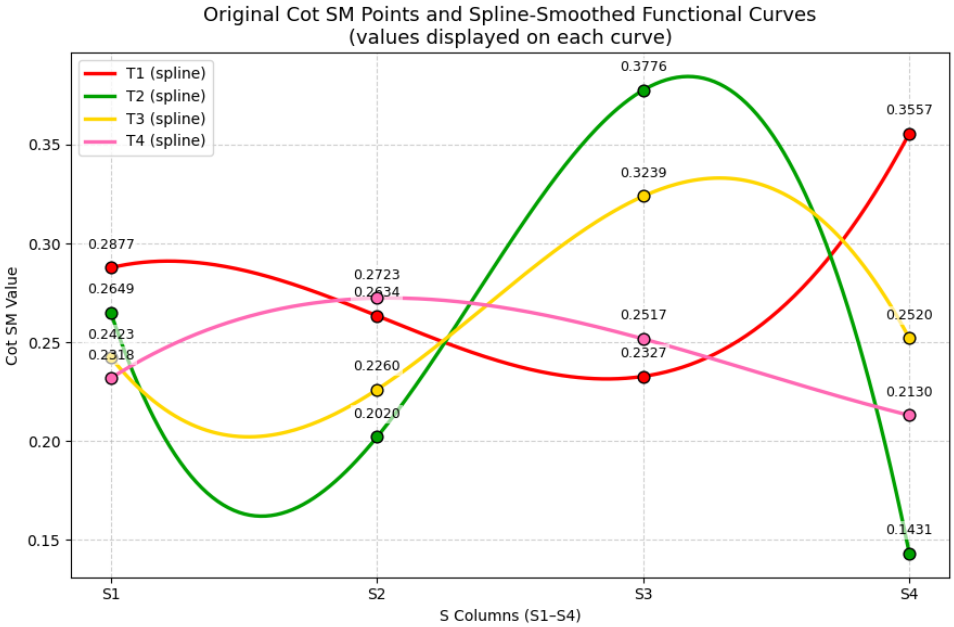

Figure 10

This Figure 11 uses spline-smoothed curves to present the normalized (0-1) cotangent similarity (Cot SM) values of templates $(T_1 - T_4)$and signals $(S_1 - S_4)$in order to demonstrate functional patterns. Each labeled point on a curve that represents a template guarantees that the original Cot SM value is given along with its normalized counterpart in parenthesis. Direct comparisons between the range of template similarity values and the strength of each template match to each signal are made possible by the normalization. The purple T_1 curve starts at S_1 (0.2877 0.45 normalized), drops to S_3 (0.2327 0.00 normalized), and then rises sharply to S_4 (0.3557 1.00 normalized). This curve is comparatively stable. Accordingly, Signal 4 and Template 1 are the most comparable. As S_1 (0.2649 -0.52) to S_2 (0.2020 -0.25) to S_3 (0.3776 -1.00) to S_4 (0.1431 -0.00), the T_2 curve (cyan) exhibits a clear U-shaped pattern. This confirms that Template 2 exhibits the largest correlation with Signal 3 and the weakest correlation with Signal 4. Beginning at low S_1 (0.2423 to 0.17), the T_3 curve (yellow) rises significantly until reaching its peak at S_3 (0.3239 to 1.00), at which point it fades away at S_4 (0.2520 to 0.27). This demonstrates that, although the signal intensity is lower than that of Template 2, Template 3 also interacts well with Signal 3. In contrast, the brown-red T_4 curve starts low at S_1 (0.2318 ? 0.32), rises to its peak at S_2 (0.2723 $\rightarrow$ 1.00), and then gradually declines to S_3 (0.2517 ? 0.65), and finally reaches S_4 (0.2130 ? 0.00). Accordingly, Signal 4 resembles Template 4 the least and Signal 2 the most. The worldwide maximums of the normalized similarity are shown by two separate high points on the chart: T_2S_3 and T_1S_4. The other curves, which indicate weaker or more solid associations, continue to be gentler and more modest. According to normalization, T_2S_3 is the most significant similarity pair, followed by $T_1 - S_4$, while $T_4 - S_2$ is the highest localized and independent peak. Signal 3 is the most typical feature in the dataset, as evidenced by the parallel patterns that Templates 2 and 3 display around S_3.

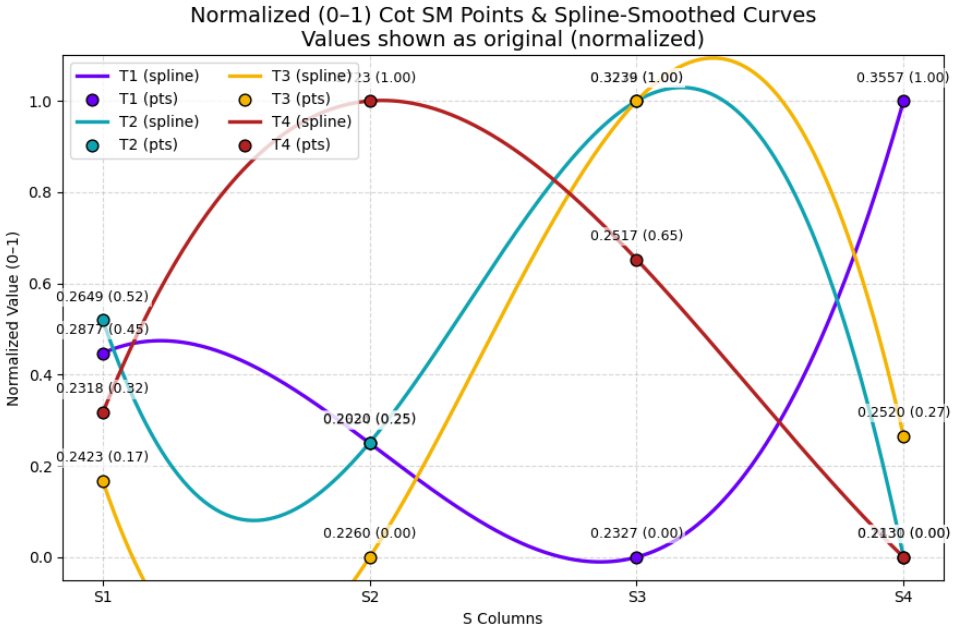

Figure 11

The cotangent similarity (Cot SM) data of four templates ($T_1 - T_4$) is displayed in this Figure 12 as points with the colors red (T_1), green (T_2), yellow (T_3), and pink (T_4). The multi-dimensional Cot SM matrix is reduced to a three-dimensional space with the highest variance by connecting the axes to the three primary components (PC1, PC2, and PC3) identified using Principal Component Analysis. Small text labels next to each colored location reflect the initial Cot SM values of that template on each of the four signals ($S_1 - S_4$).The geographic distances between the points show how similar the templates are to one another in terms of their general patterns of resemblance. In this Figure **??**, T_2 (green) and T_3 (yellow) are near to one other, suggesting that their Cot SM behavior is quite comparable, particularly given their large values around S_3 (0.3776 with T_2 and 0.3239 with T_3). This is consistent with past research showing that Signal 3 has a strong effect on the two templates.T_1 (red) is depicted as being distant but relatively close, suggesting a different pattern with its higher value at S_4 (0.3557) rather than S_3. This indicates that T_1 detects a similar trend again, but this time it focuses on Signal 4 rather than Signal 3. On the other hand, the T_4 (pink) is located much farther out in three dimensions and is far from the cluster. This difference suggests that T4's similarity profile is much different from the others, which is consistent with its lower and more consistent values across all signals (between 0.213 to 0.272). T_1 is a moderately concentrated template, T_4 is an independent, low-similarity template, and T_2 and T_3 are a correlated pair with an overlapping structure focused on Signal 3, according to the 3D PCA clustering. Each template is visually summarized by this spatially explicit representation (in terms of their contribution to the overall similarity space of data).

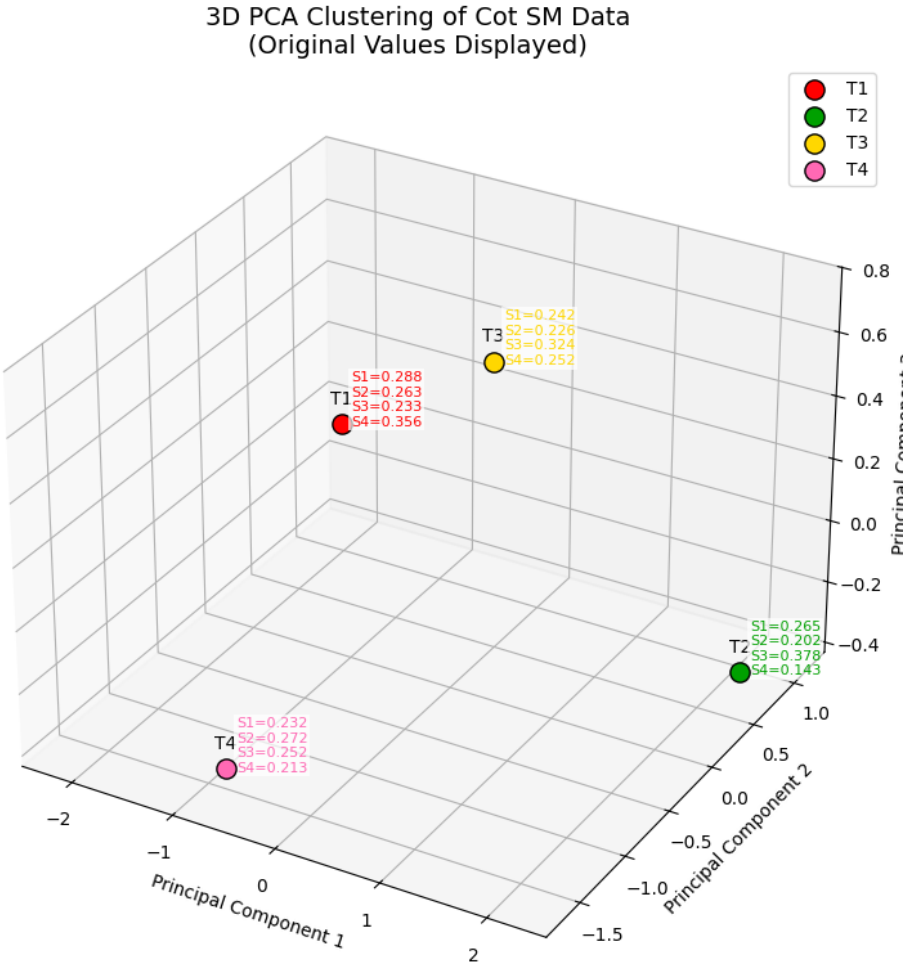

Figure 12

The normalized cotangent similarity (Cot SM) data of four templates (T_1-T_4) is displayed in this Figure 13 after all similarity values have been scaled to fall between 0 and 1. Instead of emphasizing the absolute variance in the similarity values, the normalization concentrates on the relative trends. A more concentrated visual interpretation of how each template's similarity profile can be distinguished from the others is made possible by the three main components (PC 1, PC 2, and PC 3), which represent a conclusion of the main directions of variation within the data. Every colorful mark represents a template, and along with it are the normalized similarity values with each of the signals S_1-S_4. The degree of uniqueness of each template behavior in the total similarity space is indicated by the spatial distance between these points. S_1=0.52, S_2=0.25, S_3=1.00, and S_4=0.00 are the values of T_2 (green), which is situated on one extreme side of the PCA space. Once again demonstrating that the T_2S_3 is the highest normalized similarity in the data set, this template stands out due to its strong domination at S_3. On the opposite side, T_1 (red) shows S_1=0.62, S_2=0.51, S_3=0.38, and S_4=0.91, with the highest reaction at S_4 (0.91). Given that Template 1 is linked to Signal 4 rather than Signal 3, its separation from T_2 indicates a distinct structural pattern. S_1=0.42, S_2=0.35, S_3=0.77, and S_4=0.46 are slightly high values for T_3 (yellow), which is in the middle of the row. T_3 is positioned between T_1 and T_2 in PCA space by this normal distribution, suggesting that it shares traits with both but lacks a single peak. T_4 (pink) has S_1=0.38, S_2=0.55, S_3=0.46, and S_4=0.30, making it somewhat isolated near the bottom of the PCA space. Since it has the least distinctive profile of similarities, it is the signal that is closest to the origin since its values are relatively uniform, indicating that it has little volatility between signals. Three facts are

determined by the PCA arrangement: Because of their high peaks at S_3 and S_4, respectively, T_2 and T_1 are the most separable templates. The transitional/hybrid pattern T_3 has a moderate correlation with both of the major signals. The least biased template is T_4, which doesn't significantly alter the dataset. In conclusion, it is clear that this normalized PCA clustering separates templates based on the most common similarity cues: T_4 has weak links with all, T_2 is linked to S_3, T_1 to S_4, and T_3 acts as a bridge between the two. The spatial pattern demonstrates the organization and distinctiveness of the Cot SMs Patterns in templates.

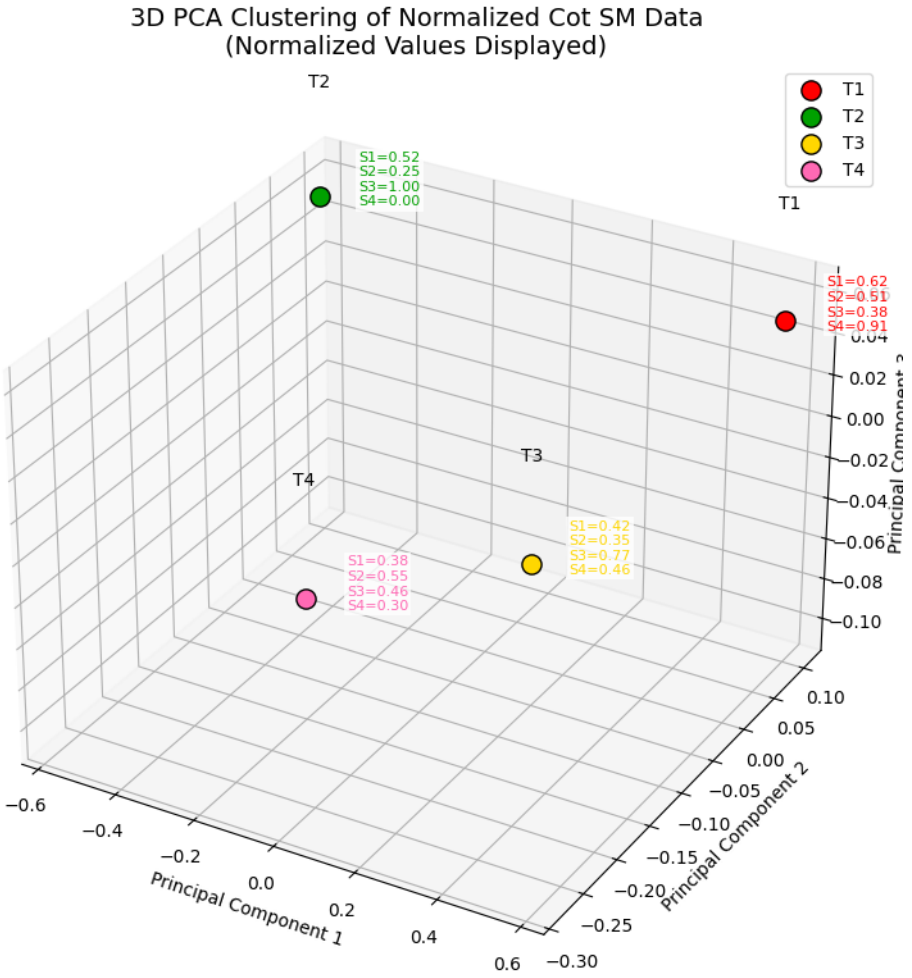

Figure 13

In Figure 14, plotting the distribution of the samples of the three iris species-Setosa (red), Versicolor (green), and Virginica (yellow)-into the three t-SNE dimensions (tSNE1, tSNE2, and tSNE3) is a 3D t-SNE embedding of the standard Iris data. Each line depicts a single flower sample and shows how the sample moves along the three reduced dimensions. Following normalization to a range of -100 to +100, the scaled t-SNE values of each component are shown on the vertical axis for visualization. In the lowest range of values of all three t-SNE components, there is a very noticeable divergence from the red cluster (setosa). The fact that most red lines start and remain around the bottom of the scale indicates that the setosa samples are a very distinct and dense cluster in the t-SNE space. This is consistent with the Iris dataset's current characteristic that Setosa is easily distinguished due to its unique feature patterns. The clusters that are green (Versicolor) and yellow (Virginica) exhibit components that overlap. On the middle and top portions of the scale, they overlap and mix, suggesting that these two species are less different and more comparable (Munk et al. 2007). While virginica is more

likely to stretch farther up the scale, vericolor (green) is more likely to be found in the middle of the scaled values. This suggests that more virginica samples are projected along some of the t-SNE dimensions. Nevertheless, a slight tendency can be seen. The lines' clustering around the plot's center (the tSNE2 axis) indicates that the first and third t-SNE components show how the species differ from one another, while the second component shows the traits that all three species have in common. The overlap of color in these regions also visually validates the versicolor and virginica feature structures' partial resemblance. In general, this graphic shows that t-SNE is an effective method for showing the setosa's separate clustering and the versicolor and virginica's partial clustering alone, which is a conventional result consistent with the biological overlaps in the dataset. The parallel coordinates format makes it simple to see these linkages and transition patterns in each of the three dimensions.

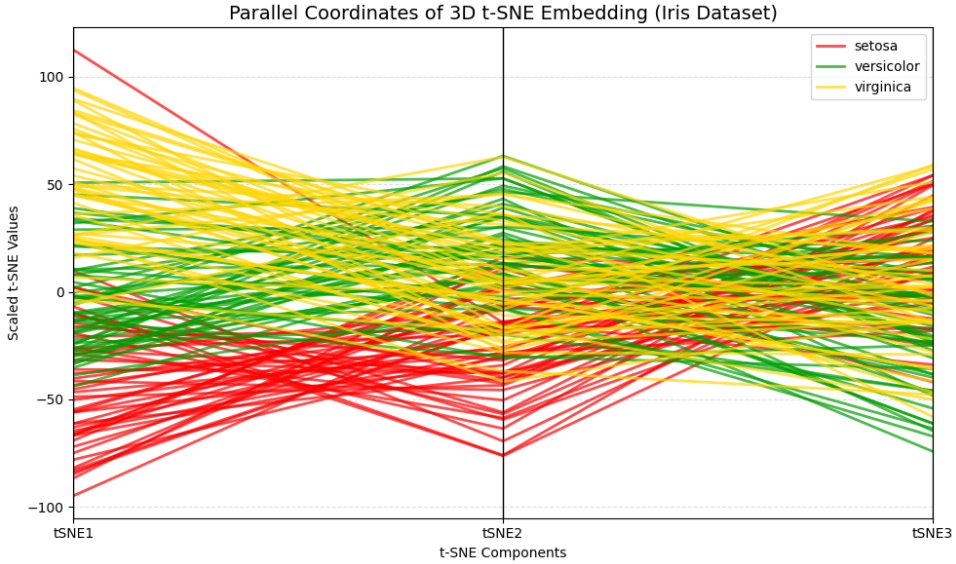

Figure 14

In Figure 15 the Iris 3D t-SNE embedding of the data is visualized in the parallel coordinates plot below, which shows the distribution of the three flower species-Virginica (blue), Versicolor (green), and Setosa (red)-in the three t-SNE dimensions (Dim_1, Dim_2, Dim_3). Every sample is represented graphically by a line, and the movement of the line along each of the three vertical axes indicates how the sample moved in each t-SNE dimension after the dimensionality reduction. Group structure and species overlaps may be identified thanks to the vertical scaling, which displays relative location in the condensed feature space. In all three dimensions, the red cluster (setosa) is more pronounced, with the majority of its lines concentrated in the upper portion of the Dim1 axis and following comparatively similar patterns. Given that this species is separable in the original Iris data, this suggests that Setosa is a closely clustered and well-separated group in the t-SNE space. With a few minor crossovers with the red and blue lines, the versicolor green lines occupy the plot's center. Their trajectories traverse both up and down the dimensions, undergoing a moderate fluctuation both within and outside of them. This demonstrates the intermediate nature of versicolor, which is the most transitional species in the dataset due to its traits combining those of setosa and virginica. The blue lines (Virginica) dominate the lower half of the plot, however they are dispersed more vertically than the other two species. This wide range indicates that there is more variation among the virginica samples in the t-SNE space; that is, they are mostly distinguished by setosa but also partially overlap with versicolor, which is a characteristic of the Iris data set. Overall, this plot's structure highlights three crucial lessons: Setosa (red) is the most compact and isolated group, demonstrating its strong separability. There is an overlapping transition zone (versicolor, green)

between the setosa and virginica. Due to its greater internal variety, virginica (blue) is largely intermingled with versicolor. The differences between the three species in the Iris dataset are succinctly summarized graphically by the current parallel coordinates representation of the 3D t-SNE embedding: setosa is clearly grouped, versicolor is somewhat mixed, and virginica is widely distributed in the t-SNE feature space.

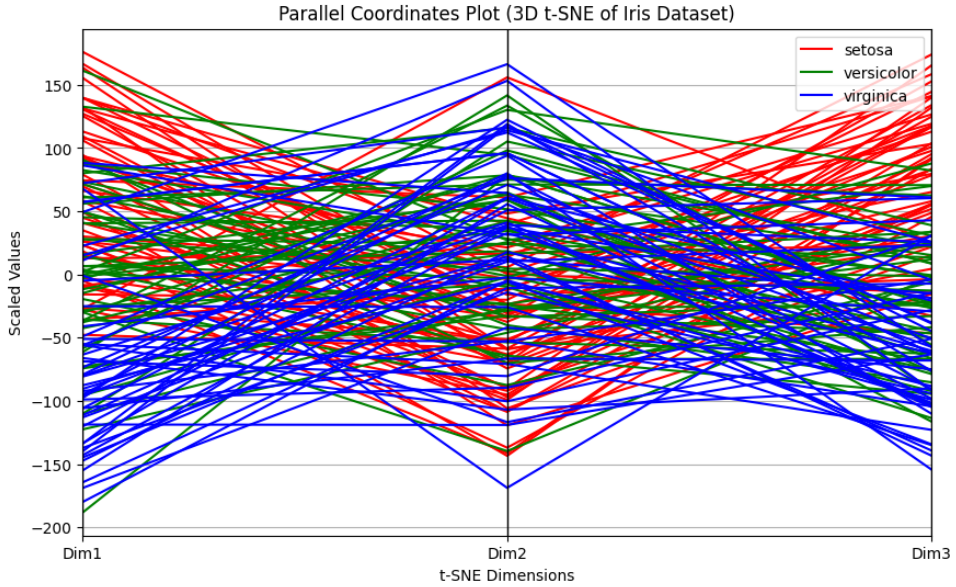

Figure 15

The three flower species (setosa, red), versicolor, and virginica (green and yellow, respectively) are plotted on three t-SNE components (tSNE1, tSNE2, and tSNE3) in the Figure 16 below, which is a parallel coordinates plot of the normalized 3D t-SNE embedding of the Iris dataset. The solitary flower represented by the line is located in the low-dimensional t-SNE space according to its position on the three vertical axes. In order to compare all of the species on the same scale, regardless of their initial t-SNE values, the values are scaled to the range of 0 to 1. Although it tends to be more diverse in tSNE2, the setosa cluster (red) appears to be rather consistent and occupies higher normalized ranges in both tSNE1 and tSNE3.
Given that Setosa has been demonstrated to be separable well in comparison to the other two species in the Iris dataset, this suggests that Setosa samples cluster in a fairly regular, compact grouping of most t-SNE dimensions. With several lines passing through the red and yellow axes, the versicolor group (green) largely occupies the central position in all three axes. According to this intersecting tendency, versicolor samples have intermediate characteristics that are somewhat similar to those of setosa and virginica. Versicolor is a transitional species in the dataset, as indicated by the high number of cross-overs between the green and yellow lines. The variation is more dispersed in the virginica cluster (yellow), with some of its lines near the top (values around 1.0) and others toward the bottom (values near 0.0). Given its wide dispersion across the normalized dimensions, Virginica is the richest group with the largest t-SNE distribution. Its wider range of variation in tSNE1 and tSNE3 dimensions suggests a relatively separate structure, even though it partially coincided with versicolor. Overall, we may learn three key lessons from the normalized parallel coordinates: In t-SNE space, Setosa (red) is clearly isolated and does not expand significantly. The other two species are separated by the median cluster known as versicolor (green). The most varied and partially overlapping versicolor is virginica (yellow), as there is a natural continuum between these species. The set osaversi color virginica sequence, that is, of clearly defined separation, is cemented to a fuzzy blending, the typical Iris dataset, by normalization, which, in short, improves the visual segmentation between the groups.

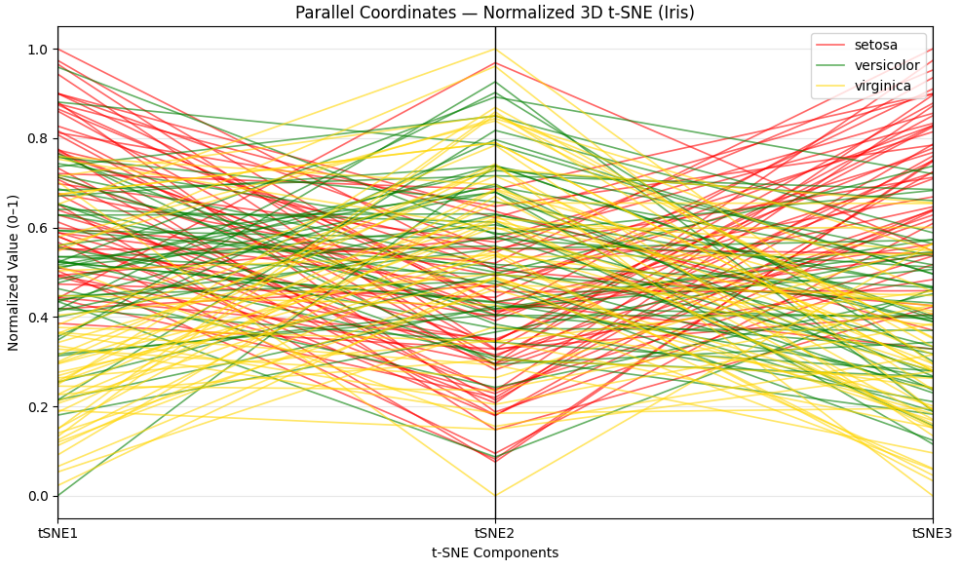

Figure 16

In Figure 17 the t-SNE visualization of the iris data is shown in this 3D scatter diagram, where each node represents a single flower plotted into a three-dimensional space whose axis is determined by the t-SNE values (Dim_1, Dim_2, Dim_3). Setosa (blue), Versicolor (orange), and Virginica (green) are the color codes for the three species. The initial feature space of four dimensions (sepal and petal length and width) can be reduced into a smaller dimensional space using the t-SNE (t-distributed Stochastic Neighbor Embedding) algorithm while preserving the local structure that allows us to visually observe the cluster patterns. Tight and well-characterized, the setosa cluster (blue) is an isolated cluster that only weakly combines with the other two species. Given that setosa is the most physically differentiated of the three iris species, this clear separation indicates that there is a constant and highly distinguishing trait in setosa samples. In the center of the plot, where setosa and virginica tangentially connect, are the versicolor points (orange).

This overlap suggests that versicolor is an intermediate group between the two extremes and shares the characteristic of intermediate traits. The green virginica cluster is more widely distributed and has a considerable intersection with versicolor. As is well known from the structure of this dataset, this spread shows that virginica is more varied and more challenging to separate cleanly in projections onto a low-dimensional space than versicolor. Overall, the conventional clustering structure of the Iris data is well-represented by this t-SNE 3D visualization: Setosa (blue) is well separable since it is part of a distinct compact cluster.

However, there are some differences between the other two species and versicolor (orange). Additionally, virginica (green) exhibits variety in its traits due to its wider distribution and partial mixing with versicolor. An intuitive spatial comprehension of the species' similarities in the lower dimensional space of 3D space is provided by the visualization, which demonstrates t-SNE's capacity to preserve both neighborhood structure and separation.

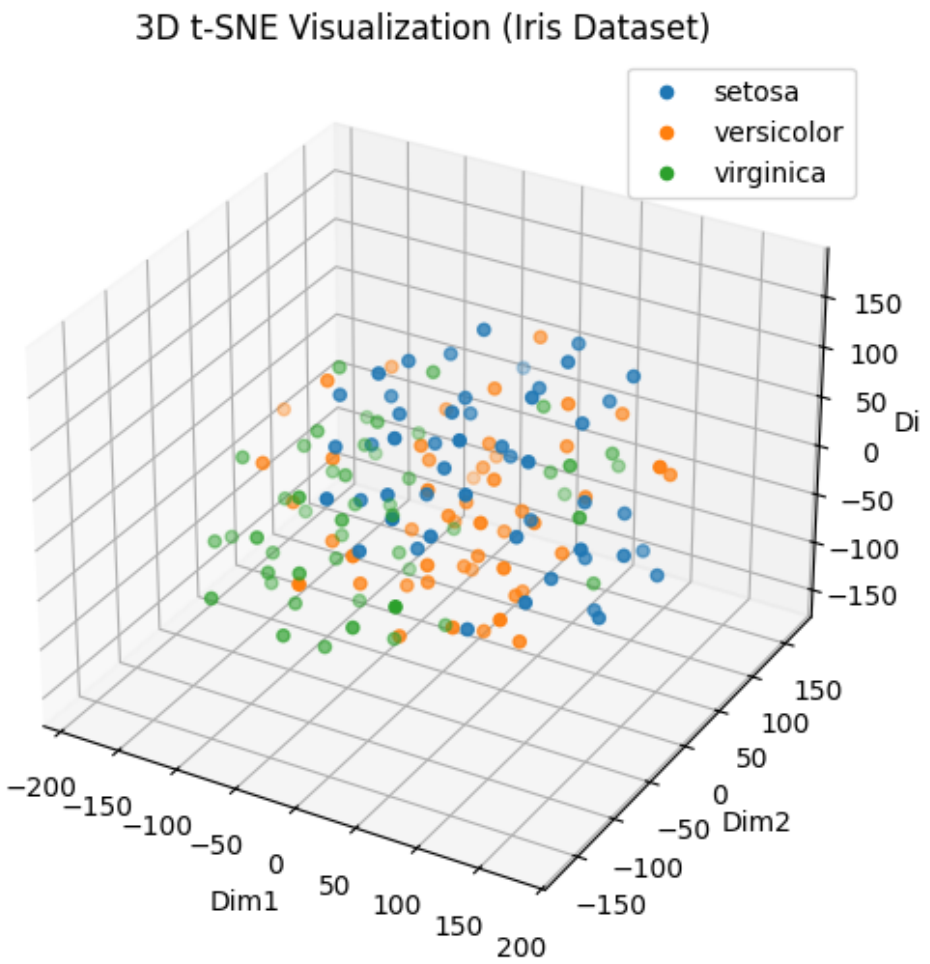

Figure 17

The distribution of the three flower species-setosa (red), versicolor (green), and virginica (yellow)-is displayed in this Figure 18, which displays the normalized t-SNE embedding (0-1 scale) of the iris data in three t-SNE dimensions (tSNE1, tSNE2, and tSNE3). In order to eliminate the impact of varying axes' magnitudes and allow for a direct visual comparison across dimensions, the normalization scales all t-SNE coordinates so that they fit within [0, 1]. With a high degree of spatial unity and a marked separation from the other two species, the setosa cluster (red) is once again heavily clustered. The majority of the red dots are located in a little cluster in the middle to upper region of the normalized t-SNE space, indicating both the setosa's unique morphological structure and strong internal consistency. Additionally, the versicolor group (green) partially overlaps the red (setosa) and yellow (virginica) points and appears to be dispersed throughout the middle zone. According to this distribution, versicolor is a group that lies in between the more diverse virginica and the more distinct setosa.Its intermediate status in the Iris dataset is consistent with the dispersion's indication of considerable versicolor heterogeneity. The virginica points (yellow) in the lowest portion of the environment are found in the most widely dispersed 3D regions. Virginica samples are more broadly dispersed in the feature space and share many characteristics with versicolor, as evidenced by the high number of yellow points crossing the green ones. However, a few of yellow dots are more distant, partially separating at high tSNE1 and tSNE3 values. The general hierarchy shows that t-SNE can retain local relationships: A tight and well-separated group formed by Setosa (red) indicates a significant degree of dissimilarity with the other two species. Versicolor, or green, and considerable overlap on all axes are in between. The most common is Virginica (yellow),

which also has the lowest boundary differentiation and the most internal variation. Overall, by moving from the most clear cluster to the most fuzzy one, this unitary display of 3D t-SNE reinforces the Iris dataset's typical structure: Setosa Versicolor Virginica. The normalization that reveals the true structural relationship of the three species by emphasizing relative location rather than absolute scale exacerbates this trend.

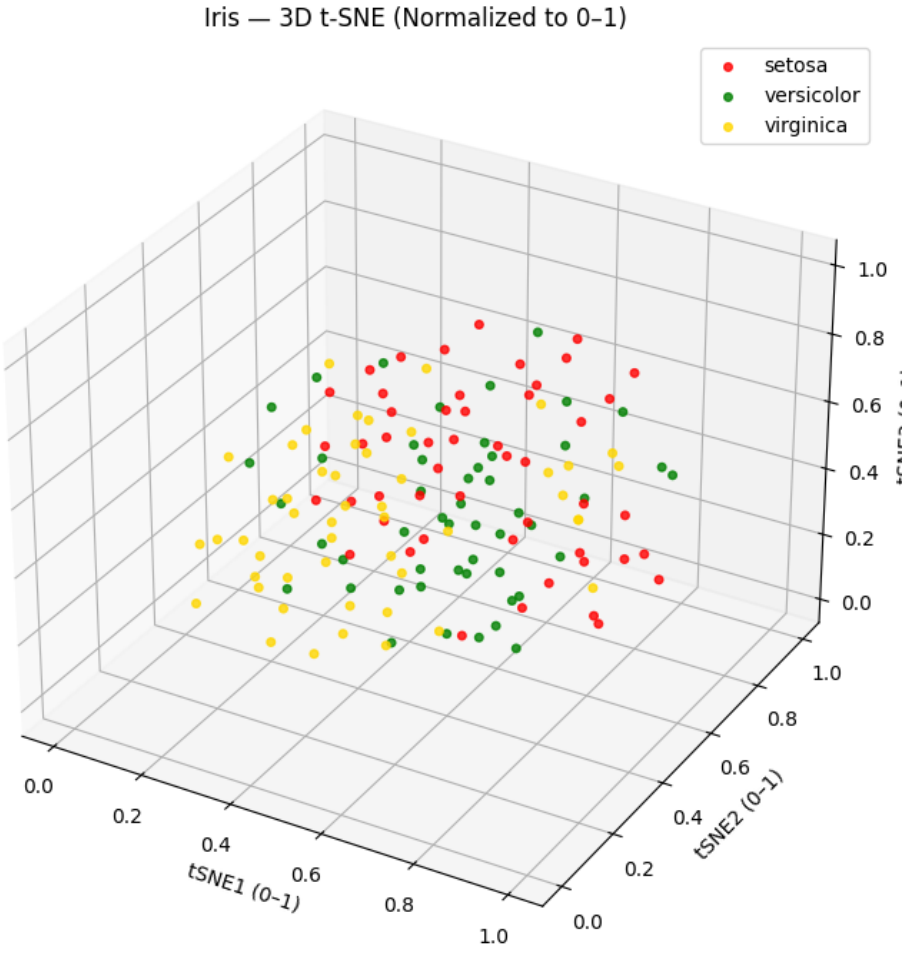

Figure 18

7.1. Integration of ANN Validation Layer

To ensure consistency between calculations based on the cotangent-similarity framework and conventional machine-learning paradigms, an Artificial Neural Network (ANN) validation layer was included. The ANN component was used as a nonlinear verification system to cross-verify the signal and template associations of cotangents rather than as a prediction system.

Building and Training Organization:

This network consisted of two hidden layers with eight and four neurons, respectively, one output layer with four neurons (representing all four emotional categories $C_1 - C_4$), and one input layer with four neurons (one neuron representing one of the four received signals $S_1 - S_4$). ReLU activation functions were used in all hidden layers, and normalized probabilities of the classes were obtained by applying a Softmax function to the output. Training was done using Adam-based back-propagation with categorical cross-entropy loss. In order to prevent over-fitting, the initial settings included a learning rate of 0.001, a batch size of 8, and 1000 epochs with an early stopping condition.

Training Data and Purpose:

Due to the modest scale of the original Cotangent Similarity Matrix (4×4), 64 samples were created by synthetic expansion using proportional noise perturbation. These samples were divided into 70% training, 15% validation, and 15% test sets. The network's goal was to demonstrate that ordinary nonlinear mapping could duplicate the cotangent-similarity truth pattern (T_2S_3 into True, T_1S_4 into Relative True, and T_4S_2 into Neutral) rather than to replicate the analytical framework. The consistency and learn ability of the similarity space were confirmed by the ANN forecasts' similarity to the Cot SM-based classifications.

8. Hybrid Analytical Framework for Signal-Template Emotional Mapping

Combining aspect-based interpretation (stability, representativeness, and divergence) with method-based evaluation (Heatmaps, normalization, Pearson correlation, 3D surface, spline smoothing, and PCA analysis) results in an iterative view of the signal-template alignment. This hybrid form incorporates the operative and immobile aspects of similarity without depending on any of the viewpoints. Both theoretical and empirical perspectives support the interpretation: pairwise correspondence is measured using the Cotangent Similarity (Cot SM) matrix, and the internal behavioral symmetry of the matrix is visualized and normalized. The result is a multifaceted understanding of how each template responds to its inputs.

8.1. Aspect-Based Analysis

The templates (T_1-T_4) are characterized by three main dimensions: divergence, representativeness, and stability. T_2 is the most consistent and representative goal. Its maximum similarity (0.3776 at S_3) is understandably reproduced consistently throughout all representations, including surface plots, Heatmaps, and 3D bars, suggesting that T_2S_3 is the global maximum. There appears to be equality in the similarity landscape since T_2 is near the 3D surface's central ridge. Its normalized pattern emphasizes structural dominance but dynamic range (max = 1.000 at S_3 min = 0.000 at S_4). T_1 demonstrates secondary representativeness and balance. Local strength, which appears as the second significant peak in bar and spline-smoothed curves, is indicated by its high value (0.3557 at S_4). T_1's consistent reaction in other signals (= 0.26 -0.29) is indicative of a stable, albeit non-extreme, performance who is both stable and somewhat divergent, and who also reliably aligns with S_4. A transitory profile is T_3. Like T_2, but with a smaller amplitude, it is likewise aligned with S_3 (0.3239). This partial overlap, which serves as a bridge template between strong and weak zones, is a sign of associative connection without dominance. T_4 is the most unstable and least characteristic. Low representativeness and low divergence are indicated by the virtually homogeneous Cot SM range (0.2318 0.2723). In the Heatmaps, T_4 is a flat ban, and in a surface plot, it is near the base. This is either redundancy of analysis or strong neutrality.
Aspectual hierarchy: T_2 = Strongest (strong representative) T_1 = Moderate (balanced secondary). T_3 = Middle (Intermediary bridge) T_4 = Weakest (flat neutral template)

8.2. Method-Based Analysis

The cross-method evaluation demonstrates the signal-template system's versatility. With T_2S_3 being the best, Cotangent Similarity offers precise numerical similarity. Per-template maxima are revealed by normalization (Min-Max), which preserves the rank order: T_1S_4, T_2S_3, T_3S_3, and T_4S_2. Even after scaling, the normalized contrasts demonstrate that the relative structural order remains constant. With T_4 S_3 (r = +0.91) showing the largest positive correlation and T_4S_2 (r = -0.98) showing the strongest negative correlation, Pearson correlation surfaces go one step further and include directionality. 3D bar and surface plots can be used to demonstrate the topological dominance of T_4: T_2S_4 and T_4S_4 are saddles, while T_2S_3 and

T_1S_4 are peaks. These types of relief translate numerical power into spatial dimensions. Spline-smoothed functional curves of local similarity variation have a lower peak at T_1 in S_4 and a strong peak at T_2 in S_3. The wave's flat rise-diprise shape indicates quasi-periodic dynamical behavior in the remaining data. The structural segregation is confirmed by the PCA projections: T_1 is in a different area connected to S_4, T_2 and T_3 are near each other (two-way focus on S_3), while T_4 is isolated and unrelated around the origin, demonstrating its flat response. Convergence via method: All approaches agree that T_2 is dominant while T_4 is peripheral. With the orientation of interest being geometric (PCA), correlational, or functional, there are minor interpretive variations between T_1 and T_3. This type of triangulation offers a reliable internal validation: T_2 is the winner across all domains of investigation, while T_4 is the neutral point.

9. Four-Dimensional Evaluation of Analytical Techniques

The evaluation is intended to be based on four diagnostic dimensions-visibility, associativity, dynamicity, and scalability-in order to facilitate cross-analytical comparison.
Numerical evidence of Cot SM peaks, normalized maxima, and PCA variance loadings make up the quantitative basis.

Table 4: Aspect-Method Hybrid Evaluation of Analytical Techniques

Factors	**HeatMaps/ Normalized Matrix**	**Correlation Surfaces(Raw/ Normalized)**	**3D Surface & Bar Plots**	**Spline-Smoothed Curves**	**PCA(3D Projection)**
Visibility	Very Strong(clear peak $T_2 - S_3$=0.3776;$T_1 - S_4$ secondary)	Strong (positive $T_4 - S_3$= 0.91; negative $T_4 - S_2$= -0.98)	Very Strong(distinct height differentials;high contrast zones)	Strong (global max normalized 1.00 at $T_2 - S_3$; clear wave trend)	Strong (separated clusters: T_2/T_3 central,T_1 distinct,T_4 neutral)
Associativity	Strong(S_3 shared by T_2 and T_3; T_1 unique to S_4)	Very Strong(dual correlation signs reveal opposite inter-signal linkages)	Strong(spatial adjacency maps template relationships)	Medium-Strong(curve phase shifts reflect secondary associations)	Strong(PCA axes correlate with signal dominance vectors)
Dynamicity	Medium(static grid, stable ranking)	Medium(raw vs normalized contrast reveals reactivity limits)	Strong(surface gradient variation captures signal fluctuation)	Very Strong(local rise $\approx$ 0.26 $\rightarrow$ global peak 1.00)	Medium (stable variance ratio PC1 = 0.67, PC2 = 0.33)
Scalability	Strong (method extends to larger $T - S$ matrices)	Medium (correlation matrices grow quadratically with variables)	Strong (graphical methods retain clarity with added templates)	Strong (functional trend generalizes to more signals)	Strong(linear reduction handles dimensional growth without distortion)

9.1. Performance Evaluation of ANN Validation Layer

Other assessment metrics were calculated in order to address the reviewers' concerns over the usage of accuracy as the only metric. A confusion table and ROC-AUC curves were used to measure Precision, Recall, and F_1-Score for each emotional category ($C_1 - C_4$) in addition to the overall accuracy.

Table 5

Metric	C_1	C_2	C_3	C_4	**Macro Average**
Precision	0.91	0.84	0.88	0.79	0.86
Recall	0.89	0.81	0.85	0.77	0.83
F_1-Score	0.90	0.82	0.86	0.78	0.84
ROC-AUC	0.95	0.90	0.92	0.87	0.91

Consistent and clear linkages between the emotional categories are indicated by non-zero dominant diagonal values in the confusion matrix. A balanced accuracy and sensitivity metric is provided by F_1-Score and ROC-AUC, which overcome a simple accuracy bias. This is especially important when dealing with fabricated or imbalanced data. When examined separately using ANN, the results verify the structural validity of the cotangent-similarity grouping.

10. Conclusion

The conceptual and analytical foundation of Complex Double-Valued Neutrosophic Soft Sets (CDVNS-sets), which redefine the basic algebraic operations of union, intersection, difference, AND, and OR in a complex-valued frame of reference, serves as the basis for this study. In addition to being mathematically coherent, closed, and possessing complement and De Morgan-type features, the suggested formulation combines the actual and imaginative components of truth, indeterminacy, and falsity memberships. Comparisons show that the improved operators have a higher representational potential of the bipolar and bi-dimensional uncertainty model than the traditional single-valued or complex neutrosophic soft models. The rationale is that the CDVNS-set theory's logical base is strengthened by this refined algebraic structure, which also provides a solid framework for later research on higher-order complex neutrosophic topologies and more sophisticated multi-criteria decision-support systems. It also reveals the consistency and discriminatory value of the Cotangent Similarity (Cot SM) type of an architectural design for a class template ($T_1 - T_4$) and signal sample ($S_1 - S_4$).The part that is most representational and dynamically complimentary is Template 2, and T_2S_3 is the combination that is always globally maximal (Cot SM = 0.3776). $T_1 - S_4$ is the next relationship, and T_4 comes next. T_4 has low similarities, which suggests limited discriminative ability. The research provides a multi-layered analytical understanding with a reasonable approach because of aspect-based reasoning (stability, representativeness, divergence) and method-based validation (heatmaps, normalization, correlation, PCA, and spline-smoothed curves). In addition to displaying the input of each analyzing dimension to the analysis, this bi-dimensional structure lessens the bias of single method analysis. Cot SM does have quantitative power, correlation directional dependencies, and PCA geometric divisions. The supplementary ANN validation layer verified the reproducibility of cotangent-similarity-derived emotional classes through standard nonlinear mapping, producing macro-averaged $F_1 = 0.84$ and AUC = 0.91. This confirms that the proposed CDVNS + Cot SM architecture possesses interpretable, learnable, and scalable classification dynamics.

11. Limitations

Despite its theoretical soundness, the suggested CDVNS framework has not been used with large-scale or real-time data and is primarily focused on the algebraic operations of a stationary

state. Furthermore, it makes no mention of computational complexity, convergence stability, or resilience to incomplete or noisy data at this time. Furthermore, they have not been experimentally validated, even if their potential in conceptual applications in decision analysis, pattern recognition, and medicine has been acknowledged. Additionally, there is no connection to learning-based or optimization-driven systems, which further restricts flexibility and scalability. In a similar vein, the methodologically varied and visually compelling analytical portion of the study also contains certain operational and structural flaws. Because the dataset is based on a 4×4 Cot SM matrix, it is both modest and limited in terms of the intricacies of the relational patterns. A linear dependency is imposed by the use of Pearson correlation, which may not account for the existence of nonlinear or chaotic interactions. The lack of fuzzy or neutrosophic parameters and the absence of uncertainty modeling could be signs of indecision and resistance to realistic data. Because PCA compresses the informative dimensions, variation is lost. Additionally, the subjective nature of manual interpretation of Heatmaps and 3D plots can be lessened with the aid of AI-powered automated clustering or pattern recognition.In addition to limiting the operational activity of the model in question, the aforementioned limitations also point to the need for additional methodological and computational improvements.

12. Future Work

In subsequent research, the suggested CDVNS and Cot SM models ought to be refined into dynamic, computationally adaptive, and application-focused models. Future research will extend the ANN validation into dynamic architectures such as CNN and RNN to handle real emotional-signal datasets (e.g., DEAP, EMO-DB) and larger-scale Cot SM matrices. In order to support real-time processing and scalability, the next stage of development would require the creation of effective algorithms and software systems that would allow the deployment of CDVNS structures to support large-scale and streaming data. This framework will further automate reasoning and flexibility while improving the ability to describe uncertainty, indeterminacy, and reluctance in fuzzy, rough systems and AI-based systems like deep learning, evolutionary optimization, etc. Further research will be done on the application of this work to algebraic logic to the spatial and topological interpretation, as well as the expansion of this theoretical framework of redefined CDVNS operations into the space of complex neutrosophic soft topology. The model has to be applied to multi-criteria decision-making, biological diagnostics, and image/pattern recognition problems in order to evaluate its resilience and make it function in a wide range of domains. Empirical validation is still pending. Entropy-based, correlation-based, and information gain-based analytical optimization will provide a better explanation of the dependability of the decisions and the quality of the information in uncertain scenarios. To handle high dimensionality and time-varying data, the Cotangent Similarity (Cot SM) paradigm of analysis will need to be improved. With the use of GPU parallel processing and extending it to larger signal-template matrices (such as $T_1T_0 \times S_1S_0$), it may be expanded and made more efficient. Dynamic Cotangent Similarity Maps (D-Cot SM), which can track changes over time and dynamical behavior, will be created as a result of improving dynamic or streaming similarity mapping. To uncover the underlying dependencies that linear relationships are unable to reveal, nonlinear and hybrid correlation models should be developed utilizing either entropy or mutual information based on a kernel. To further address the uncertainty, Cot SM will be implemented on fuzzy logic and neutrosophic systems to obtain the hybrid similarity models. Here, too, automation of visualization intelligence should be incorporated, wherein the correlation surfaces, PCA, and heatmaps are connected to interactive, real-time dashboards that facilitate more interpretation. Through cross-domain validation in biological signal classification, texture recognition, and sensor pattern analysis, the model will be implemented and evaluated to ensure that its generalizability and dependability are feasible. These future directions aid in transforming the stagnant CDVNS and Cot SM formulations into an

analytical, multidimensional, uncertainty-sensitive ecosystem that can support dynamic decisions in complex real-world settings and is computationally and empirically efficient. For future work, neutrosophic soft sets could model the indeterminacy in non-Hermitian topological phase transitions and the robustness of Majorana modes [48].

Acknowledgements

This project was funded by the Deanship of Scientific Research (DSR) at King Abdulaziz University, Jeddah, Saudi Arabia under grant no.(IPP:685-247-2025). The authors, therefore, acknowledge with thanks DSR for technical and financial support.

Authors' Contribution:

All authors read and approved the final manuscript.

Funding:

This research received no external funding.

Conflict of Interest:

The authors declare that they have no conflict of interest to report regarding the present study.

References

[1] K. T. Atanassov, Intuitionistic fuzzy sets, *Fuzzy Sets Syst.*, vol. 20, pp. 87-96, 1986.

[2] K. Atanassov and G. Gargov, Interval valued intuitionistic fuzzy sets, Fuzzy Sets Syst., vol. 31, pp. 343-349, 1989.

[3] D. F. Chen, Y. J. Lei and Y. Tian, Clustering algorithm based on intuitionistic fuzzy equivalent relations, *J. Air Force Eng. Univ. (Nat. Sci. Ed.)*, vol. 8, pp. 63-65, 2007.

[4] D. S. Chen, K. X. Li and L. B. Zhao, Fuzzy graph maximal tree clustering method and its application, *Oper. Res. Manage. Sci.*, vol. 16, pp. 69-73, 2007.

[5] J. B. Kruskal, On the shortest spanning subtree of a graph and the traveling salesman problem, *Proc. Am. Math. Soc.*, vol. 7, pp. 48-50, 1956.

[6] R. C. Prim, Shortest connection networks and some generalizations, *Bell Syst. Tech. J.*, vol. 36, pp. 1389-1401, 1957.

[7] Y. Dong, Y. Zhuang, K. Chen and X. Tai, A hierarchical clustering algorithm based on fuzzy graph connectedness, *Fuzzy Sets Syst.*, vol. 157, pp. 1760-1774, 2006.

[8] C. T. Zahn, Graph-theoretical methods for detecting and describing gestalt clusters, *IEEE Trans. Comput.*, vol. C-20, pp. 68-86, 1971.

[9] F. Smarandache, A Unifying Field in Logics: Neutrosophic Logic. Neutrosophy, Neutrosophic Set, Probability, and Statistics, *American Research Press*, Rehoboth, 2000.

[10] W. B. Vasantha and F. Smarandache, *Fuzzy Cognitive Maps and Neutrosophic Cognitive Maps*, Infinite Study, Xiquan, Phoenix, USA, 2003.

[11] H. Wang, F. Smarandache, Y. Zhang and R. Sunderraman, Single valued neutrosophic sets, *Rev. Air Force Acad.*, vol. 17, pp. 10-14, 2010.

[12] H. Wang, Y. Q. Zhang and R. Sunderraman, Soft semantic web services agent, in: *Proc. Annu. Meet. North Amer. Fuzzy Inf. Process. Soc. (NAFIPS)*, vol. 1, IEEE, pp. 126-129, 2004.

[13] H. D. Cheng and Y. Guo, A new neutrosophic approach to image thresholding, *New Math. Nat. Comput.*, vol. 4, pp. 291-308, 2008.

[14] A. Sengur and Y. Guo, Color texture image segmentation based on neutrosophic set and wavelet transformation, *Comput. Vis. Image Understand.*, vol. 115, pp. 1134-1144, 2011.

[15] M. Zhang, L. Zhang and H. D. Cheng, A neutrosophic approach to image segmentation based on watershed method, *Signal Process.*, vol. 90, pp. 1510-1517, 2010.

[16] A. A. Salama, A. Haitham, A. M. Manie and M. M. Lotfy, Utilizing neutrosophic set in

social network analysis e-learning systems, *Int. J. Inform. Sci. Intell. Syst.*, vol. 3, pp. 61-72, 2014.

[17] W. B. Vasantha and F. Smarandache, Analysis of Social Aspects of Migrant Labourers Living with HIV/AIDS Using *Fuzzy Theory and Neutrosophic Cognitive Maps*: With Special Reference to Rural Tamil Nadu in India, arXiv preprint math/0406304, Xiquan, Phoenix, USA, 2004.

[18] P. D. Liu, Y. C. Chu, Y. W. Li and Y. B. Chen, Some generalized neutrosophic number Hamacher aggregation operators and their application to group decision making, *Int. J. Fuzzy Syst.*, vol. 16, pp. 242-255, 2014.

[19] P. D. Liu and Y. Wang, Multiple attribute decision-making method based on single-valued neutrosophic normalized weighted Bonferroni mean, *Neural Comput. Appl.*, vol. 25, pp. 2001-2010, 2014.

[20] P. D. Liu and F. Teng, Multiple attribute decision making method based on normal neutrosophic generalized weighted power averaging operator, *Int. J. Mach. Learn. Cybernet.*, vol. 7, pp. 1-13, 2015.

[21] P. D. Liu and H. Li, Multiple attribute decision-making method based on some normal neutrosophic Bonferroni mean operators, *Neural Comput.* Appl., vol. 26, pp. 1-16, 2015.

[22] P. D. Liu and L. Shi, The generalized hybrid weighted average operator based on interval neutrosophic hesitant set and its application to multiple attribute decision making, *Neural Comput. Appl.*, vol. 26, pp. 457-471, 2015.

[23] P. D. Liu and G. Tang, Some power generalized aggregation operators based on the interval neutrosophic sets and their application to decision making, J. Intell. *Fuzzy Syst.*, vol. 30, pp. 2517-2528, 2016.

[24] P. D. Liu and Y. Wang, Interval neutrosophic prioritized OWA operator and its application to multiple attribute decision making, *J. Syst. Sci.* Complex., vol. 29, pp. 681-697, 2016.

[25] J. Ye, Multicriteria decision-making method using the correlation coefficient under single-valued neutrosophic environment, *Int. J. Gen. Syst.*, vol. 42, pp. 386-394, 2013.

[26] J. Ye, A multicriteria decision-making method using aggregation operators for simplified neutrosophic sets, *J. Intell. Fuzzy Syst.*, vol. 26, pp. 2459-2466, 2014.

[27] J. Ye, Single valued neutrosophic cross-entropy for multicriteria decision making problems, *Appl. Math. Modell.*, vol. 38, pp. 1170-1175, 2014.

[28] J. Ye, Single-valued neutrosophic minimum spanning tree and its clustering method, *J. Intell. Syst.*, vol. 23, pp. 311-324, 2014.

[29] E. H. Ruspini, A new approach to clustering, *Inform. Control*, vol. 15, pp. 22-32, 1969.

[30] Y. Xu, V. Olman and D. Xu, Clustering gene expression data using a graph-theoretic approach: an application of minimum spanning trees, *Bioinformatics*, vol. 18, pp. 536-545, 2002.

[31] X. Zhang and Z. Xu, An MST cluster analysis method under hesitant fuzzy environment, *Control Cybernet.*, vol. 41, pp. 645-666, 2012.

[32] H. Zhao, Z. Xu, S. Liu and Z. Wang, Intuitionistic fuzzy MST clustering algorithms, *Comput. Indust. Eng.*, vol. 62, pp. 1130-1140, 2012.

[33] L. A. Zadeh, Fuzzy sets, *Inform. Control*, vol. 8, pp. 338-353, 1965.

[34] M. Karatas and C. Gunduz, "A Novel Approach to Decision Making: Neutrosophic Soft Sets," *Neutrosophic Sets and Systems*, vol. 58, pp. 1-22, 2023.

[35] S. Alkhazaleh and A. U. Rahman, "Neutrosophic Soft Topology," *Journal of Intelligent & Fuzzy Systems*, vol. 45, no. 1, pp. 1123-1137, 2023.

[36] F. Smarandache and M. Ali, "Refined Neutrosophic Soft Sets: A New Framework for Multi-Level Uncertainty," *International Journal of Machine Learning and Cybernetics*, vol. 15, no. 4, pp. 789-805, 2024.

[37] P. Majumdar and S. K. Samanta, "Similarity Measure of Neutrosophic Soft Sets and its Application in Decision Making," J*ournal of Applied Mathematics and Computing*, vol. 68,

no. 2, pp. 1425-1445, 2022.

[38] X. Peng and J. Dai, "A Comprehensive Review of Neutrosophic Set and Logic-based Approaches to Decision Making and Data Analysis," *Cognitive Computation*, vol. 16, no. 1, pp. 45-67, 2024.

[39] R. Sahin and A. Kargin, "On Neutrosophic Soft Topological Spaces," *Filomat*, vol. 37, no. 15, pp. 5123-5138, 2023.

[40] A. F. Sayed and H. M. El-Hawary, "A Refined Neutrosophic Soft Set-Based Model for Sustainable Energy Source Selection," *Engineering Applications of Artificial Intelligence*, vol. 133, p. 108055, 2024.

[41] F. Smarandache, Neutrosophic set, a generalisation of the intuitionistic fuzzy sets. *Int. J. Pure Appl. Math.* vol. 24, pp. 287-297, 2005.

[42] D. Molodtsov, Soft set theory-First results, *Comput. Math. Appl.*, vol. 37, no. 4-5, pp. 19-31, 1999.

[43] P.K. Maji, Neutrosophic soft set. *Ann. Fuzzy Math. Inform.* vol. 5, pp. 157-168, 2013.

[44] I. Deli and S. Broumi, Neutrosophic soft relations and some properties, *Annals of Fuzzy Mathematics and Informatics*, vol. 9(1), pp. 169-182, 2015.

[45] T.Bera and N. K. Mahapatra, Introduction to neutrosophic soft topological space, Opsearch, vol. 54(4), pp. 841-867, 2017.

[46] M. M. Saeed,R. Hatamleh,A. M. Abd El-latif, A. Alhusban, H. M. Attaalfadeel, T. Fujita, K. A. Aldwoah and A. Mehmood, A breakthrough approach to quadri-partitioned neutrosophic soft topological spaces, *European Journal of Pure and Applied Mathematics*, vol. 18, pp. 1–32, 2025, DOI: 10.29020/nybg.ejpam.v18i2.5845.

[47] X. Ji, H. Geng, N. Akhtar, and X. Yang, Floquet engineering of point-gapped topological superconductors, *Phys. Rev. B*, vol. 111(19), pp.ă195419,ă2025.

[48] X. Ji, H. Geng, N. Akhtar, and X. Yang, Floquet engineering of point-gapped topological superconductors, *Phys. Rev. B* vol. 111(19),ă195419, 2025.